

University of Groningen

Causal and unitary scattering amplitudes compliant with crossing symmetry at low energy

Stoica, Simona

IMPORTANT NOTE: You are advised to consult the publisher's version (publisher's PDF) if you wish to cite from it. Please check the document version below.

Document Version

Publisher's PDF, also known as Version of record

Publication date:

2012

[Link to publication in University of Groningen/UMCG research database](#)

Citation for published version (APA):

Stoica, S. (2012). *Causal and unitary scattering amplitudes compliant with crossing symmetry at low energy*. s.n.

Copyright

Other than for strictly personal use, it is not permitted to download or to forward/distribute the text or part of it without the consent of the author(s) and/or copyright holder(s), unless the work is under an open content license (like Creative Commons).

The publication may also be distributed here under the terms of Article 25fa of the Dutch Copyright Act, indicated by the "Taverne" license. More information can be found on the University of Groningen website: <https://www.rug.nl/library/open-access/self-archiving-pure/taverne-amendment>.

Take-down policy

If you believe that this document breaches copyright please contact us providing details, and we will remove access to the work immediately and investigate your claim.

Downloaded from the University of Groningen/UMCG research database (Pure): <http://www.rug.nl/research/portal>. For technical reasons the number of authors shown on this cover page is limited to 10 maximum.

RIJKSUNIVERSITEIT GRONINGEN

**Causal and Unitary Scattering Amplitudes
Compliant with Crossing Symmetry at Low Energy**

Proefschrift

ter verkrijging van het doctoraat in de
Wiskunde en Natuurwetenschappen
aan de Rijksuniversiteit Groningen
op gezag van de
Rector Magnificus, dr. E. Sterken,
in het openbaar te verdedigen op
vrijdag 11 mei 2012
om 12:45 uur

door

Simona Stoica

geboren op 28 september 1982
te Mangalia, Roemenië

Promotor: Prof. dr. O. Scholten
Copromotor: Dr. M.F.M. Lutz

Beoordelingscommissie: Prof. dr. D. Bettoni
Prof. dr. K. Nakayama
Prof. dr. K. Peters

This work is sponsored by the Helmholtzzentrum für Schwerionenforschung GmbH (GSI), Germany - KVI University of Groningen collaboration agreement.

PRINTED BY: GVO drukkers & vormgevers B.V. Ponsen &Looijen

Contents

1	Introduction	1
1.1	Non-perturbative QCD	1
1.2	Reaction mechanism	3
1.3	Analytic properties of the scattering matrix	5
1.4	Approaches to construct a scattering matrix	8
2	Kinematical constraints in fermion-antifermion systems	11
2.1	Introduction	11
2.2	Wave functions and conventions	13
2.3	Invariant amplitudes	15
2.4	Partial-wave decomposition	21
2.5	Covariant partial-wave projectors	23
2.6	Conclusions	32
3	Effective field theory	35
3.1	Symmetries of QCD	35
3.1.1	Color	36
3.1.2	Flavor	37
3.2	Effective interaction	38
3.3	Isospin decomposition	42
3.3.1	Isospin decomposition of \mathcal{L}_{PB}	44
3.3.2	Isospin decomposition of \mathcal{L}_{VB}	45
3.3.3	Coupled-channel states	46

3.4	The scattering of spin-1/2 particles	47
3.4.1	Invariant amplitudes for the t-channel exchange of a pseudoscalar meson	52
3.4.2	Invariant amplitudes for the t-channel exchange of a vector meson	53
4	Dynamically generated resonances in the N/D method	61
4.1	N/D method	62
4.2	Single-channel calculation	66
4.3	Coupled-channel effects	71
4.3.1	Zero coupling	71
4.3.2	Intermediate coupling	73
4.3.3	Strong coupled-channel interaction	75
5	Summary and conclusions	77
A	Expansion in Legendre polynomials	81
B	Projectors for the $\frac{1}{2} \bar{1} \rightarrow \frac{1}{2} \bar{1}$ reaction	83
C	Projectors for the $\frac{1}{2} \bar{1} \rightarrow \frac{3}{2} \bar{1}$ reaction	85
	Nederlandse samenvatting	87
	Acknowledgments	91
	References	93

INTRODUCTION

The future international Facility for Antiproton and Ion Research (FAIR) [1] in Darmstadt, Germany, will be one of the most advanced facilities for investigating antiproton-proton collisions. Based on the existing facility at the Helmholtzzentrum für Schwerionenforschung GmbH (GSI), it will provide beams with exceptional intensity, quality and energies.

The AntiProton ANihilation at DArmstadt experiment ($\bar{\text{P}}\text{ANDA}$) [2] is one of the large detectors at FAIR, allowing for spectroscopic studies of baryons and mesons with unprecedented statistics and precision. Spectroscopy is an important tool in physics and has played a major role in the development of quantum mechanics and the standard model of physics. Spectroscopy experiments within hadron physics are *the* tool to investigate the dynamics governing the interaction of fundamental particles, as well as the existence of new forms of matter. $\bar{\text{P}}\text{ANDA}$ features a broad scientific programme [3–7], with key areas being the study of exotic hadrons (hybrids, glueballs, multi-quark states), strange and charmed baryons, charmonium spectroscopy, the hadron properties in the nuclear medium, γ -ray spectroscopy of hypernuclei, and the structure of the nucleon.

1.1 Non-perturbative QCD

Quantum Chromo Dynamics (QCD) is generally accepted to be the fundamental underlying theory of the strong interaction. However, our knowledge of the behavior at large distances is still rather primitive. QCD is the color $SU(3)$ gauge theory with

quarks (q) as the fundamental particles and gluons (g) as gauge fields. Because QCD has a non-Abelian symmetry, the gluons can interact with themselves, causing the coupling constant to decrease with energy. This means that the quarks are asymptotically free at large energies, according to the renormalization group equations. On the other hand, the coupling constant becomes large in the low-energy region, where the perturbative calculations break down. In this non-perturbative region, due to the color confinement, the fundamental degrees of freedom are no longer the quarks and gluons.

As opposed to the charge-neutral photons, which are the gauge fields of quantum electrodynamics (QED), the gluons, which are the gauge fields of QCD, can interact with each other because they carry color charge. The self-coupling of gluons in QCD allows the prediction of hadronic systems that differ from the classical quark model states $\bar{q}q$ and qqq . There are exotic possibilities to construct color singlets, such as glueballs, which would correspond to bound states of gluons (gg or ggg), hybrids, which are states made up of quarks with a strong gluon component ($q\bar{q}g$) or states with exotic flavor content like tetraquarks ($qq\bar{q}\bar{q}$) for mesons or pentaquarks ($qqq\bar{q}q$) for baryons. The additional degrees of freedom carried by gluons allow all exotic states to have spin-exotic quantum numbers, J^{PC} , that are forbidden for $q\bar{q}$ mesons and other fermion-antifermion systems. J , P and C stand for the total angular momentum, parity, and charge conjugation, respectively. States with exotic quantum numbers provide a good opportunity to identify gluonic hadrons. Moreover, there is another class of nonconventional hadrons, which have ordinary quantum numbers but lie at a too low energy to fit in the simplistic quark constituent model. These states can be identified and separated from conventional hadrons if we have a reasonably complete description of the background of ordinary hadrons. The identification of any anomalous state will be identified by an overpopulation of states in a given energy range.

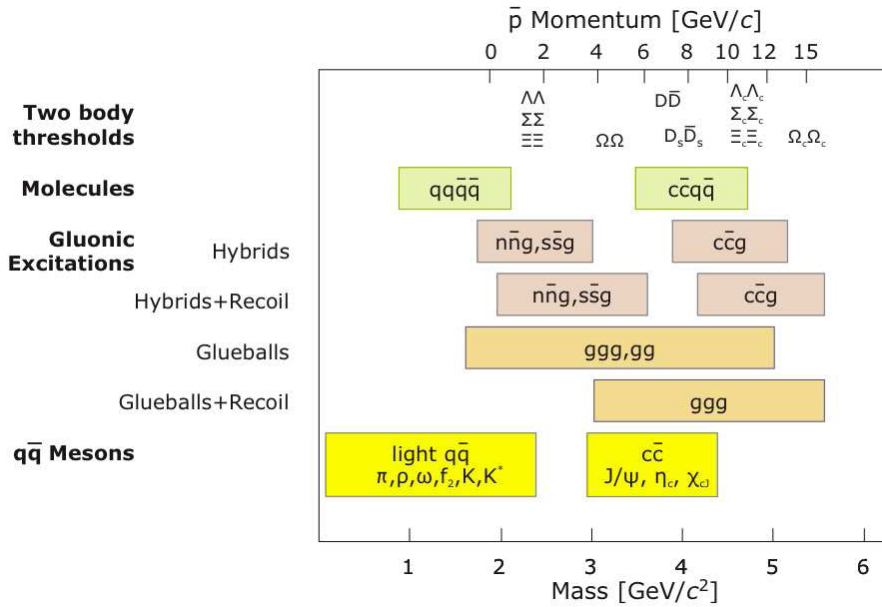


Figure 1.1: An overview of the various quark and gluon configurations of hadrons and their corresponding mass range. The \bar{P} ANDA experiment uses antiproton beams in the momentum range of 1.5 - 15 GeV/c, corresponding to a mass range of 2.2 - 5.5 GeV/c² in antiproton-proton collisions, thereby having access to glueballs, charmed hybrids, and charm-rich four-quark states.

1.2 Reaction mechanism

\bar{P} ANDA will be in an unique position to study the structure of non-perturbative QCD. The interactions of high-intensity, phase-space cooled antiproton beams, of momenta in the range of 1.5 - 15 GeV/c, with a fixed proton target are an excellent tool to access both the states with exotic and non-exotic quantum numbers. Figure 1.1 from [3] shows an overview of the various quark and gluon configurations of hadrons and their corresponding mass range. These predictions have been obtained with *ab initio* calculations from Lattice QCD [8]. Moreover, recent findings from running experiments at B-factories (see e.g. [9]) show the existence of unexpected narrow states unaccounted for in the naive quark models. A typical example of such a state is the threshold en-

hancement observed by the BES collaboration [10] in the invariant mass spectrum of the $J/\psi \rightarrow \gamma p\bar{p}$ with assigned quantum numbers $J^{PC} = 0^{-+}$, and a mass and width of $M = 1859$ MeV and $\Gamma < 30$ MeV, respectively, given by a Breit-Wigner fit. Later, another signal was observed in the $J/\psi \rightarrow \gamma X(1835) \rightarrow \gamma \eta' \pi^+ \pi^-$ channel. The mass and width of either the threshold enhancement or the X(1835) does not match any known particle around this mass range. There have been many speculations of the underlying structure of the X(1835) in the literature [11–14]. Proposed theoretical schemes include the t-channel pion exchange, some kind of threshold kinematical effects, a new resonance below threshold, even a $p\bar{p}$ bound state, etc. However, there is no strong experimental evidence that the $p\bar{p}$ threshold enhancement and X(1835) have the same underlying structure. Very probably they are two different states even if the enhancement arises from a sub-threshold resonance. For example, the mass, total decay width, production rate and decay pattern of X(1835) are consistent with its assignment as the second radial excitation of the η' meson [15].

This sort of examples stress the need for experiments focussed on the abundant production and systematic studies of these states, that should, preferably, be performed using hadronic probes due to the large expected cross sections. Results of high precision are a decisive element to be able to identify and extract features of these exotic states. Hadron beams are advantageous also for the production of hadrons with non-exotic quantum numbers, as these can be formed directly with high cross sections.

In order to be able to access physics of resonances and to be able to disentangle gluonic states from resonances, we have to first improve our understanding of the reaction mechanism. In view of the difficulties presented by QCD, many approaches that study hadronic interactions are based on effective theories. The idea is to use the symmetries of the QCD Lagrangian to construct Lagrangians for the interaction of hadrons instead of quarks. One of the most successful theories in this direction is chiral perturbation theory [16], that makes use of the approximate chiral symmetry of QCD. In this approach, the mesons and baryons are the effective degrees of freedom of the theory. If the interaction between two hadrons is attractive and strong enough, it could bind these two particles in a new state, or generate resonances. This picture is called the molecular picture and it differs from the tetraquark or pentaquark pic-

ture, since the quarks in the molecular picture case are correlated inside two different hadrons. The molecular states that appear within this method are usually called dynamically generated resonances, since they appear from the dynamical interaction of the particles included explicitly as building blocks of the framework.

1.3 Analytic properties of the scattering matrix

So far, there are several established approaches to describe the properties of the hadronic resonances [17–19], that start from the analytic properties of the most general scattering amplitude like unitarity, covariance, analyticity and crossing symmetry. Unitarity, derived from the principle of conservation of probability, is expressed as

$$S^\dagger S = S S^\dagger = \mathbb{1} , \quad (1.1)$$

where S is the scattering matrix operator. The relation between the scattering matrix operator S , the scattering amplitude T and the phases-space density ρ is given as

$$S = \mathbb{1} + 2i\sqrt{\rho} T \sqrt{\rho} . \quad (1.2)$$

Unitarity in coupled channels for the imaginary part of $T_{ab}^{(JP)}$ reads

$$\begin{aligned} \Im T_{ab}^{(JP)}(\sqrt{s}) &= \frac{1}{2i} [T(\sqrt{s} + i\epsilon) - T(\sqrt{s} - i\epsilon)] \\ &= \sum_{c,d} \left[T_{ac}^{(JP)}(\sqrt{s}) \right]^\dagger \rho_{cd}^{(JP)}(\sqrt{s}) T_{db}^{(JP)}(\sqrt{s}) . \end{aligned} \quad (1.3)$$

where $\rho_{cd}^{(JP)}(\sqrt{s})$ is the phases-space matrix and the subscripts a, b, c and d refer to the physical states. Using partial-wave amplitudes simplifies the computation of the scattering amplitude due to the conservation of angular momentum J and parity P . An alternative formulation of unitarity follows immediately,

$$\Im [T^{JP}(\sqrt{s})]_{ab}^{-1} = -\rho_{ab}^{JP}(\sqrt{s}) . \quad (1.4)$$

From a theoretical point of view, analyticity is strongly related to the causality condition, which requires the outgoing wave not to be present until the incoming signal has arrived. A great stride was taken when a direct connection was found

between analyticity and general properties of field operators like asymptotic relations and local commutativity [20–22]. A scattering matrix that depends only on covariant combinations of momenta is called covariant. Such invariant combinations of the momenta are the Mandelstam variables s , t and u . Given the scattering process of $a b \rightarrow c d$, as given in Figure 1.2, Mandelstam variables are defined as

$$\begin{aligned} s &= (p_1 + p_2)^2 = (p_3 + p_4)^2; \\ t &= (p_1 - p_3)^2 = (p_2 - p_4)^2; \\ u &= (p_1 - p_4)^2 = (p_2 - p_3)^2. \end{aligned} \quad (1.5)$$

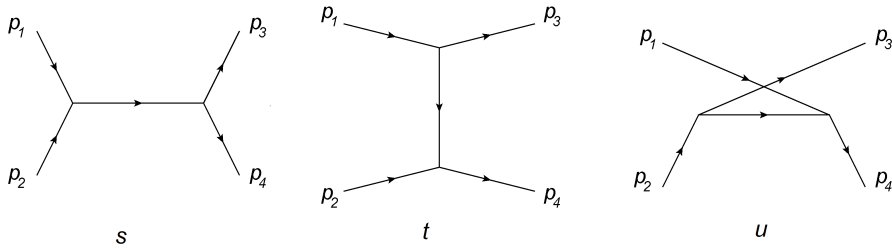


Figure 1.2: s -, t - and u -channel type diagrams.

A scattering matrix that is expressed by the same analytic function independent of the permutation of initial and final particles is called crossing symmetric. An important consequence of crossing symmetry is that the different kinematical variables can take the roles of both energy and momentum transfer depending on the channel that is considered. This information can only be used if some analytic procedure allows one to continue the amplitude from one physical region to the other. The dispersion-integral representation proposed by Mandelstam [23] for the scattering amplitude is a way to obtain amplitudes that satisfy the requirements imposed by unitarity and by crossing symmetry. There are two kinds of dispersion integrals: causal and acausal. Causal dispersion relations are related to positive decay widths.

The two-body scattering amplitude in the complex energy plane has several cuts or discontinuities. The unitarity relation together with the Schwarz reflection principle implies that the scattering amplitude must have a branch-cut on the real axis for

energies larger than the two-particle threshold. The cut comes from the existence of an imaginary part of the T -matrix in the region where the s -channel process becomes on-the-mass-shell. This discontinuity is called the left-hand cut or physical cut. Similarly, the T -matrix amplitude also has an imaginary part in the region where the u - and t -channel processes become on-the-mass-shell, which leads to the unphysical cut. Additionally, the s -, t - and u - exchange diagrams given in Figure 1.2 give rise to a simple pole in the complex energy plane and t - and u -channel cuts, respectively, produced by the propagating particle becoming on-the-mass-shell.

This work investigates different methods of building a scattering matrix obeying the constraints from unitarity, analyticity and crossing symmetry. This thesis is organized as follows. In chapter 2, the analytical structure of partial-wave amplitudes describing spin-1/2 and spin-3/2 fermion-antifermion scattering is investigated. Even though it is straightforward to calculate partial-wave amplitudes expressed in the helicity formalism of Jacob and Wick [24], they will have either poles or be correlated at certain energies, even if the S -matrix elements themselves are regular at the corresponding points. These singularities are in a sense spurious, reflecting only the nature of the decomposition; such singularities have been called kinematical singularities. The kinematical constraints in the helicity partial-wave amplitudes are eliminated by means of nonunitary transformation matrices that map the initial and final helicity states to new covariant states. Kinematically unconstrained amplitudes are useful for partial-wave analysis or effective field theory approaches which consider the consequences of micro causality in terms of partial-wave dispersion-integral representations [25–28]. A related approach based on the study of the spin structure of the spin-1/2 baryon and spinless meson production amplitudes in photo and hadronic reactions has been presented in [29, 30]. In chapter 3 we cover the theoretical framework upon which the effective field theories are built. We discuss the symmetries of QCD and construct an effective Lagrangian with the pseudoscalar Goldstone bosons, vector mesons, octet baryons, and decuplet baryons as effective degrees of freedom. Subsequently, for the scattering of spin-1/2 fermions, the covariant amplitudes describing the t -channel exchange of a pseudoscalar meson and a vector meson are built. In chapter 4, the resulting potential is used as the driving interaction for a coupled-channel calculation of scattering amplitudes. The dynam-

ics of the process in a coupled-channel scattering problem may generate resonances. These resonances can be thought of as the result of real-valued self energies generated by loop contributions to the amplitude. For the energy of the resonances the real contributions from the loop integrals are essential. As the imaginary contributions of the loop integrals contribute to the inelasticities it can be seen that it is important to require that the real and imaginary parts of the scattering matrix are consistent.

1.4 Approaches to construct a scattering matrix

The most straightforward method for building unitary scattering amplitudes is the K -matrix approach [31, 32]. In this approach a unitarity-violating tree level amplitude is iterated in such a way that the final amplitude is unitary, whereas the original amplitude is recovered in an expansion at low energies [33]. The K -matrix approach is a simplification of the unitarization via the Bethe-Salpeter equation [34]. By taking into account only on-shell intermediate states and ignoring the real parts of the loop functions, the solution of the Bethe-Salpeter equation is reduced to an algebraic equation. The K -matrix is related to the scattering matrix S by

$$S = \mathbb{1} + 2i \frac{K}{\mathbb{1} - iK}, \quad (1.6)$$

where S and K are matrices in channel space at a fixed total angular momentum J and parity P and a fixed invariant mass \sqrt{s} . It can easily be seen that the scattering matrix is unitary when the kernel K is Hermitian [35].

The matrix elements of the kernel can be expressed as

$$K_{ij} = \sqrt{\rho_i \rho_j} U_{ij} \quad (1.7)$$

where the phase-space factor ρ_i is *identically zero* below the threshold μ_i of channel i and the physics of the problem is reflected in the choice of the matrix elements U_{ij} . The K -matrix has been used with much success in many phenomenological applications, see e.g. [36], where usually the kernel K is taken as the sum of tree-level diagrams including resonance contributions. The main problem is that the amplitude is not an analytic function of energy and as a consequence does not obey a dispersion

relation, thus violating causality. The reason for this lies in the definition of the phase-space factor which vanishes below the threshold of a particular reaction channel. This means that in the K -matrix only physical states are included in the model space at a particular energy. Since the model space thus changes abruptly when the energy crosses a reaction threshold, it is no surprise that the calculated scattering amplitude is not an analytic function of energy. This can be repaired by taking an analytic continuation of the amplitude in the complex energy plane.

Another method for constructing a unitary and analytic scattering amplitude is the N/D approach [37, 38]. The N/D method allows one to obtain a general solution of the unitarity relation making use of the left-hand discontinuities of the amplitude $T_{ab}^{J\pm}(\sqrt{s})$. It linearizes the nonlinear integral equation derived from unitarity and the partial-wave dispersion relation with a finite number of subtractions. In this case, unitarity is implemented via the right-hand, physical cut. Expressing the amplitude in a dispersion relation, the unitary amplitude is obtained by matching the amplitude to the chiral perturbative results at a matching scale. This unitary method provides automatically the basic analytic properties of the scattering amplitude.

We will show that partial-wave amplitudes that are free of kinematical constraints can be readily used for the implementation of the N/D , avoiding any additional relations that try to correct for the constraints that relate the amplitudes at the kinematical points. This approach will lead to the calculation of covariant partial-wave amplitudes that obey unitarity, analyticity and are not correlated at the thresholds or pseudothresholds.

KINEMATICAL CONSTRAINTS IN FERMION-ANTIFERMION SYSTEMS¹

2.1 Introduction

This chapter addresses an important aspect arising in the study of fermion-antifermion annihilation. Though it is straightforward to introduce partial-wave scattering amplitudes in the helicity formalism of Jacob and Wick [24], it is a nontrivial task to derive transformations that lead to amplitudes that are kinematically unconstrained. Much work has gone in the derivation of kinematically unconstrained amplitudes for spin-1/2 scattering, see for example Ref. [39]. Such amplitudes have so far not been established for systems involving spin-1/2 and spin-3/2 fermions. Kinematically unconstrained amplitudes are useful for partial-wave analysis or effective field theory approaches which consider the consequences of micro causality in terms of partial-wave dispersion-integral representations [25–28]. It is the purpose of the present work to derive such amplitudes by suitable transformations of the helicity partial-wave scattering amplitudes. Our results will be relevant for the PANDA experiment at FAIR, where protons and antiprotons may be annihilated into systems of spin-3/2 states.

The technique applied in this work has been used previously in studies of two-body scattering systems with photons, pions and nucleons [25, 39–47]. More recent work addressed the scattering of pseudoscalar off vector particles [48].

¹This chapter follows closely: S. Stoica, M.F.M. Lutz, O. Scholten, "On kinematical constraints in fermion-antifermion systems", published in Phys. Rev. D84 (2011) 125001 .

In an initial step we decompose the scattering amplitude into invariant functions. For on-shell kinematics such a decomposition is not unique for systems involving particles with nonzero spin. The task is to find a basis of invariant functions that are free of kinematical constraints. Such amplitudes are expected to satisfy a Mandelstam dispersion-integral representation [23, 40]. At this point we distinguish kinematical from dynamical singularities. Kinematical singularities are dependent on the particularities of the used basis and typically occur at thresholds or pseudo-thresholds. Dynamical singularities are related to interesting physics such as resonances.

In a second step we consider partial-wave projections of the scattering amplitude. Our goal is to establish partial-wave amplitudes with convenient analytic properties that justify the use of uncorrelated dispersion-integral relations. In particular we want to avoid cumbersome constraints relating different partial-wave amplitudes. Our starting point are the helicity partial-wave amplitudes. It is well known that different helicity partial-wave amplitudes are correlated at various kinematical conditions. This is readily seen if the helicity partial-wave amplitudes are expressed in terms of a basis of invariant functions. The kinematical constraints in the helicity partial-wave amplitudes are eliminated by means of nonunitary transformation matrices that map the initial, respectively final helicity states to new covariant states. Since the mapping procedure is based on the exclusive use of on-shell matrix elements there is no model-dependent off-shell dependence in our considerations.

The work is organized as follows. Section 2.2 introduces the conventions used for the kinematics and the spin-1/2 and spin-3/2 helicity wave functions. It follows a section where the scattering amplitudes are decomposed into sets of invariant amplitudes. We consider all two-body reactions possible with spin-1/2 and spin-3/2 fermions. In section 2.4 the helicity partial-wave amplitudes are constructed within the given convention. The central results are presented in section 2.5, where the transformation to partial-wave amplitudes free of kinematical constraints are derived and discussed.

2.2 Wave functions and conventions

We introduce the 4-momenta p_1 and \bar{p}_1 of the incoming and outgoing particles and those of the anti-particles, p_2 and \bar{p}_2 . In the center of mass frame we write

$$\begin{aligned} p_1^\mu &= (E_1, 0, 0, +p) , & \bar{p}_1^\mu &= (\bar{E}_1, +\bar{p} \sin \theta, 0, +\bar{p} \cos \theta) , \\ E_1 &= \sqrt{M_1^2 + p^2} , & \bar{E}_1 &= \sqrt{\bar{M}_1^2 + \bar{p}^2} , \\ p_2^\mu &= (E_2, 0, 0, -p) , & \bar{p}_2^\mu &= (\bar{E}_2, -\bar{p} \sin \theta, 0, -\bar{p} \cos \theta) , \\ E_2 &= \sqrt{M_2^2 + p^2} , & \bar{E}_2 &= \sqrt{\bar{M}_2^2 + \bar{p}^2} , \end{aligned} \quad (2.1)$$

where θ is the scattering angle, p and \bar{p} are the magnitudes of the initial and final three-momenta. The relative momenta can be expressed in terms of the total energy \sqrt{s} of the system

$$w^\mu = p_1^\mu + p_2^\mu = \bar{p}_1^\mu + \bar{p}_2^\mu , \quad s = w^2 . \quad (2.2)$$

It holds

$$\begin{aligned} p^2 &= \frac{(s - (M_1 + M_2)^2)(s - (M_1 - M_2)^2)}{4s} \\ \bar{p}^2 &= \frac{(s - (\bar{M}_1 + \bar{M}_2)^2)(s - (\bar{M}_1 - \bar{M}_2)^2)}{4s} . \end{aligned} \quad (2.3)$$

We continue with the specification of helicity eigenstates. This is an important part of the documentation since there are various distinct phase conventions being used in the literature. For the spin-1/2 fermions the Dirac spinors for the outgoing states are

$$\begin{aligned} u(\bar{p}_1, \pm \tfrac{1}{2}) &= \begin{pmatrix} \sqrt{\frac{\bar{E}_1 + \bar{M}_1}{2\bar{M}_1}} e^{-\frac{i}{2} \sigma_y \theta} \chi_\pm \\ \pm \sqrt{\frac{\bar{E}_1 - \bar{M}_1}{2\bar{M}_1}} e^{-\frac{i}{2} \sigma_y \theta} \chi_\pm \end{pmatrix} , \\ u(\bar{p}_2, \pm \tfrac{1}{2}) &= \begin{pmatrix} \sqrt{\frac{\bar{E}_2 + \bar{M}_2}{2\bar{M}_2}} e^{-\frac{i}{2} \sigma_y \theta} \chi_\mp \\ \pm \sqrt{\frac{\bar{E}_2 - \bar{M}_2}{2\bar{M}_2}} e^{-\frac{i}{2} \sigma_y \theta} \chi_\mp \end{pmatrix} , \\ \chi_+ &= \begin{pmatrix} 1 \\ 0 \end{pmatrix} , & \chi_- &= \begin{pmatrix} 0 \\ 1 \end{pmatrix} . \end{aligned} \quad (2.4)$$

The spinors of the incoming states are recovered by setting $\theta = 0$ and removing the bars in (2.4). It holds the completeness relation

$$\sum_{\lambda=\pm\frac{1}{2}} u(p, \lambda) \bar{u}(p, \lambda) = \frac{\not{p} + M}{2M}. \quad (2.5)$$

We specify the helicity states for a spin-3/2 particle [49]. Most conveniently they are expressed in terms of spin-1/2 and spin-1 wave functions

$$\begin{aligned} u^\mu(\bar{p}_1, \pm\frac{3}{2}) &= \epsilon^\mu(\bar{p}_1, \pm 1) u(\bar{p}_1, \pm\frac{1}{2}), \\ u^\mu(\bar{p}_1, \pm\frac{1}{2}) &= \sqrt{\frac{2}{3}} \epsilon^\mu(\bar{p}_1, 0) u(\bar{p}_1, \pm\frac{1}{2}) + \sqrt{\frac{1}{3}} \epsilon^\mu(\bar{p}_1, \pm 1) u(\bar{p}_1, \mp\frac{1}{2}), \\ \epsilon^\mu(\bar{p}_1, \pm 1) &= \begin{pmatrix} 0 \\ \frac{\pm \cos \theta}{\sqrt{2}} \\ \frac{-i}{\sqrt{2}} \\ \frac{\pm \sin \theta}{\sqrt{2}} \end{pmatrix}, \quad \epsilon^\mu(\bar{p}_1, 0) = \begin{pmatrix} \frac{\bar{p}}{M_1} \\ \frac{\bar{E}_1}{M_1} \sin \theta \\ 0 \\ \frac{\bar{E}_1}{M_1} \cos \theta \end{pmatrix}, \end{aligned} \quad (2.6)$$

and

$$\begin{aligned} u^\mu(\bar{p}_2, \pm\frac{3}{2}) &= \epsilon^\mu(\bar{p}_2, \pm 1) u(\bar{p}_2, \pm\frac{1}{2}) \\ u^\mu(\bar{p}_2, \pm\frac{1}{2}) &= \sqrt{\frac{2}{3}} \epsilon^\mu(\bar{p}_2, 0) u(\bar{p}_2, \pm\frac{1}{2}) - \sqrt{\frac{1}{3}} \epsilon^\mu(\bar{p}_2, \pm 1) u(\bar{p}_2, \mp\frac{1}{2}), \\ \epsilon^\mu(\bar{p}_2, \pm 1) &= \begin{pmatrix} 0 \\ \frac{\pm \cos \theta}{\sqrt{2}} \\ \frac{-i}{\sqrt{2}} \\ \frac{\mp \sin \theta}{\sqrt{2}} \end{pmatrix}, \quad \epsilon^\mu(\bar{p}_2, 0) = \begin{pmatrix} \frac{\bar{p}}{M_2} \\ -\frac{\bar{E}_2}{M_2} \sin \theta \\ 0 \\ -\frac{\bar{E}_2}{M_2} \cos \theta \end{pmatrix}. \end{aligned} \quad (2.7)$$

Again the spinor of the corresponding initial states is recovered with $\theta = 0$ and by removing the bars in (2.6, 2.7). The main properties of the spinors are recalled by

$$\begin{aligned} \sum_{\lambda=\pm\frac{3}{2}, \pm\frac{1}{2}} u^\mu(p, \lambda) \bar{u}^\nu(p, \lambda) &= \frac{(\not{p} + M)}{2M} \left[-g^{\mu\nu} + \frac{1}{3} \gamma^\mu \gamma^\nu \right. \\ &\quad \left. + \frac{2}{3M^2} p^\mu p^\nu - \frac{1}{3M} (p^\mu \gamma^\nu - p^\nu \gamma^\mu) \right], \\ \gamma^\mu u_\mu(p, \lambda) &= 0, \quad p^\mu u_\mu(p, \lambda) = 0. \end{aligned} \quad (2.8)$$

It remains to detail the phase convention of the anti-particles spinors. We use

$$\begin{aligned}\bar{v}(p_1, \lambda) &= u^t(p_1, \lambda) C, & v(\bar{p}_1, \lambda) &= C^{-1} \bar{u}^t(\bar{p}_1, \lambda), \\ \bar{v}(p_2, \lambda) &= u^t(p_2, \lambda) C, & v(\bar{p}_2, \lambda) &= C^{-1} \bar{u}^t(\bar{p}_2, \lambda),\end{aligned}\tag{2.9}$$

$$\begin{aligned}\bar{v}_\mu(p_1, \lambda) &= u_\mu^t(p_1, \lambda) C, & v_\mu(\bar{p}_1, \lambda) &= C^{-1} \bar{u}_\mu^t(\bar{p}_1, \lambda), \\ \bar{v}_\mu(p_2, \lambda) &= u_\mu^t(p_2, \lambda) C, & v_\mu(\bar{p}_2, \lambda) &= C^{-1} \bar{u}_\mu^t(\bar{p}_2, \lambda),\end{aligned}$$

where $C = i \gamma_2 \gamma_0$ is the charge-conjugation matrix and λ is the helicity of the spinor.

It follows

$$\begin{aligned}v(\bar{p}_2, \pm \tfrac{1}{2}) &= \begin{pmatrix} \mp \sqrt{\frac{\bar{E}_2 - \bar{M}_2}{2\bar{M}_2}} i \sigma_y e^{-\frac{i}{2} \sigma_y \theta} \chi_\mp \\ \sqrt{\frac{\bar{E}_2 + \bar{M}_2}{2\bar{M}_2}} i \sigma_y e^{-\frac{i}{2} \sigma_y \theta} \chi_\mp \end{pmatrix}, \\ v_\mu(\bar{p}_2, \pm \tfrac{3}{2}) &= \epsilon_\mu^*(\bar{p}_2, \pm 1) v(\bar{p}_2, \pm \tfrac{1}{2}) \\ v_\mu(\bar{p}_2, \pm \tfrac{1}{2}) &= \sqrt{\tfrac{2}{3}} \epsilon_\mu^*(\bar{p}_2, 0) v(\bar{p}_2, \pm \tfrac{1}{2}) - \sqrt{\tfrac{1}{3}} \epsilon_\mu^*(\bar{p}_2, \pm 1) v(\bar{p}_2, \mp \tfrac{1}{2}).\end{aligned}\tag{2.10}$$

2.3 Invariant amplitudes

We decompose the scattering amplitudes into sets of invariant functions. For this purpose it is convenient to introduce some further notation

$$k = \tfrac{1}{2} (p_1 - p_2), \quad \bar{k} = \tfrac{1}{2} (\bar{p}_1 - \bar{p}_2).\tag{2.11}$$

We will consider first the scattering of spin-1/2 particles. It is described by the on-shell scattering amplitude

$$\begin{aligned}T_{\frac{1}{2} \frac{1}{2} \rightarrow \frac{1}{2} \frac{1}{2}} &= \sum_{i=1}^4 \sum_{\pm} F_i^\pm \langle T_\pm^{(i)} \rangle_{\frac{1}{2} \frac{1}{2} \rightarrow \frac{1}{2} \frac{1}{2}} \\ &= \sum_{i=1}^4 \sum_{\pm} F_i^\pm \langle T^{(i)} \rangle_{\frac{1}{2} \frac{1}{2} \rightarrow \frac{1}{2} \frac{1}{2}}^\pm, \\ T^{(1)} &= \mathbb{1} \times \mathbb{1}, & T^{(2)} &= \gamma_\mu \times \gamma^\mu, \\ T^{(3)} &= \mathbb{1} \times \bar{k}, & T^{(4)} &= \not{k} \times \mathbb{1},\end{aligned}\tag{2.12}$$

in terms of eight scalar functions F_i^\pm . The on-shell particle and antiparticle spinors are implied by the $\langle \dots \rangle$ and $\langle \dots \rangle^\pm$ notations used in (2.12),

$$\begin{aligned} \langle \bar{\Gamma} \times \Gamma \rangle_{\frac{1}{2} \frac{1}{2} \rightarrow \frac{1}{2} \frac{1}{2}}^\pm &= \langle \bar{\Gamma} P_\pm \otimes P_\pm \Gamma \rangle_{\frac{1}{2} \frac{1}{2} \rightarrow \frac{1}{2} \frac{1}{2}}^\pm = \\ &= \left(\bar{u}(\bar{p}_1) \bar{\Gamma} P_\pm v(\bar{p}_2) \right) \left(\bar{v}(p_2) P_\pm \Gamma u(p_1) \right), \\ P_+ &= \mathbb{1}, \quad P_- = \gamma_5, \end{aligned} \quad (2.13)$$

where for notational clarity the reference to the helicities of initial and final states is not made explicit.

The number of invariant amplitudes needed is determined by the number of helicity amplitudes. Since we are assuming parity conservation the total number of independent helicity amplitudes is

$$\frac{1}{2} (2 S_1 + 1) (2 S_2 + 1) (2 \bar{S}_1 + 1) (2 \bar{S}_2 + 1), \quad (2.14)$$

where S_1, S_2 and \bar{S}_1, \bar{S}_2 are the spins of the initial and final particles.

We assure that our decomposition (2.12) and the ones presented below imply that the invariant amplitudes F_i^\pm satisfy a Mandelstam dispersion-integral representation free of kinematical constraints. They are functions of the Mandelstam variables s, t and u .

The particular choice of tensors in (2.12) is not unique. The scattering amplitude considered at off-shell kinematics requires a more general decomposition. For instance the structure $\not{p} \gamma_5 \otimes \gamma_5$, which is not considered in (2.12), is on-the-mass-shell equivalent to $(\bar{M}_1 + \bar{M}_2) \gamma_5 \otimes \gamma_5$.

Our bases are characterized by this property: if any structure that is not part of a basis, is decomposed into the basis set, no kinematical singularities arise in the on-shell limit. The identification of such basis sets is a nontrivial task getting more and more tedious as the spin of the involved particles increase. A good starting point are tensors which involve minimal powers of momenta.

We continue with the reactions involving a single spin-3/2 particle only. There are four cases to be considered. A decomposition analogous to (2.12) is established. While (2.12) involves eight scalar functions F_{1-4}^\pm the replacement of a spin-1/2 by a spin-3/2 particle leads to 16 scalar functions. For notational convenience the invariant

amplitudes are denoted with F_{1-8}^\pm , even though this implies a conflict of notation for some amplitudes. Given the local context a misinterpretation is excluded. We consider first the two spin-3/2 production amplitudes

$$T_{\frac{1}{2}\frac{1}{2} \rightarrow \frac{3}{2}\frac{1}{2}} = \sum_{i=1}^8 \sum_{\pm} F_i^\pm \langle T_\mu^{(i)} \rangle_{\frac{1}{2}\frac{1}{2} \rightarrow \frac{3}{2}\frac{1}{2}}^{\pm, \mu}, \quad (2.15)$$

$$\langle \bar{\Gamma} \times \Gamma \rangle_{\frac{1}{2}\frac{1}{2} \rightarrow \frac{3}{2}\frac{1}{2}}^{\pm, \mu} = \left(\bar{u}^\mu(\bar{p}_1) \bar{\Gamma} P_\mp v(\bar{p}_2) \right) \left(\bar{v}(p_2) P_\pm \Gamma u(p_1) \right),$$

$$T_{\frac{1}{2}\frac{1}{2} \rightarrow \frac{1}{2}\frac{3}{2}} = \sum_{i=1}^4 \sum_{\pm} F_i^\pm \langle T_\mu^{(i)} \rangle_{\frac{1}{2}\frac{1}{2} \rightarrow \frac{1}{2}\frac{3}{2}}^{\pm, \mu}, \quad (2.16)$$

$$\langle \bar{\Gamma} \times \Gamma \rangle_{\frac{1}{2}\frac{1}{2} \rightarrow \frac{1}{2}\frac{3}{2}}^{\pm, \mu} = \left(\bar{u}(\bar{p}_1) \bar{\Gamma} P_\mp v^\mu(\bar{p}_2) \right) \left(\bar{v}(p_2) P_\pm \Gamma u(p_1) \right),$$

$$\begin{aligned} T_\mu^{(1)} &= 1 \times \gamma_\mu, & T_\mu^{(2)} &= \not{k} \times \gamma_\mu, \\ T_\mu^{(3)} &= k_\mu \times 1, & T_\mu^{(4)} &= w_\mu \gamma^\tau \times \gamma_\tau, \\ T_\mu^{(5)} &= w_\mu \times 1, & T_\mu^{(6)} &= w_\mu \times \not{k}, \\ T_\mu^{(7)} &= w_\mu \not{k} \times 1, & T_\mu^{(8)} &= k_\mu \not{k} \times 1. \end{aligned}$$

For the inverse reactions we use a convention generated unambiguously by the tensor choice in (2.15, 2.16), where any tensor T_μ is replaced by a corresponding tensor \bar{T}_μ generated using the following rule

$$T_\mu^{(i)} = \bar{\Gamma} \times \Gamma \rightarrow \bar{T}_\mu^{(i)} = \gamma_0 \Gamma^\dagger \gamma_0 \times \gamma_0 \bar{\Gamma}^\dagger \gamma_0 \Big|_{k \leftrightarrow \bar{k}}. \quad (2.17)$$

The decomposition of the inverse reactions is formally analogous to (2.15, 2.16) where the role of the tensors T_μ is taken over by \bar{T}_μ . The bracket notation is extended naturally with

$$\begin{aligned} \langle \bar{\Gamma} \times \Gamma \rangle_{\frac{3}{2}\frac{1}{2} \rightarrow \frac{1}{2}\frac{1}{2}}^{\pm, \mu} &= \left(\bar{u}(\bar{p}_1) \bar{\Gamma} P_\pm v(\bar{p}_2) \right) \left(\bar{v}(p_2) P_\mp \Gamma u^\mu(p_1) \right), \\ \langle \bar{\Gamma} \times \Gamma \rangle_{\frac{1}{2}\frac{3}{2} \rightarrow \frac{1}{2}\frac{1}{2}}^{\pm, \mu} &= \left(\bar{u}(\bar{p}_1) \bar{\Gamma} P_\pm v(\bar{p}_2) \right) \left(\bar{v}^\mu(p_2) P_\mp \Gamma u(p_1) \right). \end{aligned}$$

We proceed with reactions involving two spin-3/2 particles. There are six different cases to be studied. It suffices to detail two reactions, the remaining ones are implied unambiguously within our notations and conventions. The first four cases

are introduced by

$$T_{\frac{3}{2} \frac{1}{2} \rightarrow \frac{3}{2} \frac{1}{2}} = \sum_{i=1}^{16} \sum_{\pm} F_i^{\pm} \langle T_{\bar{\mu}\mu}^{(i)} \rangle_{\frac{3}{2} \frac{1}{2} \rightarrow \frac{3}{2} \frac{1}{2}}^{\pm, \bar{\mu}\mu}, \quad (2.18)$$

$$\langle \bar{\Gamma} \times \Gamma \rangle_{\frac{3}{2} \frac{1}{2} \rightarrow \frac{3}{2} \frac{1}{2}}^{\pm, \bar{\mu}\mu} = \left(\bar{u}^{\bar{\mu}}(\bar{p}_1) \bar{\Gamma} P_{\mp} v(\bar{p}_2) \right) \left(\bar{v}(p_2) P_{\mp} \Gamma u^{\mu}(p_1) \right),$$

with the tensors $T_{\bar{\mu}\mu}^{(i)}$ defined below:

$$\begin{aligned} T_{\bar{\mu}\mu}^{(1)} &= g_{\bar{\mu}\mu} \mathbb{1} \times \mathbb{1}, & T_{\bar{\mu}\mu}^{(2)} &= \gamma_{\mu} \times \gamma_{\bar{\mu}} \\ T_{\bar{\mu}\mu}^{(3)} &= w_{\mu} \times \gamma_{\bar{\mu}}, & T_{\bar{\mu}\mu}^{(4)} &= \gamma_{\mu} \times w_{\bar{\mu}}, \\ T_{\bar{\mu}\mu}^{(5)} &= \bar{k}_{\mu} \times \gamma_{\bar{\mu}}, & T_{\bar{\mu}\mu}^{(6)} &= \gamma_{\mu} \times k_{\bar{\mu}}, \\ T_{\bar{\mu}\mu}^{(7)} &= w_{\mu} \times w_{\bar{\mu}}, & T_{\bar{\mu}\mu}^{(8)} &= w_{\mu} \gamma_{\tau} \times \gamma^{\tau} w_{\bar{\mu}}, \\ T_{\bar{\mu}\mu}^{(9)} &= w_{\mu} \times k_{\bar{\mu}}, & T_{\bar{\mu}\mu}^{(10)} &= w_{\mu} \gamma_{\tau} \times \gamma^{\tau} k_{\bar{\mu}}, \\ T_{\bar{\mu}\mu}^{(11)} &= \bar{k}_{\mu} \times w_{\bar{\mu}}, & T_{\bar{\mu}\mu}^{(12)} &= \bar{k}_{\mu} \gamma_{\tau} \times \gamma^{\tau} w_{\bar{\mu}}, \\ T_{\bar{\mu}\mu}^{(13)} &= w_{\mu} \not{k} \times w_{\bar{\mu}}, & T_{\bar{\mu}\mu}^{(14)} &= w_{\mu} \times \not{k} w_{\bar{\mu}}, \\ T_{\bar{\mu}\mu}^{(15)} &= w_{\mu} \not{k} \times k_{\bar{\mu}}, & T_{\bar{\mu}\mu}^{(16)} &= \bar{k}_{\mu} \times \not{k} w_{\bar{\mu}}. \end{aligned}$$

Any of the three additional reactions which involve a spin-3/2 particle or antiparticle in the initial and final state is decomposed in terms of the tensors introduced in (2.16, 2.18). The corresponding bracket notation follows from (2.16, 2.18) upon moving the Lorentz indices to the appropriate spinors.

It is left to detail the reactions involving a spin-3/2 particle and antiparticle in either the initial or final state. We write

$$T_{\frac{3}{2} \frac{3}{2} \rightarrow \frac{1}{2} \frac{1}{2}} = \sum_{i=1}^{16} \sum_{\pm} F_i^{\pm} \langle T_{\mu\nu}^{(i)} \rangle_{\frac{3}{2} \frac{3}{2} \rightarrow \frac{1}{2} \frac{1}{2}}^{\pm, \mu\nu}, \quad (2.19)$$

$$\langle \bar{\Gamma} \times \Gamma \rangle_{\frac{3}{2} \frac{3}{2} \rightarrow \frac{1}{2} \frac{1}{2}}^{\pm, \mu\nu} = \left(\bar{u}(\bar{p}_1) \bar{\Gamma} P_{\pm} v(\bar{p}_2) \right) \left(\bar{v}^{\nu}(p_2) P_{\pm} \Gamma u^{\mu}(p_1) \right),$$

with the tensors $T_{\mu\nu}^{(i)}$ defined below:

$$\begin{aligned} T_{\mu\nu}^{(1)} &= g_{\mu\nu} \mathbb{1} \times \mathbb{1}, & T_{\mu\nu}^{(2)} &= g_{\mu\nu} \gamma_{\tau} \times \gamma^{\tau}, \\ T_{\mu\nu}^{(3)} &= g_{\mu\nu} \not{k} \times \mathbb{1}, & T_{\mu\nu}^{(4)} &= g_{\mu\nu} \mathbb{1} \times \not{k}, \end{aligned}$$

$$\begin{aligned}
T_{\mu\nu}^{(5)} &= \gamma_\mu \times w_\nu, & T_{\mu\nu}^{(6)} &= \gamma_\mu \times \bar{k}_\nu, \\
T_{\mu\nu}^{(7)} &= w_\mu \times w_\nu, & T_{\mu\nu}^{(8)} &= w_\mu \gamma_\tau \times \gamma^\tau w_\nu, \\
T_{\mu\nu}^{(9)} &= \bar{k}_\mu \times \bar{k}_\nu, & T_{\mu\nu}^{(10)} &= \bar{k}_\mu \gamma_\tau \times \gamma^\tau \bar{k}_\nu, \\
T_{\mu\nu}^{(11)} &= \bar{k}_\mu \times w_\nu, & T_{\mu\nu}^{(12)} &= w_\mu \gamma_\tau \times \gamma^\tau \bar{k}_\nu, \\
T_{\mu\nu}^{(13)} &= w_\mu \not{k} \times w_\nu, & T_{\mu\nu}^{(14)} &= w_\mu \times \not{k} w_\nu, \\
T_{\mu\nu}^{(15)} &= \bar{k}_\mu \times \not{k} \bar{k}_\nu, & T_{\mu\nu}^{(16)} &= w_\mu \times \not{k} \bar{k}_\nu,
\end{aligned}$$

and refer to (2.17) as a definition of the inverse reaction.

We continue with the reactions involving three spin-3/2 particles. There are four cases to be studied.

$$T_{\frac{3}{2}\frac{1}{2} \rightarrow \frac{3}{2}\frac{3}{2}} = \sum_{i=1}^{32} \sum_{\pm} F_i^{\pm} \langle T_{\bar{\mu}\bar{\nu}\mu}^{(i)} \rangle_{\frac{3}{2}\frac{1}{2} \rightarrow \frac{3}{2}\frac{3}{2}}^{\pm, \bar{\mu}\bar{\nu}\mu}, \quad (2.20)$$

$$\langle \bar{\Gamma} \times \Gamma \rangle_{\frac{3}{2}\frac{1}{2} \rightarrow \frac{3}{2}\frac{3}{2}}^{\pm, \bar{\mu}\bar{\nu}\mu} = \left(\bar{u}^{\bar{\mu}}(\bar{p}_1) \bar{\Gamma} P_{\pm} v^{\bar{\nu}}(\bar{p}_2) \right) \left(\bar{v}(p_2) P_{\pm} \Gamma u^{\mu}(p_1) \right),$$

$$T_{\frac{1}{2}\frac{3}{2} \rightarrow \frac{3}{2}\frac{3}{2}} = \sum_{i=1}^{32} \sum_{\pm} F_i^{\pm} \langle T_{\bar{\mu}\bar{\nu}\mu}^{(i)} \rangle_{\frac{1}{2}\frac{3}{2} \rightarrow \frac{3}{2}\frac{3}{2}}^{\pm, \bar{\mu}\bar{\nu}\mu}, \quad (2.21)$$

$$\langle \bar{\Gamma} \times \Gamma \rangle_{\frac{1}{2}\frac{3}{2} \rightarrow \frac{3}{2}\frac{3}{2}}^{\pm, \bar{\mu}\bar{\nu}\mu} = \left(\bar{u}^{\bar{\mu}}(\bar{p}_1) \bar{\Gamma} P_{\pm} v^{\bar{\nu}}(\bar{p}_2) \right) \left(\bar{v}^{\mu}(p_2) P_{\pm} \Gamma u(p_1) \right),$$

$$\begin{aligned}
T_{\bar{\mu}\bar{\nu}\mu}^{(1)} &= g_{\bar{\mu}\bar{\nu}} \gamma_\mu \times \mathbb{1}, & T_{\bar{\mu}\bar{\nu}\mu}^{(2)} &= g_{\bar{\mu}\mu} \mathbb{1} \times \gamma_{\bar{\nu}}, \\
T_{\bar{\mu}\bar{\nu}\mu}^{(3)} &= g_{\bar{\mu}\bar{\nu}} \mathbb{1} \times w_\mu, & T_{\bar{\mu}\bar{\nu}\mu}^{(4)} &= g_{\bar{\mu}\bar{\nu}} \gamma_\tau \times \gamma^\tau w_\mu, \\
T_{\bar{\mu}\bar{\nu}\mu}^{(5)} &= g_{\bar{\mu}\mu} w_{\bar{\nu}} \times \mathbb{1}, & T_{\bar{\mu}\bar{\nu}\mu}^{(6)} &= w_{\bar{\mu}} \gamma_\mu \times \gamma_{\bar{\nu}}, \\
T_{\bar{\mu}\bar{\nu}\mu}^{(7)} &= g_{\bar{\mu}\bar{\nu}} \mathbb{1} \times \bar{k}_\mu, & T_{\bar{\mu}\bar{\nu}\mu}^{(8)} &= g_{\bar{\mu}\bar{\nu}} \gamma_\mu \times \not{k}, \\
T_{\bar{\mu}\bar{\nu}\mu}^{(9)} &= g_{\bar{\mu}\mu} k_{\bar{\nu}} \times \mathbb{1}, & T_{\bar{\mu}\bar{\nu}\mu}^{(10)} &= g_{\bar{\mu}\mu} \not{k} \times \gamma_{\bar{\nu}}, \\
T_{\bar{\mu}\bar{\nu}\mu}^{(11)} &= g_{\bar{\mu}\bar{\nu}} \not{k} \times w_\mu, & T_{\bar{\mu}\bar{\nu}\mu}^{(12)} &= g_{\bar{\mu}\bar{\nu}} \times \not{k} w_\mu, \\
T_{\bar{\mu}\bar{\nu}\mu}^{(13)} &= w_{\bar{\nu}} \times \gamma_{\bar{\mu}} w_\mu, & T_{\bar{\mu}\bar{\nu}\mu}^{(14)} &= w_{\bar{\mu}} w_{\bar{\nu}} \gamma_\mu \times \mathbb{1}, \\
T_{\bar{\mu}\bar{\nu}\mu}^{(15)} &= g_{\bar{\mu}\bar{\nu}} \mathbb{1} \times \not{k} \bar{k}_\mu, & T_{\bar{\mu}\bar{\nu}\mu}^{(16)} &= k_{\bar{\mu}} \times \gamma_{\bar{\nu}} w_\mu, \\
T_{\bar{\mu}\bar{\nu}\mu}^{(17)} &= g_{\bar{\nu}\mu} w_{\bar{\mu}} \not{k} \times \mathbb{1}, & T_{\bar{\mu}\bar{\nu}\mu}^{(18)} &= w_{\bar{\nu}} \times \gamma_{\bar{\mu}} \bar{k}_\mu, \\
T_{\bar{\mu}\bar{\nu}\mu}^{(19)} &= g_{\bar{\mu}\mu} k_{\bar{\nu}} \not{k} \times \mathbb{1}, & T_{\bar{\mu}\bar{\nu}\mu}^{(20)} &= w_{\bar{\mu}} w_{\bar{\nu}} \times w_\mu, \\
T_{\bar{\mu}\bar{\nu}\mu}^{(21)} &= w_{\bar{\mu}} w_{\bar{\nu}} \gamma_\tau \times \gamma^\tau w_\mu, & T_{\bar{\mu}\bar{\nu}\mu}^{(22)} &= k_{\bar{\mu}} w_{\bar{\nu}} \times w_\mu,
\end{aligned}$$

$$\begin{aligned}
T_{\bar{\mu}\bar{\nu}\mu}^{(23)} &= w_{\bar{\mu}} w_{\bar{\nu}} \times \bar{k}_{\mu}, & T_{\bar{\mu}\bar{\nu}\mu}^{(24)} &= k_{\bar{\mu}} k_{\bar{\nu}} \times w_{\mu}, \\
T_{\bar{\mu}\bar{\nu}\mu}^{(25)} &= k_{\bar{\mu}} k_{\bar{\nu}} \gamma_{\tau} \times \gamma^{\tau} w_{\mu}, & T_{\bar{\mu}\bar{\nu}\mu}^{(26)} &= w_{\bar{\mu}} w_{\bar{\nu}} \gamma_{\mu} \times \bar{k}, \\
T_{\bar{\mu}\bar{\nu}\mu}^{(27)} &= w_{\bar{\mu}} \not{k} \times \gamma_{\bar{\nu}} w_{\mu}, & T_{\bar{\mu}\bar{\nu}\mu}^{(28)} &= w_{\bar{\mu}} w_{\bar{\nu}} \not{k} \times w_{\mu}, \\
T_{\bar{\mu}\bar{\nu}\mu}^{(29)} &= w_{\bar{\mu}} w_{\bar{\nu}} \times \bar{k} w_{\mu}, & T_{\bar{\mu}\bar{\nu}\mu}^{(30)} &= w_{\bar{\mu}} k_{\bar{\nu}} \not{k} \times w_{\mu}, \\
T_{\bar{\mu}\bar{\nu}\mu}^{(31)} &= w_{\bar{\mu}} w_{\bar{\nu}} \times \bar{k} \bar{k}_{\mu}, & T_{\bar{\mu}\bar{\nu}\mu}^{(32)} &= k_{\bar{\mu}} k_{\bar{\nu}} \not{k} \times w_{\mu}.
\end{aligned}$$

We use (2.17) to obtain the tensors for the other two inverse reactions.

The scattering of spin-3/2 -particles is described by the on-shell scattering amplitude

$$\begin{aligned}
T_{\frac{3}{2}\frac{3}{2} \rightarrow \frac{3}{2}\frac{3}{2}} &= \sum_{i=1}^{64} \sum_{\pm} F_i^{\pm} \langle T_{\bar{\mu}\bar{\nu}\mu\nu}^{(i)} \rangle_{\frac{3}{2}\frac{3}{2} \rightarrow \frac{3}{2}\frac{3}{2}}^{\pm, \bar{\mu}\bar{\nu}\mu\nu}, \\
\langle \bar{\Gamma} \times \Gamma \rangle_{\frac{3}{2}\frac{3}{2} \rightarrow \frac{3}{2}\frac{3}{2}}^{\pm, \bar{\mu}\bar{\nu}\mu\nu} &= \left(\bar{u}^{\bar{\mu}}(\bar{p}_1) \bar{\Gamma} P_{\pm} v^{\bar{\nu}}(\bar{p}_2) \right) \left(\bar{v}^{\nu}(p_2) P_{\pm} \Gamma u^{\mu}(p_1) \right),
\end{aligned} \tag{2.22}$$

where the tensors $T_{\bar{\mu}\bar{\nu}\mu\nu}^{(i)}$ are given below:

$$\begin{aligned}
T_{\bar{\mu}\bar{\nu}\mu\nu}^{(1)} &= g_{\bar{\mu}\bar{\nu}} \mathbb{1} \times \mathbb{1} g_{\mu\nu} & T_{\bar{\mu}\bar{\nu}\mu\nu}^{(2)} &= g_{\bar{\mu}\bar{\nu}} \gamma_{\tau} \times \gamma^{\tau} g_{\mu\nu} \\
T_{\bar{\mu}\bar{\nu}\mu\nu}^{(3)} &= g_{\bar{\nu}\nu} g_{\bar{\mu}\mu} \mathbb{1} \times \mathbb{1} & T_{\bar{\mu}\bar{\nu}\mu\nu}^{(4)} &= g_{\bar{\nu}\nu} g_{\bar{\mu}\mu} \gamma_{\tau} \times \gamma^{\tau} \\
T_{\bar{\mu}\bar{\nu}\mu\nu}^{(5)} &= g_{\bar{\mu}\bar{\nu}} \not{k} \times \mathbb{1} g_{\mu\nu} & T_{\bar{\mu}\bar{\nu}\mu\nu}^{(6)} &= g_{\bar{\mu}\bar{\nu}} \mathbb{1} \times \bar{k} g_{\mu\nu} \\
T_{\bar{\mu}\bar{\nu}\mu\nu}^{(7)} &= w_{\bar{\nu}} \times \gamma_{\bar{\mu}} g_{\mu\nu} & T_{\bar{\mu}\bar{\nu}\mu\nu}^{(8)} &= g_{\bar{\mu}\bar{\nu}} \gamma_{\mu} \times w_{\nu} \\
T_{\bar{\mu}\bar{\nu}\mu\nu}^{(9)} &= k_{\bar{\mu}} \times \gamma_{\bar{\nu}} g_{\mu\nu} & T_{\bar{\mu}\bar{\nu}\mu\nu}^{(10)} &= g_{\bar{\mu}\bar{\nu}} \gamma_{\mu} \times \bar{k}_{\nu} \\
T_{\bar{\mu}\bar{\nu}\mu\nu}^{(11)} &= g_{\bar{\nu}\nu} w_{\bar{\mu}} \gamma_{\mu} \times \mathbb{1} & T_{\bar{\mu}\bar{\nu}\mu\nu}^{(12)} &= g_{\bar{\mu}\bar{\nu}} \mathbb{1} \times \gamma_{\bar{\nu}} w_{\mu} \\
T_{\bar{\mu}\bar{\nu}\mu\nu}^{(13)} &= g_{\bar{\nu}\nu} g_{\bar{\mu}\mu} \not{k} \times \mathbb{1} & T_{\bar{\mu}\bar{\nu}\mu\nu}^{(14)} &= g_{\bar{\nu}\nu} g_{\bar{\mu}\mu} \mathbb{1} \times \bar{k} \\
T_{\bar{\mu}\bar{\nu}\mu\nu}^{(15)} &= w_{\bar{\mu}} w_{\bar{\nu}} \times \mathbb{1} g_{\mu\nu} & T_{\bar{\mu}\bar{\nu}\mu\nu}^{(16)} &= w_{\bar{\mu}} w_{\bar{\nu}} \gamma_{\tau} \times \gamma^{\tau} g_{\mu\nu} \\
T_{\bar{\mu}\bar{\nu}\mu\nu}^{(17)} &= g_{\bar{\mu}\bar{\nu}} \mathbb{1} \times w_{\mu} w_{\nu} & T_{\bar{\mu}\bar{\nu}\mu\nu}^{(18)} &= g_{\bar{\mu}\bar{\nu}} \gamma_{\tau} \times \gamma^{\tau} w_{\mu} w_{\nu} \\
T_{\bar{\mu}\bar{\nu}\mu\nu}^{(19)} &= g_{\bar{\mu}\mu} w_{\bar{\nu}} \times w_{\nu} & T_{\bar{\mu}\bar{\nu}\mu\nu}^{(20)} &= g_{\bar{\nu}\nu} w_{\bar{\mu}} \gamma_{\tau} \times \gamma^{\tau} w_{\mu} \\
T_{\bar{\mu}\bar{\nu}\mu\nu}^{(21)} &= k_{\bar{\mu}} w_{\bar{\nu}} \times \mathbb{1} g_{\mu\nu} & T_{\bar{\mu}\bar{\nu}\mu\nu}^{(22)} &= g_{\bar{\mu}\bar{\nu}} \mathbb{1} \times \bar{k}_{\mu} w_{\nu} \\
T_{\bar{\mu}\bar{\nu}\mu\nu}^{(23)} &= k_{\bar{\mu}} k_{\bar{\nu}} \times \mathbb{1} g_{\mu\nu} & T_{\bar{\mu}\bar{\nu}\mu\nu}^{(24)} &= k_{\bar{\mu}} k_{\bar{\nu}} \gamma_{\tau} \times \gamma^{\tau} g_{\mu\nu} \\
T_{\bar{\mu}\bar{\nu}\mu\nu}^{(25)} &= g_{\bar{\mu}\bar{\nu}} \times \bar{k}_{\mu} \bar{k}_{\nu} & T_{\bar{\mu}\bar{\nu}\mu\nu}^{(26)} &= g_{\bar{\mu}\bar{\nu}} \gamma_{\tau} \times \gamma^{\tau} \bar{k}_{\mu} \bar{k}_{\nu} \\
T_{\bar{\mu}\bar{\nu}\mu\nu}^{(27)} &= g_{\bar{\mu}\bar{\nu}} \gamma_{\nu} \times \bar{k} w_{\mu} & T_{\bar{\mu}\bar{\nu}\mu\nu}^{(28)} &= g_{\bar{\mu}\mu} k_{\bar{\nu}} \times w_{\nu}
\end{aligned}$$

$$\begin{aligned}
T_{\bar{\mu}\bar{\nu}\mu\nu}^{(29)} &= g_{\bar{\mu}\mu} w_{\bar{\nu}} \times \bar{k}_{\nu} & T_{\bar{\mu}\bar{\nu}\mu\nu}^{(30)} &= w_{\bar{\mu}} \not{k} \times \gamma_{\bar{\nu}} g_{\mu\nu} \\
T_{\bar{\mu}\bar{\nu}\mu\nu}^{(31)} &= g_{\bar{\mu}\nu} k_{\bar{\nu}} \gamma_{\tau} \times \gamma^{\tau} w_{\mu} & T_{\bar{\mu}\bar{\nu}\mu\nu}^{(32)} &= g_{\bar{\nu}\nu} w_{\bar{\mu}} \gamma_{\tau} \times \gamma^{\tau} \bar{k}_{\mu} \\
T_{\bar{\mu}\bar{\nu}\mu\nu}^{(33)} &= w_{\bar{\mu}} w_{\bar{\nu}} \not{k} \times \mathbb{1} g_{\mu\nu} & T_{\bar{\mu}\bar{\nu}\mu\nu}^{(34)} &= w_{\bar{\mu}} w_{\bar{\nu}} \times \not{k} g_{\mu\nu} \\
T_{\bar{\mu}\bar{\nu}\mu\nu}^{(35)} &= g_{\bar{\mu}\nu} \not{k} \times w_{\mu} w_{\nu} & T_{\bar{\mu}\bar{\nu}\mu\nu}^{(36)} &= g_{\bar{\mu}\bar{\nu}} \mathbb{1} \times \not{k} w_{\mu} w_{\nu} \\
T_{\bar{\mu}\bar{\nu}\mu\nu}^{(37)} &= w_{\bar{\mu}} w_{\bar{\nu}} \gamma_{\mu} \times w_{\nu} & T_{\bar{\mu}\bar{\nu}\mu\nu}^{(38)} &= w_{\bar{\nu}} \times \gamma_{\bar{\mu}} w_{\mu} w_{\nu} \\
T_{\bar{\mu}\bar{\nu}\mu\nu}^{(39)} &= w_{\bar{\mu}} k_{\bar{\nu}} \not{k} \times g_{\mu\nu} & T_{\bar{\mu}\bar{\nu}\mu\nu}^{(40)} &= g_{\bar{\mu}\bar{\nu}} \mathbb{1} \times \not{k} w_{\mu} \bar{k}_{\nu} \\
T_{\bar{\mu}\bar{\nu}\mu\nu}^{(41)} &= g_{\bar{\nu}\mu} w_{\bar{\mu}} \not{k} \times w_{\nu} & T_{\bar{\mu}\bar{\nu}\mu\nu}^{(42)} &= k_{\bar{\mu}} \times \gamma_{\bar{\nu}} w_{\mu} w_{\nu} \\
T_{\bar{\mu}\bar{\nu}\mu\nu}^{(43)} &= w_{\bar{\mu}} w_{\bar{\nu}} \gamma_{\mu} \times \bar{k}_{\nu} & T_{\bar{\mu}\bar{\nu}\mu\nu}^{(44)} &= g_{\bar{\mu}\nu} w_{\bar{\nu}} \times \not{k} w_{\mu} \\
T_{\bar{\mu}\bar{\nu}\mu\nu}^{(45)} &= k_{\bar{\mu}} k_{\bar{\nu}} \not{k} \times \mathbb{1} g_{\mu\nu} & T_{\bar{\mu}\bar{\nu}\mu\nu}^{(46)} &= g_{\bar{\mu}\bar{\nu}} \mathbb{1} \times \not{k} \bar{k}_{\mu} \bar{k}_{\nu} \\
T_{\bar{\mu}\bar{\nu}\mu\nu}^{(47)} &= k_{\bar{\mu}} k_{\bar{\nu}} \gamma_{\mu} \times w_{\nu} & T_{\bar{\mu}\bar{\nu}\mu\nu}^{(48)} &= w_{\bar{\nu}} \times \gamma_{\bar{\mu}} \bar{k}_{\mu} \bar{k}_{\nu} \\
T_{\bar{\mu}\bar{\nu}\mu\nu}^{(49)} &= w_{\bar{\mu}} w_{\bar{\nu}} \times w_{\mu} w_{\nu} & T_{\bar{\mu}\bar{\nu}\mu\nu}^{(50)} &= w_{\bar{\mu}} w_{\bar{\nu}} \gamma_{\tau} \times \gamma^{\tau} w_{\mu} w_{\nu} \\
T_{\bar{\mu}\bar{\nu}\mu\nu}^{(51)} &= k_{\bar{\mu}} k_{\bar{\nu}} \times w_{\mu} w_{\nu} & T_{\bar{\mu}\bar{\nu}\mu\nu}^{(52)} &= k_{\bar{\mu}} k_{\bar{\nu}} \gamma_{\tau} \times \gamma^{\tau} w_{\mu} w_{\nu} \\
T_{\bar{\mu}\bar{\nu}\mu\nu}^{(53)} &= w_{\bar{\mu}} w_{\bar{\nu}} \times \bar{k}_{\mu} \bar{k}_{\nu} & T_{\bar{\mu}\bar{\nu}\mu\nu}^{(54)} &= w_{\bar{\mu}} w_{\bar{\nu}} \gamma_{\tau} \times \gamma^{\tau} \bar{k}_{\mu} \bar{k}_{\nu} \\
T_{\bar{\mu}\bar{\nu}\mu\nu}^{(55)} &= k_{\bar{\mu}} w_{\bar{\nu}} \times w_{\mu} w_{\nu} & T_{\bar{\mu}\bar{\nu}\mu\nu}^{(56)} &= w_{\bar{\mu}} w_{\bar{\nu}} \times \bar{k}_{\mu} w_{\nu} \\
T_{\bar{\mu}\bar{\nu}\mu\nu}^{(57)} &= w_{\bar{\mu}} \not{k} \times \gamma_{\bar{\nu}} w_{\mu} w_{\nu} & T_{\bar{\mu}\bar{\nu}\mu\nu}^{(58)} &= w_{\bar{\mu}} w_{\bar{\nu}} \gamma_{\nu} \times \not{k} w_{\mu} \\
T_{\bar{\mu}\bar{\nu}\mu\nu}^{(59)} &= w_{\bar{\mu}} w_{\bar{\nu}} \not{k} \times w_{\mu} w_{\nu} & T_{\bar{\mu}\bar{\nu}\mu\nu}^{(60)} &= w_{\bar{\mu}} w_{\bar{\nu}} \times \not{k} w_{\mu} w_{\nu} \\
T_{\bar{\mu}\bar{\nu}\mu\nu}^{(61)} &= w_{\bar{\mu}} k_{\bar{\nu}} \not{k} \times w_{\mu} w_{\nu} & T_{\bar{\mu}\bar{\nu}\mu\nu}^{(62)} &= w_{\bar{\mu}} w_{\bar{\nu}} \times \not{k} w_{\mu} \bar{k}_{\nu} \\
T_{\bar{\mu}\bar{\nu}\mu\nu}^{(63)} &= k_{\bar{\mu}} k_{\bar{\nu}} \not{k} \times w_{\mu} w_{\nu} & T_{\bar{\mu}\bar{\nu}\mu\nu}^{(64)} &= w_{\bar{\mu}} w_{\bar{\nu}} \times \not{k} \bar{k}_{\mu} \bar{k}_{\nu}
\end{aligned}$$

2.4 Partial-wave decomposition

The helicity matrix elements of the scattering operator, T , are decomposed into partial-wave amplitudes characterized by the total angular momentum J . Given a specific process together with our convention of the helicity wave functions it suffices to specify the helicity projection of the initial and final wave functions λ_1, λ_2 and $\bar{\lambda}_1, \bar{\lambda}_2$. We write

$$\begin{aligned}
\langle \bar{\lambda}_1 \bar{\lambda}_2 | T | \lambda_1 \lambda_2 \rangle &= \sum_J (2J+1) \langle \bar{\lambda}_1 \bar{\lambda}_2 | T_J | \lambda_1 \lambda_2 \rangle d_{\lambda, \bar{\lambda}}^{(J)}(\theta), \\
d_{\lambda, \bar{\lambda}}^{(J)}(\theta) &= (-)^{\lambda - \bar{\lambda}} d_{-\lambda, -\bar{\lambda}}^{(J)}(\theta) = (-)^{\lambda - \bar{\lambda}} d_{\bar{\lambda}, \lambda}^{(J)}(\theta) = d_{-\bar{\lambda}, -\lambda}^{(J)}(\theta), \quad (2.23)
\end{aligned}$$

$$\langle \bar{\lambda}_1 \bar{\lambda}_2 | T_J | \lambda_1 \lambda_2 \rangle = \int_{-1}^{-1} \frac{d \cos \theta}{2} \langle \bar{\lambda}_1 \bar{\lambda}_2 | T | \lambda_1 \lambda_2 \rangle d_{\lambda, \bar{\lambda}}^{(J)}(\theta),$$

with $\lambda = \lambda_1 - \lambda_2$ and $\bar{\lambda} = \bar{\lambda}_1 - \bar{\lambda}_2$. The Wigner rotation functions $d_{\lambda, \bar{\lambda}}^{(J)}(\theta)$ are used in a convention as characterized by (2.23).

It is useful to introduce parity eigenstates of good total angular momentum J , formed in terms of the helicity states $|\lambda_1, \lambda_2\rangle_J$ [24]. The phase conventions assumed in this work imply the relation

$$\langle -\bar{\lambda}_1 - \bar{\lambda}_2 | T | -\lambda_1 - \lambda_2 \rangle = (-)^{S_1 - S_2 + \bar{S}_1 - \bar{S}_2 + \lambda - \bar{\lambda}} \langle \bar{\lambda}_1 \bar{\lambda}_2 | T | \lambda_1 \lambda_2 \rangle \quad (2.24)$$

The various parity eigenstates are readily identified. We introduce for the $\frac{1}{2} \frac{1}{2}$ system:

$$\begin{aligned} |1_{\pm}, J\rangle &= \frac{1}{\sqrt{2}} (|+\frac{1}{2}, +\frac{1}{2}\rangle_J \pm |-\frac{1}{2}, -\frac{1}{2}\rangle_J), \\ |2_{\pm}, J\rangle &= \frac{1}{\sqrt{2}} (|+\frac{1}{2}, -\frac{1}{2}\rangle_J \pm |-\frac{1}{2}, +\frac{1}{2}\rangle_J), \end{aligned} \quad (2.25)$$

for the $\frac{3}{2} \frac{1}{2}$ system:

$$\begin{aligned} |1_{\pm}, J\rangle &= \frac{1}{\sqrt{2}} (|+\frac{1}{2}, +\frac{1}{2}\rangle_J \mp |-\frac{1}{2}, -\frac{1}{2}\rangle_J), \\ |2_{\pm}, J\rangle &= \frac{1}{\sqrt{2}} (|+\frac{1}{2}, -\frac{1}{2}\rangle_J \mp |-\frac{1}{2}, +\frac{1}{2}\rangle_J), \\ |3_{\pm}, J\rangle &= \frac{1}{\sqrt{2}} (|+\frac{3}{2}, +\frac{1}{2}\rangle_J \mp |-\frac{3}{2}, -\frac{1}{2}\rangle_J), \\ |4_{\pm}, J\rangle &= \frac{1}{\sqrt{2}} (|+\frac{3}{2}, -\frac{1}{2}\rangle_J \mp |-\frac{3}{2}, +\frac{1}{2}\rangle_J), \end{aligned} \quad (2.26)$$

for the $\frac{1}{2} \frac{3}{2}$ system:

$$\begin{aligned} |1_{\pm}, J\rangle &= \frac{1}{\sqrt{2}} (|+\frac{1}{2}, +\frac{1}{2}\rangle_J \mp |-\frac{1}{2}, -\frac{1}{2}\rangle_J), \\ |2_{\pm}, J\rangle &= \frac{1}{\sqrt{2}} (|+\frac{1}{2}, -\frac{1}{2}\rangle_J \mp |-\frac{1}{2}, +\frac{1}{2}\rangle_J), \\ |3_{\pm}, J\rangle &= \frac{1}{\sqrt{2}} (|-\frac{1}{2}, -\frac{3}{2}\rangle_J \mp |+\frac{1}{2}, +\frac{3}{2}\rangle_J), \\ |4_{\pm}, J\rangle &= \frac{1}{\sqrt{2}} (|+\frac{1}{2}, -\frac{3}{2}\rangle_J \mp |-\frac{1}{2}, +\frac{3}{2}\rangle_J), \end{aligned} \quad (2.27)$$

and for the $\frac{3}{2}\frac{3}{2}$ system:

$$\begin{aligned}
|1_{\pm}, J\rangle &= \frac{1}{\sqrt{2}} \left(|+\frac{1}{2}, +\frac{1}{2}\rangle_J \pm |-\frac{1}{2}, -\frac{1}{2}\rangle_J \right), \\
|2_{\pm}, J\rangle &= \frac{1}{\sqrt{2}} \left(|+\frac{3}{2}, +\frac{3}{2}\rangle_J \pm |-\frac{3}{2}, -\frac{3}{2}\rangle_J \right), \\
|3_{\pm}, J\rangle &= \frac{1}{\sqrt{2}} \left(|+\frac{1}{2}, -\frac{1}{2}\rangle_J \pm |-\frac{1}{2}, +\frac{1}{2}\rangle_J \right), \\
|4_{\pm}, J\rangle &= \frac{1}{\sqrt{2}} \left(|+\frac{3}{2}, +\frac{1}{2}\rangle_J \pm |-\frac{3}{2}, -\frac{1}{2}\rangle_J \right), \\
|5_{\pm}, J\rangle &= \frac{1}{\sqrt{2}} \left(|-\frac{1}{2}, -\frac{3}{2}\rangle_J \pm |+\frac{1}{2}, +\frac{3}{2}\rangle_J \right), \\
|6_{\pm}, J\rangle &= \frac{1}{\sqrt{2}} \left(|+\frac{1}{2}, -\frac{3}{2}\rangle_J \pm |-\frac{1}{2}, +\frac{3}{2}\rangle_J \right), \\
|7_{\pm}, J\rangle &= \frac{1}{\sqrt{2}} \left(|+\frac{3}{2}, -\frac{1}{2}\rangle_J \pm |-\frac{3}{2}, +\frac{1}{2}\rangle_J \right), \\
|8_{\pm}, J\rangle &= \frac{1}{\sqrt{2}} \left(|+\frac{3}{2}, -\frac{3}{2}\rangle_J \pm |-\frac{3}{2}, +\frac{3}{2}\rangle_J \right). \tag{2.28}
\end{aligned}$$

The partial-wave helicity amplitudes $t_{\pm,ij}^J$ that carry good angular momentum J and good parity are defined by

$$t_{\pm,ij}^J = \langle i_{\pm}, J | T | j_{\pm}, J \rangle, \tag{2.29}$$

where i and j label the states. The unitarity condition takes the simple form

$$\Im \left[t_{\pm}^J(s) \right]_{ij}^{-1} = -\frac{M_1 M_2}{2\pi} \frac{p_i}{\sqrt{s}} \delta_{ij}, \tag{2.30}$$

where M_1 and M_2 are the masses of the particles of the intermediate state.

2.5 Covariant partial-wave projectors

From a field theoretical point of view a two-body scattering amplitude is determined by the Bethe-Salpeter equation in terms of an interaction kernel defined by two-particle irreducible Feynman diagrams and a fully dressed two-particle propagator. To establish a connection we consider first the limit of short-range forces. Correspondingly, we consider quasi-local two-body interaction terms as they arise

naturally in any type of effective field theory. It is almost obvious that for such structures the Bethe-Salpeter equation can be solved by algebraic methods (see e.g. [19, 48, 50–54]).

The off-shell scattering amplitude

$$T(\bar{k}, k, w) = \sum_{J, \pm, a, b} T_{\pm, ab}^J(s) \mathcal{Y}_{\pm, ab}^J(\bar{k}, k, w) + T^{\text{off-shell}}(\bar{k}, k, w) \quad (2.31)$$

can be decomposed into on-shell partial-wave amplitudes $T_{\pm, ab}^J(s)$ and a set of projectors $\mathcal{Y}_{\pm, ab}^J(\bar{k}, k, w)$ that carry well defined total angular momentum J and parity [19, 48, 51, 53]. The indices a, b reflect the possible states with given total angular momentum and parity (see (2.25-2.28)). The remainder $T^{\text{off-shell}}(\bar{k}, k, w)$ vanishes for on-shell kinematics. While the partial-wave amplitudes $T_{\pm, ab}^J(s)$ depend on the total energy s only, the projectors are fully off-shell quantities. The latter are nothing but suitably constructed polynomials in the 4-momenta $\bar{k}_\mu, k_\mu, w_\mu$, and γ_μ . Depending on the reaction considered they may carry open Lorentz indices. By construction a partial-wave projector $\mathcal{Y}_{\pm, ab}^J(\bar{k}, k, w)$ is non-vanishing only for its associated angular momentum J and parity in the center of mass frame. As a consequence the projectors are a convenient tool to solve the Bethe-Salpeter equation in the limit of short-range forces.

In the absence of spin the construction of the projectors \mathcal{Y}_{\pm}^J is trivial. It is implied by the identification

$$Y_J = \left(\frac{\bar{r}^2 r^2}{s^2} \right)^{J/2} P_J \left(-\frac{\bar{r} \cdot r}{\sqrt{\bar{r}^2 r^2}} \right), \quad (2.32)$$

where we have introduced the notation

$$\begin{aligned} \bar{r}^\mu &= \bar{k}^\mu - \frac{\bar{k} \cdot w}{s} w^\mu, \\ r^\mu &= k^\mu - \frac{k \cdot w}{s} w^\mu, \end{aligned} \quad (2.33)$$

with the Legendre polynomials P_J . For a given angular momentum J the projector as given in (2.32) is a polynomial in the three off-shell momenta \bar{r}, r, w after multiplication with the factor s^J . The latter reflects a particular normalization of the projectors that imply their associated phase-space function to be asymptotically bounded.

While in the scalar case the covariant partial-wave amplitudes $T_{\pm}^J(s)$ are obtained from the helicity partial-wave amplitudes $t_{\pm}^J(s)$ by dividing out the phase-space factor $(\bar{p}p/s)^J$, for the cases of interest in this work the analogous relations are significantly more complicated. They take the form

$$T_{\pm}^J(s) = \left(\frac{s}{\bar{p}p} \right)^J [\bar{U}_{\pm}^J(s)]^T t_{\pm}^J(s) U_{\pm}^J(s), \quad (2.34)$$

with nontrivial matrices $U_{\pm}(s)$ and $\bar{U}_{\pm}(s)$ characterizing the transformation for the initial and final states from the helicity basis to the new kinematic-free basis. This implies a change in the phase-space distribution:

$$\begin{aligned} \rho_{\pm}^J(s) &= -\Im \left[T_{\pm}^J(s) \right]^{-1} \\ &= \frac{M_1 M_2}{2\pi} \left(\frac{p}{\sqrt{s}} \right)^{2J+1} \left[U_{\pm}^J(s) \right]^{-1} \left[U_{\pm}^J(s) \right]^{T,-1}. \end{aligned} \quad (2.35)$$

Like in the scalar case we adapt a convention for the transformation matrices that lead to an asymptotically bounded phase-space matrix, i.e. we require

$$\lim_{s \rightarrow \infty} \det \rho_{\pm}^J(s) = \text{const} \neq 0. \quad (2.36)$$

It is important to realize that all covariant partial-wave amplitudes are subject to kinematical constraints at $s = 0$. Dividing out powers of s will not introduce additional kinematical singularities, but it will just change their realization.

The significance of introducing the kinematic-free basis lies in the identification and elimination of kinematical constraints. Helicity partial-wave amplitudes are correlated at specific kinematical conditions. This is seen once the amplitudes $t_{\pm,ij}^J(\sqrt{s})$ are expressed in terms of the invariant functions $F_i^{\pm}(s, t)$. If one ignores such correlations it is impossible to reconstruct the invariant functions from the partial-wave amplitudes in an unambiguous manner. This is a well known problem related to the use of the helicity basis in co-variant models, see for example the review Ref. [39]. In contrast, covariant partial-wave amplitudes $T_{\pm}^J(s)$ are free of kinematical constraints and can therefore be used efficiently in partial-wave dispersion relations.

In the following we will present the required transformation matrices relevant for this work. To the best of our knowledge, they are novel and not presented in the

literature before. We provide a particularly detailed presentation for the $\frac{1}{2}\bar{\frac{1}{2}} \rightarrow \frac{1}{2}\bar{\frac{1}{2}}$ case, but refrain from giving the tedious details for the remaining cases.

Any scattering matrix can be expressed in terms of the tensor set (2.12). To construct the kinematic-free basis, it is therefore a necessary condition that the matrix elements of the tensors (2.12) evaluated in the new basis are free from singularities. After some calculations this condition leads to the transformation:

$$\begin{aligned}
 U_{\pm, \frac{1}{2}\bar{\frac{1}{2}}}^J &= \begin{pmatrix} \frac{\sqrt{2J+1}\sqrt{s}}{\sqrt{2}\alpha_{\mp}} & 0 \\ \mp \frac{\sqrt{J(2J+1)}\beta_{\pm}\sqrt{s}}{\sqrt{2(J+1)}\alpha_{\pm}\alpha_{\mp}} & \frac{\sqrt{2J+1}p}{\sqrt{2J(J+1)}\alpha_{\pm}} \end{pmatrix}, \\
 \bar{\alpha}_{\pm} &= \sqrt{\frac{\bar{E}_1 + \bar{M}_1}{2\bar{M}_1}} \sqrt{\frac{\bar{E}_2 \pm \bar{M}_2}{2\bar{M}_2}} + \sqrt{\frac{\bar{E}_1 - \bar{M}_1}{2\bar{M}_1}} \sqrt{\frac{\bar{E}_2 \mp \bar{M}_2}{2\bar{M}_2}}, \\
 \bar{\beta}_{\pm} &= \sqrt{\frac{\bar{E}_1 + \bar{M}_1}{2\bar{M}_1}} \sqrt{\frac{\bar{E}_2 \pm \bar{M}_2}{2\bar{M}_2}} - \sqrt{\frac{\bar{E}_1 - \bar{M}_1}{2\bar{M}_1}} \sqrt{\frac{\bar{E}_2 \mp \bar{M}_2}{2\bar{M}_2}}. \quad (2.37)
 \end{aligned}$$

The expressions for α_{\pm} and β_{\pm} follow from the definition above by removing the bars.

The phase-space distribution becomes:

$$\begin{aligned}
 \rho_{\pm, \frac{1}{2}\bar{\frac{1}{2}}}^J(s) &= \frac{1}{(2J+1)\pi} \left(\frac{p}{\sqrt{s}} \right)^{2J-1} \\
 &\times \begin{pmatrix} \frac{p^2(s-M_{\pm}^2)}{4s^2} & \frac{Jp^2 M_{\pm}}{2s\sqrt{s}} \\ \frac{Jp^2 M_{\pm}}{2s\sqrt{s}} & \frac{J(s-M_{\pm}^2)((J+1)s+JM_{\pm}^2)}{4s^2} \end{pmatrix}, \quad (2.38)
 \end{aligned}$$

where $M_{\pm} = M_1 \pm M_2$. We observe the consistency of the phase-space distribution (2.38) with the desired asymptotic behavior (2.36).

The construction of the associated projectors involves the polynomials introduced already in (2.32) and their derivatives defined as

$$\begin{aligned}
 Y_J' &= \left(\frac{\bar{r}^2 r^2}{s^2} \right)^{(J-1)/2} P_J' \left(-\frac{\bar{r} \cdot r}{\sqrt{\bar{r}^2 r^2}} \right), \\
 Y_J'' &= \left(\frac{\bar{r}^2 r^2}{s^2} \right)^{(J-2)/2} P_J'' \left(-\frac{\bar{r} \cdot r}{\sqrt{\bar{r}^2 r^2}} \right), \quad (2.39)
 \end{aligned}$$

obeying identities that can easily be derived from those of the Legendre polynomials

such as

$$\begin{aligned}
 (2J+1)Y_J &= Y'_{J+1} - \frac{\bar{r}^2 r^2}{s^2} Y'_{J-1}, \\
 (J+1)Y_{J+1} &= -\frac{\bar{r} \cdot r}{s} (2J+1)Y_J - \frac{\bar{r}^2 r^2}{s^2} J Y_{J-1}, \\
 (J-n)Y_J^{(n)} &= -\frac{\bar{r} \cdot r}{s} Y_J^{(n+1)} - \frac{\bar{r}^2 r^2}{s^2} Y_{J-1}^{(n+1)},
 \end{aligned} \tag{2.40}$$

where n denotes the order of the derivative. The projectors read

$$\begin{aligned}
 \mathcal{Y}_{\pm,11}^J &= \frac{\mp 1}{s} \left(P_{\pm} \otimes P_{\pm} \right) Y_J, \\
 \mathcal{Y}_{\pm,12}^J &= \frac{\mp 1}{s} \left(P_{\pm} \otimes P_{\pm} \tilde{\gamma}_{\nu} \right) \left[\frac{\bar{r}^{\nu}}{\sqrt{s}} Y'_J + \frac{r^{\nu}}{\sqrt{s}} \frac{\bar{r}^2}{s} Y'_{J-1} \right], \\
 \mathcal{Y}_{\pm,21}^J &= \frac{\mp 1}{s} \left(\tilde{\gamma}_{\mu} P_{\pm} \otimes P_{\pm} \right) \left[\frac{r^{\mu}}{\sqrt{s}} Y'_J + \frac{\bar{r}^{\mu}}{\sqrt{s}} \frac{r^2}{s} Y'_{J-1} \right], \\
 \mathcal{Y}_{\pm,22}^J &= \frac{\pm 1}{s} \left(\tilde{\gamma}_{\mu} P_{\pm} \otimes P_{\pm} \tilde{\gamma}_{\nu} \right) \left[g^{\mu\nu} Y'_J + 2 \frac{\bar{r}^{\mu} r^{\nu}}{s} Y'_{J-1} \right. \\
 &\quad \left. - \frac{\bar{r}^{\nu}}{\sqrt{s}} \left(\frac{r^{\mu}}{\sqrt{s}} Y''_J + \frac{\bar{r}^{\mu}}{\sqrt{s}} \frac{r^2}{s} Y''_{J-1} \right) \right. \\
 &\quad \left. - \frac{r^{\nu}}{\sqrt{s}} \frac{\bar{r}^2}{s} \left(\frac{r^{\mu}}{\sqrt{s}} Y''_{J-1} + \frac{\bar{r}^{\mu}}{\sqrt{s}} \frac{r^2}{s} Y''_{J-2} \right) \right],
 \end{aligned} \tag{2.41}$$

where $\tilde{\gamma}^{\mu} = \gamma^{\mu} - \not{p} w^{\mu}/s$. The important merit of the expressions (2.41) lies in their regularity in the 4-momenta. This implies that the associated partial-wave amplitudes are suitable for use in dispersion-integral equations.

The partial-wave amplitudes can be computed in terms of the invariant amplitudes $F_i^{\pm}(s, t)$. The expressions require an average over $x = \cos \theta$ of the center-of-mass frame. We established the following result

$$\begin{aligned}
 T_{\pm,11}^J &= \mp \frac{(2J+1)}{2} \left[s A_{\pm,1}^J + \bar{M}_{\mp} M_{\mp} \left(A_{\pm,2}^J + \frac{\bar{M}_{\pm}}{2} A_{\pm,3}^J + \frac{M_{\pm}}{2} A_{\pm,4}^J \right) \right. \\
 &\quad \left. + \frac{J \bar{M}_{\pm} M_{\pm}}{(J+1)} A_{\mp,2}^J - \frac{(2J+1) \bar{M}_{\pm} M_{\pm} (\bar{M}_{\mp}^2 - s) (M_{\mp}^2 - s)}{4(J+1)s^2} A_{\pm,2}^{J+1} \right. \\
 &\quad \left. - \frac{M_{\pm} \bar{p}^2 (M_{\mp}^2 - s)}{2s} A_{\pm,3}^{J+1} - \frac{\bar{M}_{\pm} p^2 (\bar{M}_{\mp}^2 - s)}{2s} A_{\pm,4}^{J+1} \right], \\
 T_{\pm,12}^J &= \mp \frac{(2J+1) \bar{M}_{\pm}}{4(J+1)\sqrt{s}} \left[(M_{\pm}^2 - s) A_{\mp,2}^J - \frac{p^2 (\bar{M}_{\mp}^2 - s)}{s} A_{\pm,2}^{J+1} \right]
 \end{aligned}$$

$$\begin{aligned}
& \mp \frac{s^{3/2}}{2} A_{\pm,3}^{J-1} \pm \frac{\bar{p}^2 p^2}{2\sqrt{s}} A_{\pm,3}^{J+1}, \\
T_{\pm,21}^J &= \frac{(2J+1)M_{\pm}}{4(J+1)\sqrt{s}} \left[(\bar{M}_{\pm}^2 - s) A_{\mp,2}^J - \frac{\bar{p}^2 (M_{\mp}^2 - s)}{s} A_{\pm,2}^{J+1} \right] \\
& \mp \frac{s^{3/2}}{2} A_{\pm,4}^{J-1} \mp \frac{\bar{p}^2 p^2}{2\sqrt{s}} A_{\pm,4}^{J+1}, \\
T_{\pm,22}^J &= \pm \frac{s}{2J} A_{\pm,2}^{J-1} \mp \frac{(2J+1)(\bar{M}_{\pm}^2 - s)(M_{\pm}^2 - s)}{8(J+J^2)s} A_{\mp,2}^J \pm \frac{\bar{p}^2 p^2 A_{\pm,2}^{J+1}}{2(J+1)s},
\end{aligned} \tag{2.42}$$

where $\bar{M}_{\pm} = \bar{M}_1 \pm \bar{M}_2$ and $M_{\pm} = M_1 \pm M_2$ and

$$\begin{aligned}
A_{\pm,i}^J(s) &= \left(\frac{s}{\bar{p}p} \right)^J \int_{-1}^1 d\cos\theta F_i^{\pm}(s,t) P_J(\cos\theta), \\
F_i^{\pm}(s,t) \Big|_{\text{on shell}} &= \sum_J \frac{2J+1}{2} A_{\pm,i}^J(s) Y_J,
\end{aligned} \tag{2.43}$$

with the Legendre polynomials $P_J(\cos\theta)$. The expressions (2.42) were obtained in application of the general results of Appendix A. From our expression for $T_{\pm,ab}^J$ and $\mathcal{Y}_{\pm,ab}^J$ it follows that there are no kinematical constraints left. Any correlation in the partial-wave amplitudes would manifest itself in a singular behavior in the expressions for the projectors. Conversely, a correlation in the projectors would lead to a singular structure in the expressions for $T_{\pm,ab}^J$. All the coefficients in front of the invariant amplitudes $A_{\pm,i}^J(s)$ are regular, thus confirming our claim that the covariant partial-wave scattering amplitudes are free of kinematical constraints.

Though the presentation given so far proves our claim, it leaves obscure how to arrive at invariant amplitudes free of kinematical constraints. The transformation U_{\pm}^J can be derived by a polynomial ansatz for the invariant function F_i , as it arises in the limit of short-range forces. As an initial condition the expressions for the partial-wave amplitudes T_{\pm}^J are made regular. This condition by itself is not sufficient since it may lead to projectors that are singular or equivalently to amplitudes T_{\pm}^J that are still correlated. The absence of such residual correlations is most efficiently proven by the construction of their associated projectors.

As an example for the construction of the projectors we elaborate the derivation of $\mathcal{Y}_{\pm,21}^J(\bar{k}, k, w)$. Given (2.37), the contribution of each of the invariant amplitudes (2.12) to the 21 partial-wave amplitudes can be calculated. The various contributions multiplied by their associated on-shell tensors define a scattering amplitude which constitutes an on-shell version of the projector $\mathcal{Y}_{\pm,ab}^J(\bar{k}, k, w)$. To be specific we obtain for the on-shell version of the projector associated with $T_{\pm,21}^J$,

$$\begin{aligned} s^{\frac{3}{2}} \mathcal{Y}_{\pm,21}^J \Big|_{\text{on-shell}} &= \mp Y_J' T_4^{\pm} \pm \bar{M}_{\mp} \frac{M_+ M_-}{2s} Y_J' T_1^{\pm} \\ &\quad \pm T_1^{\pm} Y_{J-1}' \frac{\bar{M}_{\pm}}{2s^2} (s - \bar{M}_{\mp}^2) p^2, \end{aligned} \quad (2.44)$$

expressed in terms of the on-shell tensor basis (2.12). An important property of the projectors is their independence on any mass parameter. Any mass factor M_i or \bar{M}_i occurring in (2.44) can be eliminated in favor of an appropriately chosen factor \not{p}_i or $\not{\bar{p}}_i$. This leads to the following identities,

$$\begin{aligned} \langle \bar{r}^{\mu} \left(\tilde{\gamma}_{\mu} P_{\pm} \otimes P_{\pm} \right) \rangle &= \left(\bar{M}_{\pm}/2 - \frac{\bar{k} \cdot w}{s} \bar{M}_{\mp} \right) \langle T_1^{\pm} \rangle \\ &= \frac{\bar{M}_{\pm}}{2s} (s - \bar{M}_{\mp}^2) \langle T_1^{\pm} \rangle, \\ \langle r^{\mu} \left(\tilde{\gamma}_{\mu} P_{\pm} \otimes P_{\pm} \right) \rangle &= \langle T_4^{\pm} \rangle - \frac{k \cdot w}{s} \bar{M}_{\mp} \langle T_1^{\pm} \rangle \\ &= \langle T_4^{\pm} \rangle - \frac{M_+ M_-}{2s} \bar{M}_{\mp} \langle T_1^{\pm} \rangle, \end{aligned} \quad (2.45)$$

where we used (2.33). Note also $(E_1 - E_2)\sqrt{s} = 2(w \cdot k) = M_+ M_-$ and $p^2 = -r^2$. Applying (2.45) to (2.44) leads to the result given in (2.41).

Further detailed analyses were performed for the cases where there are one or two spin-3/2 particles in the final or initial state. We derived the corresponding covariant partial-wave amplitudes $T_{\pm,ij}^J$ and the projectors $\mathcal{Y}_{\pm,ij}^J$. Since the expressions are prohibitively tedious they are not presented here. All what is needed in most practical applications are the transformation matrices from the helicity states to the covariant states. Those explicit results are provided. We assure that the implied phase-space distributions (2.35) comply with the desired asymptotic behavior (2.36). The matrices

Table 2.1: Non zero elements of the transformation matrix for the $\frac{3}{2}\bar{1}$ channel.

$(1, 1) : \frac{\sqrt{3}s}{p\alpha_{\pm}}$	$(2, 1) : \pm \sqrt{\frac{3J}{J+1}} \frac{M_{\pm}\sqrt{s}}{p\alpha_{\pm}}$
$(2, 2) : \mp \sqrt{\frac{3J}{J+1}} \frac{\sqrt{s}}{\alpha_{\mp}}$	$(3, 1) : -\sqrt{\frac{J}{J+1}} \left(\frac{2M_{\pm}^2}{\alpha_{\mp}M_1} + \frac{M_{\pm}\sqrt{s}}{\alpha_{\pm}p} \right)$
$(3, 2) : -\sqrt{\frac{J}{J+1}} \frac{M_{\pm}^2}{\alpha_{\mp}\sqrt{s}}$	$(3, 3) : \sqrt{\frac{J}{J+1}} \frac{p}{\alpha_{\pm}}$
$(4, 1) : \pm \sqrt{\frac{J(J-1)}{(J+1)(J+2)}} \left(\frac{2M_{\pm}s-8M_1p^2}{\alpha_{\mp}M_1\sqrt{s}} - \frac{M_1s-4M_{\mp}p^2}{\alpha_{\pm}M_1p} \right)$	$(4, 2) : \pm \sqrt{\frac{J(J-1)}{(J+1)(J+2)}} \frac{2(\beta_{\mp}M_1p-\alpha_{\pm}(2p^2-E_1\sqrt{s}))}{\alpha_{\mp}\alpha_{\pm}M_1}$
$(4, 3) : \pm \sqrt{\frac{J(J-1)}{(J+1)(J+2)}} \frac{pM_{\mp}}{\alpha_{\pm}\sqrt{s}}$	$(4, 4) : \pm \sqrt{\frac{J(J-1)}{(J+1)(J+2)}} \frac{p^2}{\alpha_{\mp}\sqrt{s}}$

Table 2.2: Non zero elements of the transformation matrix for the $\frac{1}{2}\bar{3}$ channel.

$(1, 1) : \frac{\sqrt{3}s}{p\alpha_{\pm}}$	$(2, 1) : \pm \sqrt{\frac{3J}{J+1}} \frac{M_{\pm}\sqrt{s}}{p\alpha_{\pm}}$
$(2, 1) : \mp \sqrt{\frac{3J}{J+1}} \frac{\sqrt{s}}{\alpha_{\mp}}$	$(3, 1) : \sqrt{\frac{J}{J+1}} \left(\mp \frac{2M_{\pm}^2}{\alpha_{\mp}M_2} + \frac{M_{\pm}\sqrt{s}}{\alpha_{\pm}p} \right)$
$(3, 2) : \sqrt{\frac{J}{J+1}} \frac{M_{\pm}^2}{\alpha_{\mp}\sqrt{s}}$	$(3, 3) : \mp \sqrt{\frac{J}{J+1}} \frac{p}{\alpha_{\pm}}$
$(4, 1) : \sqrt{\frac{J(J-1)}{(J+1)(J+2)}} \left(\frac{\pm 2M_{\pm}s-8M_2p^2}{\alpha_{\mp}M_2\sqrt{s}} - \frac{M_2s\pm 4M_{\mp}p^2}{\alpha_{\pm}M_2p} \right)$	$(4, 2) : \sqrt{\frac{J(J-1)}{(J+1)(J+2)}} \frac{2(\beta_{\mp}M_2p\pm\alpha_{\pm}(2p^2-E_2\sqrt{s}))}{\alpha_{\mp}\alpha_{\pm}M_2}$
$(4, 3) : \pm \sqrt{\frac{J(J-1)}{(J+1)(J+2)}} \frac{pM_{\mp}}{\alpha_{\pm}\sqrt{s}}$	$(4, 4) : \pm \sqrt{\frac{J(J-1)}{(J+1)(J+2)}} \frac{p^2}{\alpha_{\mp}\sqrt{s}}$

Table 2.3: Non zero elements of the transformation matrix $\tilde{U}_{\pm, \frac{3}{2}, \frac{3}{2}}^J$ for the $\frac{3}{2}, \frac{3}{2}$ channel.

$(1, 1) : \frac{3s^{3/2}}{\alpha_{\pm} p^2}$	$(2, 1) : -\frac{(3\alpha_{\pm}^2 + \alpha_{\pm}^2)s^{3/2}}{\alpha_{\pm} p^2}$
$(2, 2) : \frac{4\alpha_{\pm} s}{p}$	$(3, 1) : \mp \frac{3\beta_{\pm} \sqrt{J} s^{3/2}}{\alpha_{\pm} \sqrt{J+1} p^2}$
$(3, 3) : \frac{3s}{\alpha_{\pm} \sqrt{J} \sqrt{J+1} p}$	$(4, 1) : -\frac{\alpha_{\pm} \sqrt{J} \sqrt{J+1} p^2}{\sqrt{3} \sqrt{J} (\alpha_{\pm} E_1 + \alpha_{\pm} p) s^{3/2}}$
$(4, 3) : \mp \frac{\alpha_{\pm} \sqrt{J} \sqrt{J+1} p}{\sqrt{3} \sqrt{J} (\alpha_{\pm} E_2 + \alpha_{\pm} p) s^{3/2}}$	$(4, 4) : \pm \frac{\alpha_{\pm} \alpha_{\pm} \sqrt{J+1} M_1 p^2}{2\sqrt{3} s}$
$(5, 1) : \pm \frac{\alpha_{\pm} \alpha_{\pm} \sqrt{J+1} M_2 p^2}{\sqrt{3} (\alpha_{\pm}^2 + 3\alpha_{\pm}^2) s}$	$(5, 2) : \mp \frac{\alpha_{\pm} \sqrt{J} \sqrt{J+1} M_1}{4\sqrt{3} \beta_{\pm} \sqrt{J} s}$
$(5, 3) : -\frac{\alpha_{\pm} \sqrt{J} \sqrt{J+1} p}{4\sqrt{3} \alpha_{\pm} \sqrt{s}}$	$(5, 4) : \pm \frac{2\sqrt{3} s}{\alpha_{\pm} \sqrt{J} \sqrt{J+1} M_1}$
$(5, 5) : \frac{\sqrt{J} \sqrt{J+1}}{4\sqrt{3} \beta_{\pm} \sqrt{J-1} s}$	$(6, 1) : \frac{\alpha_{\pm} \sqrt{J-1} \sqrt{J} (\mp 2\beta_{\pm} E_2 + \alpha_{\pm} M_2) s^{3/2}}{\sqrt{3} \sqrt{J-1} \sqrt{J} (\mp 2\beta_{\pm} E_2 + \alpha_{\pm} M_2) s^{3/2}}$
$(6, 2) : \pm \frac{\alpha_{\pm} \sqrt{J+1} \sqrt{J+2} p}{2\sqrt{3} \beta_{\pm} \sqrt{J-1} s}$	$(6, 3) : \frac{\alpha_{\pm} \alpha_{\pm} \sqrt{J+1} \sqrt{J+2} M_2 p^2}{2\sqrt{3} (\alpha_{\pm} \beta_{\pm} + 3\alpha_{\pm} \beta_{\pm}) \sqrt{J-1} s}$
$(6, 4) : \mp \frac{\alpha_{\pm} \alpha_{\pm} \sqrt{J} \sqrt{J+1} \sqrt{J+2} M_1}{2\sqrt{3} \sqrt{J-1} p \sqrt{s}}$	$(6, 5) : \frac{\alpha_{\pm} \sqrt{J} \sqrt{J+1} \sqrt{J+2} p}{-4\sqrt{3} \alpha_{\pm} \beta_{\pm} \sqrt{J-1} \sqrt{s}}$
$(6, 6) : \frac{\alpha_{\pm} \sqrt{J} \sqrt{J+1} \sqrt{J+2} M_2}{4\sqrt{3} \sqrt{J-1} \sqrt{J} p s}$	$(7, 1) : \pm \frac{\alpha_{\pm} \sqrt{J} \sqrt{J+1} \sqrt{J+2}}{\sqrt{3} \sqrt{J-1} \sqrt{J} (\beta_{\pm} E_1 - \beta_{\pm} p) s^{3/2}}$
$(7, 2) : \mp \frac{\alpha_{\pm} \sqrt{J+1} \sqrt{J+2} M_1^2}{-2\sqrt{3} (\pm 4\alpha_{\pm} \alpha_{\pm} \beta_{\pm} + \beta_{\pm}) \sqrt{J-1} s}$	$(7, 3) : \frac{\alpha_{\pm} \alpha_{\pm} \sqrt{J+1} \sqrt{J+2} M_1 p^2}{-2\sqrt{3} \sqrt{J-1} (E_1 + 4\alpha_{\pm} \alpha_{\pm} p) s}$
$(7, 4) : \frac{\alpha_{\pm} \alpha_{\pm} \sqrt{J} \sqrt{J+1} \sqrt{J+2} M_1}{2\sqrt{3} \sqrt{J-1} p \sqrt{s}}$	$(7, 5) : \pm \frac{\alpha_{\pm} \sqrt{J} \sqrt{J+1} \sqrt{J+2} M_1}{4\sqrt{3} \alpha_{\pm} \sqrt{J-1} (\alpha_{\pm} E_1 + \alpha_{\pm} p) \sqrt{s}}$
$(7, 6) : \pm \frac{\alpha_{\pm} \sqrt{J} \sqrt{J+1} \sqrt{J+2} M_2}{\beta_{\pm} (3\beta_{\pm}^2 + \beta_{\pm}^2) \sqrt{J-2} \sqrt{J-1} \sqrt{J} s^{3/2}}$	$(7, 7) : \frac{\alpha_{\pm} \sqrt{J} \sqrt{J+1} \sqrt{J+2} M_1}{8\sqrt{3} \alpha_{\pm} \sqrt{J-1} p}$
$(8, 1) : \pm \frac{\alpha_{\pm} \alpha_{\pm} \sqrt{J+1} \sqrt{J+2} p^2}{2\sqrt{J-2} \sqrt{J-1} \alpha_{\pm} (3(3\pm 4\alpha_{\pm}^2) M_1^2 M_2 + 16\alpha_{\pm}^2 M_1 p^2 + 12 M_2 p^2) \sqrt{s}}$	$(8, 2) : \mp \frac{\alpha_{\pm}^2 p \sqrt{J+1} \sqrt{J+2} \sqrt{J+3} M_2}{4\sqrt{J-2} \sqrt{J-1} \sqrt{J} (\beta_{\pm}^3 M_1^2 M_2 \pm 3\beta_{\pm} M_2 p^2 + 2\alpha_{\pm} p^3) s}$
$(8, 3) : \mp \frac{4\alpha_{\pm} \sqrt{J-2} \sqrt{J-1}}{\sqrt{J} \sqrt{J+1} \sqrt{J+2} \sqrt{J+3} M_2}$	$(8, 4) : \frac{16\alpha_{\pm} \beta_{\pm} \sqrt{J-2} \sqrt{J-1} (-3\beta_{\pm} M_2 \pm 2\alpha_{\pm} p) \sqrt{s}}{\sqrt{J} \sqrt{J+1} \sqrt{J+2} \sqrt{J+3} p}$
$(8, 5) : \pm \frac{\sqrt{J} \sqrt{J+1} \sqrt{J+2} \sqrt{J+3}}{\sqrt{J} \sqrt{J+1} \sqrt{J+2} \sqrt{J+3} M_2}$	$(8, 6) : \pm \frac{8\alpha_{\pm} \beta_{\pm} \sqrt{J-2} \sqrt{J-1} p \sqrt{s}}{\alpha_{\pm} \sqrt{J} \sqrt{J+1} \sqrt{J+2} \sqrt{J+3} M_2}$
$(8, 7) : \frac{8\sqrt{J-2} \sqrt{J-1} p (\pm 3\beta_{\pm} M_2 + 2\alpha_{\pm} p)}{\sqrt{J} \sqrt{J+1} \sqrt{J+2} \sqrt{J+3} M_2}$	$(8, 8) : \pm \frac{8\alpha_{\pm} \sqrt{J-2} \sqrt{J-1} p^2}{\sqrt{J} \sqrt{J+1} \sqrt{J+2} \sqrt{J+3} \sqrt{s}}$

for the cases involving one spin-1/2 and one spin-3/2 state are shown in Tables 2.1-2.2. In Appendices B and C we show as a further example the projectors for a reaction involving one spin-3/2 particle only.

For the most tedious case with two spin-3/2 states, we have derived the transformation matrix in two steps. First we derive a set of covariant amplitudes that are free of kinematical constraints, even though at this point they do not have the appropriate asymptotic properties (2.36). This first step is defined by the transformation matrix $\tilde{U}_{\pm, \frac{3}{2} \frac{3}{2}}^J$, which is given in Table 2.3. The final transformation is

$$U_{\pm, \frac{3}{2} \frac{3}{2}}^J = \tilde{U}_{\pm, \frac{3}{2} \frac{3}{2}}^J \times \quad (2.46)$$

$$\times \begin{pmatrix} \frac{1}{M_1 M_2} & 0 & 0 & 0 & 0 & 0 & 0 & 0 \\ \frac{2}{M_1 M_2} & \frac{1}{s} & 0 & 0 & 0 & 0 & 0 & 0 \\ 0 & 0 & \frac{1}{M_1 M_2} & 0 & 0 & 0 & 0 & 0 \\ \pm \frac{2J}{M_1 M_2} & 0 & \frac{1}{M_2 \sqrt{s}} & \frac{1}{M_2 \sqrt{s}} & 0 & 0 & 0 & 0 \\ 0 & 0 & \frac{2(M_1^2 + M_2^2 + s)}{M_1 M_2 s} & \mp \frac{2}{s} & \frac{1}{s} & 0 & 0 & 0 \\ \frac{-4J}{M_1 \sqrt{s}} & 0 & -\frac{2}{M_1 M_2} & 0 & -\frac{1}{s} & \frac{1}{M_1 \sqrt{s}} & 0 & 0 \\ \frac{4J}{M_1 M_2} & \pm \frac{2J M_2}{M_1 s} & \pm \frac{2(M_1 \pm M_2)}{M_1 M_2 \sqrt{s}} & \pm \frac{2}{M_2 \sqrt{s}} & \mp \frac{1}{M_1 \sqrt{s}} & \mp \frac{1}{s} & \frac{1}{s} & 0 \\ \pm \frac{8J(M_1 \mp M_2)}{M_2^2 \sqrt{s}} & 0 & \mp \frac{4}{M_1 M_2} & 0 & \pm \frac{6}{s} & \pm \frac{2}{M_1 \sqrt{s}} & \mp \frac{2}{M_2 \sqrt{s}} & \frac{1}{s} \end{pmatrix}.$$

2.6 Conclusions

We have constructed partial-wave amplitudes for baryon-antibaryon scattering which are free from kinematical constraints and frame independent. Those amplitudes are well suited to be used in partial-wave dispersion relations. Explicit transformations from the conventional helicity states to the covariant states were derived and presented in this work. We considered the scattering of two spin-1/2, two spin-3/2 particles, and a spin-1/2 off a spin-3/2 particle.

As a necessary intermediate step we identified complete sets of invariant functions that parameterize the scattering amplitudes of the various processes and are kinematically unconstrained. The latter are expected to satisfy the Mandelstam dispersion-integral representation. Furthermore we constructed a projector algebra that solves the two-body Bethe-Salpeter scattering equation in the limit of short range forces. It was pointed out that the existence and smoothness of such a projector ba-

sis is closely related to the existence of covariant partial-wave amplitudes. Explicit expressions for such projectors were presented for the two simplest reactions.

The present paper thus offers an efficient starting point for analyzing baryon-antibaryon scattering in a covariant coupled-channel approach that takes into account the constraints set by micro-causality and coupled-channel unitarity.

EFFECTIVE FIELD THEORY

In this chapter we give a brief introduction to Quantum Chromodynamics (QCD), which is the theory describing the interaction of quarks and gluons. Section 3.1 reviews the relevant symmetries of the QCD Lagrangian. However, the description of hadron-hadron interactions based on the QCD Lagrangian is highly complicated, especially at low energies. Therefore, the common approach in describing hadron-hadron interactions is based on an effective field theory where the effective degrees of freedom are the mesons and baryons.

Based on the chiral Lagrangian written in terms of the Goldstone boson octet and the nonet of light vector mesons, as given in section 3.2, we evaluate in section 3.4 the invariant amplitudes for specific tree-level exchange diagrams involving spin-1/2 and spin-3/2 particles. The invariant amplitudes determine the specific on-shell projection of the interaction.

3.1 Symmetries of QCD

QCD is a non-Abelian theory, which describes, in the perturbative regime, the strong interactions. Quarks and gluon fields are the associated degrees of freedom [55, 56]. QCD is based on the non-Abelian gauge symmetry group $SU(3)$, introduced originally in [57]. We will denote by q_c^α the fermionic matter fields associated with *quarks*, where $\alpha = u, d, s, \dots$ is the flavor index, while $c = 1, 2, 3$ is the color index. The gauge bosons (*gluons*) belong to the adjoint representation of the gauge group G_μ^a , $a = 1, \dots, 8$. The classical QCD Lagrangian density (i.e. the density which

does not include quantum corrections) is

$$\mathcal{L} = \sum_{\alpha} \bar{q}_c^{\alpha} \left(i \not{D}^{cd} - m^{\alpha} \delta_{cd} \right) q_d^{\alpha} - \frac{1}{4} G_{\mu\nu}^a G_a^{\mu\nu}, \quad (3.1)$$

where m^{α} is the mass of the quark with flavor α and $G_{\mu\nu}^a$ is the gluonic field strength tensor. In Eq. 3.1, the Einstein summation rule is implied for the color indices. The QCD Lagrangian is invariant under the action of the discrete symmetry transformations C , P and T separately and also invariant under the $SU(3)_C$ transformation in the color space.

3.1.1 Color

The gluonic field strength tensor is given by

$$G_{\mu\nu}^a = \partial_{\mu} G_{\nu}^a - \partial_{\nu} G_{\mu}^a + g_s f^{abc} G_{\mu}^b G_{\nu}^c, \quad (3.2)$$

where g_s is the strong coupling constant and f^{abc} are the $SU(3)_C$ structure constants. The gauge-covariant derivative takes the form

$$D^{\mu} = \partial^{\mu} + i g_s \lambda^a G_a^{\mu}. \quad (3.3)$$

The λ_a denotes the Gell-Mann matrices, so that $\lambda_a/2$ are the $SU(3)_C$ generators in the fundamental representation.

At high energies, the strong coupling constant g_s is small and a perturbative expansion is possible. However, at low energies, the coupling constant grows. Moreover, the gluons, which are the gauge fields of QCD, can interact with each other because they carry color charge, in contrast to charge-neutral photons, which are the gauge fields of quantum electrodynamics (QED). The quarks, as well as gluons, are not color-neutral and, therefore, they cannot be observed as physical states but are confined with other quarks and gluons in the states of color-singlet hadrons. This mechanism is known as color confinement and it is the mechanism describing the binding of quarks into hadrons. As a consequence, one is not able to solve the QCD Lagrangian of Eq. 3.1 perturbatively at low energies. The large- N_c formulation of QCD provides a framework for studying the nonperturbative QCD dynamics of hadrons in a systematic expansion in the parameter $1/N_c$, where N_c is the number

of colors. The original theory is recovered by taking $N_c = 3$. However, an effective field theory approach at long distances turns out to be the appropriate framework.

3.1.2 Flavor

In the absence of quark masses, the QCD Lagrangian of Eq. 3.1 turns out to be

$$\mathcal{L}^0 = i \sum_{\alpha} \bar{q}_{L,c}^{\alpha} \not{D}^{cd} q_{L,d}^{\alpha} + i \sum_{\alpha} \bar{q}_{R,c}^{\alpha} \not{D}^{cd} q_{R,d}^{\alpha} - \frac{1}{4} G_{\mu\nu}^a G_a^{\mu\nu}, \quad (3.4)$$

where the \mathcal{L}^0 with the '0' index refers to the massless case and the quark fields have been split into their chiral components.

This Lagrangian is invariant under independent global $SU(n_f)_L \times SU(n_f)_R$ transformations of the left- and right-handed quarks in flavor space, where n_f is the number of flavors. Global symmetries have an influence on the spectrum, whereas local ones determine the interaction. Consistently, the global chiral symmetry, which should be approximately satisfied in the light-quark sector ($n_f = 3$), should have implications in hadron spectroscopy. However, this does not necessarily mean that the symmetry must be observed in the spectrum, since symmetries have always two possible realizations: either they are manifest, giving rise to a classification within the spectrum, or they are driven by a spontaneous symmetry breaking, with the resulting generation of the Goldstone bosons, according to Goldstone's theorem [58].

The $SU(3)_L \times SU(3)_R$ symmetry is broken in two ways. First, the non-zero masses of the light quarks lead to an explicit breaking of the symmetry. Secondly, although hadrons can be nicely classified in $SU(3)_f$ representations, degenerate multiplets with opposite parity do not exist. Moreover, the octet of pseudoscalar mesons happens to be much lighter than all the other hadronic states. This experimental evidence drives the spontaneous breaking of the symmetry $SU(3)_L \times SU(3)_R$ to $SU(3)_f$. The Nambu-Goldstone theorem states that the lost symmetry must be compensated by the presence of massless bosons (Goldstone bosons). Since there are $n_f^2 - 1 = 8$ broken axial generators of the chiral group, there should be eight lightest hadronic states with $J^P = 0^-$ (π^+ , π^- , π^0 , η , K^+ , K^- , K^0 and \bar{K}^0). Their small masses are generated by the quark-mass matrix, which explicitly breaks the global

chiral symmetry. Additionally, an effective field theory can be used at low energies in which the pseudoscalar Goldstone bosons are the relevant degrees of freedom.

3.2 Effective interaction

Chiral Perturbation Theory [59] is the effective field theory of low-energy QCD, which uses an effective Lagrangian that is invariant under global chiral transformations. The idea of constructing an effective theory in this context was first proposed by Weinberg [60]. The theory is very successful in describing the interactions of Goldstone bosons and nucleons at energies smaller than the chiral symmetry breaking scale.

We construct an effective hadronic interaction, based on the chiral Lagrangian for the Goldstone bosons, vector mesons and baryon octet fields involving u , d and s quarks

$$\mathcal{L}_{\text{int.}} = \mathcal{L}_{PB} + \mathcal{L}_{VB} + \mathcal{L}_{P\Delta B} + \mathcal{L}_{P\Delta} + \mathcal{L}_{V\Delta B} \quad (3.5)$$

where \mathcal{L}_{PB} and \mathcal{L}_{VB} describe the interaction between the octet baryons and the Goldstone bosons and vector-meson nonet, respectively, $\mathcal{L}_{P\Delta B}$ and $\mathcal{L}_{V\Delta B}$ describe the interaction of the octet mesons and vector mesons, respectively, with the octet and decuplet baryons and $\mathcal{L}_{P\Delta}$ describes the interaction between the Δ decuplet and the Goldstone bosons.

The chiral Lagrangian \mathcal{L}_{PB} describing the interaction of the pseudoscalar Goldstone bosons takes the form

$$\begin{aligned} \mathcal{L}_{PB} &= F_A \text{tr} \left(\bar{B} \gamma^\mu \gamma_5 [iU_\mu, B]_- \right) + D_A \text{tr} \left(\bar{B} \gamma^\mu \gamma_5 [iU_\mu, B]_+ \right), \\ U_\mu &= \frac{1}{2} u^\dagger \left(\partial_\mu e^{i\frac{\Phi}{f}} \right) u^\dagger, \quad u = \exp \left(i \frac{\Phi}{2f} \right), \end{aligned} \quad (3.6)$$

where B is the baryon field, Φ is the pseudoscalar meson octet field, and $[A, B]_\pm = AB \pm BA$. We first expand the building block of the chiral Lagrangian U_μ into the mesonic field. This leads to

$$U_\mu = \frac{i}{2f} \partial_\mu \Phi + \mathcal{O}(\Phi^2), \quad (3.7)$$

where higher powers of the meson field would enter at higher orders in the chiral expansion. The Lagrangian describing the interaction of the meson field with the octet baryons is:

$$\mathcal{L}_{PB} = \frac{F_A}{2f} \text{tr} (\bar{B} \gamma_5 \gamma_\mu [(\partial^\mu \Phi), B]_-) + \frac{D_A}{2f} \text{tr} (\bar{B} \gamma_5 \gamma_\mu [(\partial^\mu \Phi), B]_+) . \quad (3.8)$$

The particle content of the meson fields with $J^P = 0^-$ and baryon fields with $J^P = \frac{1}{2}^+$ is collected into the traceless matrices:

$$\begin{aligned} \Phi &= \begin{pmatrix} \pi^0 + \frac{1}{\sqrt{3}} \eta & \sqrt{2} \pi^+ & \sqrt{2} K^+ \\ \sqrt{2} \pi^- & -\pi^0 + \frac{1}{\sqrt{3}} \eta & \sqrt{2} K^0 \\ \sqrt{2} K^- & \sqrt{2} \bar{K}^0 & -\frac{2}{\sqrt{3}} \eta \end{pmatrix} , \\ B &= \begin{pmatrix} \frac{1}{\sqrt{2}} \Sigma^0 + \frac{1}{\sqrt{6}} \Lambda & \Sigma^+ & p \\ \Sigma^- & -\frac{1}{\sqrt{2}} \Sigma^0 + \frac{1}{\sqrt{6}} \Lambda & n \\ -\Xi^- & \Xi^0 & -\frac{\sqrt{2}}{\sqrt{6}} \Lambda \end{pmatrix} \end{aligned} \quad (3.9)$$

with $\bar{B} = B^\dagger \gamma_0$. The Lagrangian describing the interaction between the vector mesons and the baryon fields is described by

$$\begin{aligned} \mathcal{L}_{VB} &= \frac{F_V}{2} \text{tr} (\bar{B} \gamma_\mu [V^\mu, B]_-) + \frac{D_V}{2} \text{tr} (\bar{B} \gamma_\mu [V^\mu, B]_+) \\ &+ \frac{F_T}{4f} \text{tr} (\bar{B} \sigma_{\mu\nu} [(\partial^\mu V^\nu), B]_-) + \frac{D_T}{4f} \text{tr} (\bar{B} \sigma_{\mu\nu} [(\partial^\mu V^\nu), B]_+) \\ &+ \frac{G_V}{2} \text{tr} (\bar{B} \gamma_\mu B) \text{tr} V^\mu + \frac{G_T}{4f} \text{tr} (\bar{B} \sigma_{\mu\nu} B) \text{tr} (\partial^\mu V^\nu) , \end{aligned} \quad (3.10)$$

where V_μ is the massive vector-meson field with quantum numbers $J^P = 1^-$, whose particle content is

$$V_\mu = \begin{pmatrix} \rho_\mu^0 + \omega_\mu & \sqrt{2} \rho_\mu^+ & \sqrt{2} K_\mu^+ \\ \sqrt{2} \rho_\mu^- & -\rho_\mu^0 + \omega_\mu & \sqrt{2} K_\mu^0 \\ \sqrt{2} K_\mu^- & \sqrt{2} \bar{K}_\mu^0 & \sqrt{2} \phi_\mu \end{pmatrix} . \quad (3.11)$$

We use in our calculation a tensor-meson representation of the vector meson. The connection between the two representations is given by

$$V_{\mu\nu} = \frac{1}{m_V} (\partial_\mu V_\nu - \partial_\nu V_\mu) . \quad (3.12)$$

Here we can re-express the \mathcal{L}_{VB} in terms of $V_{\mu\nu}$ due to the Proca equation¹ as follows.

$$\partial_\nu V^{\mu\nu} = \frac{1}{m_V} (\partial^\mu \partial \cdot V - \partial^2 V^\mu) = m_V V^\mu$$

Then the Lagrangian density describing the interaction of the vector-meson fields with the baryon field described by Eq. 3.10 becomes

$$\begin{aligned} \mathcal{L}_{VB} = & \frac{F_V}{2m_V} \text{tr} (\bar{B} \gamma_\mu [\partial_\nu V^{\mu\nu}, B]_-) + \frac{D_V}{2m_V} \text{tr} (\bar{B} \gamma_\mu [\partial_\nu V^{\mu\nu}, B]_+) \\ & + \frac{G_V}{2m_V} \text{tr} (\bar{B} \gamma_\mu B) \text{tr} (\partial_\nu V^{\mu\nu}) + \frac{F_T m_V}{8f} \text{tr} (\bar{B} \sigma_{\mu\nu} [V^{\mu\nu}, B]_-) \\ & + \frac{D_T m_V}{8f} \text{tr} (\bar{B} \sigma_{\mu\nu} [V^{\mu\nu}, B]_+) + \frac{G_T m_V}{8f} \text{tr} (\bar{B} \sigma_{\mu\nu} B) \text{tr} (V^{\mu\nu}). \end{aligned} \quad (3.13)$$

The Lagrange density $\mathcal{L}_{P\Delta B}$ that describes the interaction of the octet mesons with the octet and decuplet baryons is

$$\begin{aligned} \mathcal{L}_{P\Delta B} = & C_A \text{tr} \left\{ (\bar{\Delta}_\mu \cdot iU^\mu) B - \bar{B} (iU^{\mu\dagger} \cdot \Delta_\mu) \right\} \\ & - \frac{Z_A C_A}{2} \text{tr} \left\{ (\bar{\Delta}_\mu \cdot iU_\nu) \gamma^\mu \gamma^\nu B - \bar{B} \gamma^\nu \gamma^\mu (U_\nu^\dagger \cdot \Delta_\mu) \right\}, \end{aligned} \quad (3.14)$$

where the baryon decuplet field Δ_μ^{abc} is completely symmetric, has $J^P = \frac{3}{2}^+$ quantum numbers, and is related to the physical states by

$$\begin{aligned} \Delta_\mu^{111} &= \Delta_\mu^{+++}, & \Delta_\mu^{113} &= \Sigma_\mu^+ / \sqrt{3}, & \Delta_\mu^{133} &= \Xi_\mu^0 / \sqrt{3}, & \Delta_\mu^{333} &= \Omega_\mu^-, \\ \Delta_\mu^{112} &= \Delta_\mu^+ / \sqrt{3}, & \Delta_\mu^{123} &= \Sigma_\mu^0 / \sqrt{6}, & \Delta_\mu^{233} &= \Xi_\mu^- / \sqrt{3}, \\ \Delta_\mu^{122} &= \Delta_\mu^0 / \sqrt{3}, & \Delta_\mu^{223} &= \Sigma_\mu^- / \sqrt{3}, \\ \Delta_\mu^{222} &= \Delta_\mu^-. \end{aligned} \quad (3.15)$$

At leading chiral order, after contracting the two lines in Eq. 3.14, the Lagrange density $\mathcal{L}_{P\Delta B}$ becomes

$$\mathcal{L}_{P\Delta B} = -\frac{C_A}{2f} \text{tr} \left\{ (\bar{\Delta}_\mu \cdot \partial_\nu \Phi) \left(g^{\mu\nu} - \frac{1}{2} Z_A \gamma^\mu \gamma^\nu \right) B + \text{h.c.} \right\} \quad (3.16)$$

¹ $(\partial^2 + m_V^2)V^\mu = 0$ and $\partial \cdot V = 0$

The Lagrange density describing the interaction of the vector-meson field (in the tensor representation) with the octet and decuplet fields is

$$\begin{aligned} \mathcal{L}_{V\Delta B} &= \frac{C_V}{2m_V} \text{tr} \left\{ (\bar{\Delta}_\lambda \cdot \partial_\nu V^{\mu\nu}) \left(g_\nu^\lambda - \frac{1}{2} Z_V \gamma^\lambda \gamma_\nu \right) \gamma_5 B + \text{h.c} \right\} \\ &- i \frac{m_V C_T}{8f} \text{tr} \left\{ (\bar{\Delta}_\lambda \cdot V_{\mu\nu}) \left(g^{\lambda\mu} \gamma^\nu - \frac{1}{2} Z_T \gamma^\lambda \gamma^\mu \gamma^\nu \right) \gamma_5 B + \text{h.c} \right\}. \end{aligned} \quad (3.17)$$

Finally, the Lagrange density describing the interaction of the Δ -decuplet fields with the Goldstone boson fields is

$$\begin{aligned} \mathcal{L}_{P\Delta} &= H \text{tr} \left\{ (\bar{\Delta}^\mu \cdot \gamma_\nu \gamma_5 \Delta_\mu) i U^\nu \right\} \\ &= -\frac{H}{2f} \text{tr} \left\{ (\bar{\Delta}^\mu \cdot \gamma^\nu \gamma_5 \Delta_\mu) \partial_\nu \Phi \right\}. \end{aligned} \quad (3.18)$$

The dot product in Eqs. 3.16, 3.17 and 3.18 implies

$$\begin{aligned} (\bar{\Delta}^\mu \cdot \Delta_\nu)_b^a &= \bar{\Delta}_{bcd}^\mu \Delta_\nu^{acd}, \\ (\Phi \cdot \Delta_\nu)_b^a &= \epsilon_{cdb} \Phi_e^d \Delta_\nu^{dea}, \\ (\bar{\Delta}^\mu \cdot \Phi)_b^a &= \epsilon^{cda} \bar{\Delta}_{deb}^\mu \Phi_d^e, \end{aligned} \quad (3.19)$$

where $\epsilon^{abc} = \epsilon_{abc}$ is the anti-symmetric Levi-Civita tensor. The products $(\bar{\Delta}^\mu \cdot \Delta_\nu)_b^a$, $(\Phi \cdot \Delta_\nu)_b^a$ and $(\bar{\Delta}^\mu \cdot \Phi)_b^a$ transform like octets in flavor space.

The propagators of the particles included in the theory are

$$\begin{aligned} S_{[8]}(p) &= \frac{1}{p^2 - m_{[8]}^2 + i\epsilon}, \\ S_V^{\mu\nu, \alpha\beta}(p) &= -\frac{1}{m_V^2} \frac{1}{p^2 - m_V^2 + i\epsilon} \left[(m_V^2 - p^2) g^{\mu\alpha} g^{\nu\beta} + g^{\mu\alpha} p^\nu p^\beta \right. \\ &\quad \left. - g^{\mu\beta} p^\nu p^\alpha - (m_V^2 - p^2) g^{\nu\alpha} g^{\mu\beta} - g^{\nu\alpha} p^\mu p^\beta + g^{\nu\beta} p^\mu p^\alpha \right], \\ S_B(p) &= \frac{\not{p} + M_B}{p^2 - M_B^2 + i\epsilon}, \\ S_\Delta^{\mu\nu}(p) &= \frac{\not{p} + M_\Delta}{p^2 - M_\Delta^2 + i\epsilon} \left[-g^{\mu\nu} + \frac{1}{3} \gamma^\mu \gamma^\nu + \frac{2}{3 M_\Delta^2} p^\mu p^\nu \right. \\ &\quad \left. - \frac{1}{3 M_\Delta} (p^\mu \gamma^\nu - p^\nu \gamma^\mu) \right], \end{aligned} \quad (3.20)$$

where $S_{[8]}(p)$ is the propagator of the Goldstone bosons with mass $m_{[8]}$, $S_V^{\mu\nu,\alpha\beta}(p)$ is the propagator of the vector meson (in the tensor representation) with a mass m_V , $S_B(p)$ is the propagator of an octet baryon with a mass M_B , and $S_\Delta^{\mu\nu}(p)$ is the usual Rarita-Schwinger propagator for a spin-3/2 particle with a mass M_Δ . For all propagators above, p is the four-momentum of the propagating particle.

The values of the coupling constants have been discussed in more detail in [19, 61]. We use $f = 93$ MeV in this work. The coupling constant of the nucleon to the axial vector imposes a constraint on the values $F_A + D_A \simeq 1.28$. Further constraints on the values of the other parameters describing the coupling of the pseudoscalar mesons with the octet and decuplet baryons can be imposed by performing a large- N_c operator analysis [62, 63]

$$F_A = \frac{2}{3}D_A, \quad C_A = 2D_A, \quad H = 9F_A - 3D_A. \quad (3.21)$$

The value of the parameter $Z_A = 0.72$, taken from [64], is determined by a detailed coupled-channel study of meson-baryon scattering that was based on the chiral SU(3) Lagrangian described in [19]. The parameters describing the coupling of the vector mesons to the octet and decuplet baryons can be constrained from the values of ρNN and $\rho N\Delta$ coupling constants, suggesting $F_V + D_V \simeq 6.5$ and $C_T \simeq 10.6$, together with constraints from the large- N_c analysis

$$\begin{aligned} F_T &= \frac{2}{3}D_T, & G_T &= -\frac{1}{3}D_T, & C_T &= 4D_T, \\ D_V &= 0, & F_V &= G_V, & C_V &= 0. \end{aligned} \quad (3.22)$$

3.3 Isospin decomposition

Since we assume isospin to be a perfect symmetry, pseudoscalar meson, vector-meson and baryon octet fields are decomposed into their isospin-symmetric components:

$$\begin{aligned} \Phi &= \vec{\tau} \cdot \vec{\pi}(140) + \alpha^\dagger \cdot K(494) + K^\dagger(494) \cdot \alpha + \eta(547)\lambda_8, \\ \Phi_\mu &= \vec{\tau} \cdot \vec{\rho}_\mu(770) + \alpha^\dagger \cdot K_\mu(892) + K_\mu^\dagger(892) \cdot \alpha \\ &\quad \left(\frac{2}{3} + \frac{1}{\sqrt{3}}\lambda_8 \right) \omega_\mu(782) + \left(\frac{\sqrt{2}}{3} - \sqrt{\frac{2}{3}}\lambda_8 \right) \phi_\mu(1020), \end{aligned}$$

$$\sqrt{2} B = \alpha^\dagger \cdot N(939) + \lambda_8 \Lambda(1115) + \vec{\tau} \cdot \vec{\Sigma}(1195) + \Xi^t(1315) i \sigma_2 \cdot \alpha, \quad (3.23)$$

where $\alpha^\dagger = \frac{1}{\sqrt{2}} (\lambda_4 + i\lambda_5, \lambda_6 + i\lambda_7)$ and $\vec{\tau} = (\lambda_1, \lambda_2, \lambda_3)$, with λ_i the standard Gell-Mann generators of the $SU(3)$ algebra. The numbers in brackets denote the approximate masses of the fields in units of MeV. The decomposition of the octet baryon fields, the pseudoscalar mesons, and vector mesons given in Eq. 3.23 makes use of the isospin-singlet fields $\eta, \omega_\mu, \phi_\mu$ and Λ , the isospin-doublet fields

$$\begin{aligned} K &= \begin{pmatrix} K^+ \\ K^0 \end{pmatrix}, & K^\dagger &= \begin{pmatrix} K^- \\ \bar{K}^0 \end{pmatrix}, & K_\mu &= \begin{pmatrix} K_\mu^+ \\ K_\mu^0 \end{pmatrix}, & K_\mu^\dagger &= \begin{pmatrix} K_\mu^- \\ \bar{K}_\mu^0 \end{pmatrix}, \\ N &= \begin{pmatrix} p \\ n \end{pmatrix}, & \bar{N} &= \begin{pmatrix} \bar{p} \\ \bar{n} \end{pmatrix}, & \Xi &= \begin{pmatrix} \Xi^0 \\ \Xi^- \end{pmatrix}, & \bar{\Xi} &= \begin{pmatrix} \bar{\Xi}^0 \\ \bar{\Xi}^+ \end{pmatrix} \end{aligned} \quad (3.24)$$

and the isospin triplet fields

$$\vec{\pi} = (\pi^{(1)}, \pi^{(2)}, \pi^{(3)}) , \quad \vec{\Sigma} = (\Sigma^{(1)}, \Sigma^{(2)}, \Sigma^{(3)}) , \quad \vec{\rho}_\mu = (\rho_\mu^{(1)}, \rho_\mu^{(2)}, \rho_\mu^{(3)}) . \quad (3.25)$$

The connection to the physical fields for the $\vec{\pi}, \vec{\Sigma}$ and $\vec{\rho}_\mu$ is given by

$$\begin{aligned} \pi^+ &= \frac{1}{\sqrt{2}} (\pi^{(1)} - i\pi^{(2)}) , & \Sigma^+ &= \frac{1}{\sqrt{2}} (\Sigma^{(1)} - i\Sigma^{(2)}) , & \rho_\mu^+ &= \frac{1}{\sqrt{2}} (\rho_\mu^{(1)} - i\rho_\mu^{(2)}) , \\ \pi^- &= \frac{1}{\sqrt{2}} (\pi^{(1)} + i\pi^{(2)}) , & \Sigma^- &= \frac{1}{\sqrt{2}} (\Sigma^{(1)} + i\Sigma^{(2)}) , & \rho_\mu^- &= \frac{1}{\sqrt{2}} (\rho_\mu^{(1)} + i\rho_\mu^{(2)}) . \end{aligned} \quad (3.26)$$

Note, that the isospin Pauli matrices σ_i act exclusively in the space of isospin-doublet fields K, K_μ, N, Ξ and the matrix-valued isospin doublet α . This implies, for example, $(\vec{\sigma} \cdot \alpha)_a = \sum_b \vec{\sigma}_{ab} \alpha_b$.

The isospin reduction of the $SU(3)$ -symmetric interaction terms is conveniently derived applying the set of identities

$$\begin{aligned} \vec{\tau} \cdot \alpha^\dagger &= \alpha^\dagger \cdot \vec{\sigma}, & \alpha^\dagger \cdot \vec{\tau} &= 0, & \alpha \cdot \vec{\tau} &= \vec{\sigma} \cdot \alpha, \\ \vec{\tau} \cdot \alpha &= 0, & \tau_i \lambda_8 &= \lambda_8 \tau_i & \text{tr}(\tau_i \tau_j) &= 2\delta_{ij}, \\ \text{tr}(\alpha_i \alpha_j^\dagger) &= 2\delta_{ij}, & \alpha \cdot \alpha &= 0 & \alpha^\dagger \cdot \alpha^\dagger &= 0 \end{aligned} \quad (3.27)$$

completed with the following properties of the commutators and anti-commutators

$$\begin{aligned}
[\alpha, \alpha^\dagger]_- &= -\vec{\tau} \cdot \vec{\sigma} - \sqrt{3}\lambda_8, & [\alpha, \alpha^\dagger]_+ &= \frac{4}{3}1 - \frac{1}{\sqrt{3}}\lambda_8 + \vec{\tau} \cdot \vec{\sigma}, \\
[\tau_i, \tau_j]_- &= 2i\epsilon_{ijk}\tau_k, & [\tau_i, \tau_j]_+ &= \left(\frac{2}{\sqrt{3}}\lambda_8 + \frac{4}{3}1\right)\delta_{ij} \\
[\lambda_8, \alpha^\dagger]_- &= \sqrt{3}\alpha^\dagger, & [\lambda_8, \alpha^\dagger]_+ &= -\frac{1}{\sqrt{3}}\alpha^\dagger \\
[\lambda_8, \lambda_8]_+ &= \frac{4}{3}1 - \frac{2}{\sqrt{3}}\lambda_8, & [\lambda_8, \alpha]_- &= -\sqrt{3}\alpha \\
[\lambda_8, \alpha]_+ &= -\frac{1}{\sqrt{3}}\alpha, & [\lambda_8, \tau]_+ &= \frac{2}{\sqrt{3}}\tau
\end{aligned} \tag{3.28}$$

By means of Eqs. 3.27 and 3.28 it is straightforward to decompose the interaction Lagrangian into isospin components.

3.3.1 Isospin decomposition of \mathcal{L}_{PB}

Making use of the isospin decomposition of the pseudoscalar meson fields and the baryon fields given in Eq. 3.23, together with the isospin algebra given in Eqs. 3.27 and 3.28, the interaction Lagrange density \mathcal{L}_{PB} can be decomposed in the isospin basis as follows

$$\mathcal{L}_{PB} = \mathcal{L}_\pi + \mathcal{L}_K + \mathcal{L}_\eta \tag{3.29}$$

where \mathcal{L}_π , \mathcal{L}_K , \mathcal{L}_η describe the interaction of the pion, kaon and η fields with the baryon-octet fields, respectively. The appropriate terms are collected in:

$$\begin{aligned}
\mathcal{L}_\pi &= \frac{F_A + D_A}{2f} \vec{\pi} \cdot (\bar{N} \vec{\sigma} N) + \frac{D_A}{2f} \frac{2}{\sqrt{3}} \bar{\Lambda} (\vec{\pi} \cdot \vec{\Sigma}) + \frac{D_A}{2f} \frac{2}{\sqrt{3}} (\vec{\pi} \cdot \vec{\Sigma}) \Lambda \\
&+ \frac{F_A}{2f} 2i\vec{\pi} \cdot (\vec{\Sigma} \times \vec{\Sigma}) + \frac{F_A - D_A}{2f} \vec{\pi} \cdot (\bar{\Xi} \vec{\sigma} \Xi), \\
\mathcal{L}_\eta &= \frac{3F_A - D_A}{2\sqrt{3}f} \eta (\bar{N} N) - \frac{D_A}{2f} \frac{2}{\sqrt{3}} \bar{\Lambda} \eta \Lambda \\
&+ \frac{D_A}{2f} \frac{2}{\sqrt{3}} \vec{\Sigma} \cdot (\eta \vec{\Sigma}) - \frac{3F_A + D_A}{2\sqrt{3}f} \eta (\bar{\Xi} \Xi), \\
\mathcal{L}_K &= -\frac{3F_A + D_A}{2\sqrt{3}f} (\bar{N} K) \Lambda - \frac{F_A - D_A}{2f} (\bar{N} \vec{\sigma} K) \cdot \vec{\Sigma} \\
&+ \frac{3F_A - D_A}{2\sqrt{3}f} \bar{\Lambda} (\Xi^t i\sigma_2 K) + \frac{F_A + D_A}{2f} \vec{\Sigma} \cdot (\Xi^t i\sigma_2 \vec{\sigma} K)
\end{aligned}$$

$$\begin{aligned}
& - \frac{3F_A + D_A}{2\sqrt{3}f} \bar{\Lambda} \left(K^\dagger N \right) - \frac{F_A - D_A}{2f} \vec{\Sigma} \cdot \left(K^\dagger \vec{\sigma} N \right) \\
& - \frac{3F_A - D_A}{2\sqrt{3}f} \left(K^\dagger i\sigma_2 \bar{\Xi}^t \right) \Lambda - \frac{F_A + D_A}{2f} \vec{\Sigma} \cdot \left(K^\dagger \vec{\sigma} i\sigma_2 \bar{\Xi}^t \right),
\end{aligned} \tag{3.30}$$

where we have suppressed the Lorentz structure of the vertices.

The Lagrangian given by Eq. 3.29 is invariant under $SU(3)$ flavor symmetry. By expressing the coupling constants in terms of the $NN\pi$ coupling constants g and the ratio $\alpha = F_A/(D_A + F_A)$, one gets the same coupling constants as given in [65]. However, one should note that the convention for the pseudoscalar Goldstone bosons used in this work is different, which accounts for the differences in sign for \mathcal{L}_K for the terms involving the K^\dagger fields.

3.3.2 Isospin decomposition of \mathcal{L}_{VB}

Making use of the isospin decomposition of the pseudoscalar meson fields and the baryon fields, together with the isospin algebra given in Eqs. 3.27 and 3.28, the interaction Lagrange density \mathcal{L}_{VB} can be decomposed in the isospin basis as follows

$$\mathcal{L}_{VB} = \mathcal{L}_\rho + \mathcal{L}_{K_\mu} + \mathcal{L}_\omega + \mathcal{L}_\phi \tag{3.31}$$

where \mathcal{L}_ρ , \mathcal{L}_{K_μ} , \mathcal{L}_ω and \mathcal{L}_ϕ describe the interaction of the ρ , K , ω and ϕ vector meson fields with the baryon octet fields, respectively.

$$\begin{aligned}
\mathcal{L}_\rho &= \frac{F_V + D_V}{2} \vec{\rho}_\mu \cdot (\bar{N} \vec{\sigma} N) + \frac{F_V}{2} 2i \vec{\rho}_\mu \cdot (\vec{\Sigma} \times \vec{\Sigma}) + \frac{D_V}{2} \frac{2}{\sqrt{3}} (\vec{\Sigma} \cdot \vec{\rho}_\mu) \Lambda \\
&+ \frac{D_V}{2} \frac{2}{\sqrt{3}} \bar{\Lambda} (\vec{\rho}_\mu \cdot \vec{\Sigma}) + \frac{F_V - D_V}{2} \vec{\rho}_\mu \cdot (\bar{\Xi} \vec{\sigma} \Xi), \\
\mathcal{L}_{K_\mu} &= -\frac{3F_V + D_V}{2\sqrt{3}} (\bar{N} K_\mu) \Lambda - \frac{F_V - D_V}{2} (\bar{N} \vec{\sigma} K_\mu) \cdot \vec{\Sigma} \\
&+ \frac{F_V + D_V}{2} \vec{\Sigma} \cdot (\Xi^t i\sigma_2 \vec{\sigma} K_\mu) + \frac{3F_V - D_V}{2\sqrt{3}} \bar{\Lambda} (\Xi^t i\sigma_2 K_\mu) \\
&- \frac{3F_V + D_V}{2\sqrt{3}} \bar{\Lambda} (K_\mu^\dagger N) - \frac{F_V - D_V}{2} \bar{\Sigma} \cdot (K_\mu^\dagger \vec{\sigma} N) \\
&- \frac{F_V + D_V}{2} (K_\mu^\dagger \vec{\sigma} i\sigma_2 \bar{\Xi}^t) \vec{\Sigma} - \frac{3F_V - D_V}{2\sqrt{3}} (K_\mu^\dagger i\sigma_2 \bar{\Xi}^t) \Lambda,
\end{aligned}$$

$$\begin{aligned}
\mathcal{L}_\omega &= \frac{(F_V + D_V + 2G_V)}{2} \omega_\mu (\bar{N}N) + \frac{D_V + 3G_V}{3} \bar{\Lambda} \omega_\mu \Lambda \\
&+ (D_V + G_V) \vec{\Sigma} \cdot (\omega_\mu \vec{\Sigma}) + \frac{-F_V + D_V + 2G_V}{2} \omega_\mu (\bar{\Xi}\Xi) , \\
\mathcal{L}_\phi &= \frac{-F_V + D_V + G_V}{\sqrt{2}} \phi_\mu (\bar{N}N) + \frac{4D_V + 3G_V}{3\sqrt{2}} \bar{\Lambda} \phi_\mu \Lambda \\
&+ \frac{G_V}{\sqrt{2}} (\vec{\Sigma} \vec{\Sigma}) \phi^\mu + \frac{F_V + D_V + G_V}{\sqrt{2}} \phi_\mu (\bar{\Xi}\Xi) , \tag{3.32}
\end{aligned}$$

where we have suppressed the Lorentz structure of the vertices. The same isospin decomposition holds for the part of the Lagrange density involving the tensor couplings. In this case, F_V is replaced by F_T , D_V is replaced by D_T , and G_V is replaced by G_T . As expected, the isospin decomposition of the Lagrange density describing the coupling of the isospin-triplet field η to the octet baryons is similar to the Lagrange density describing the coupling of the π field to the octet baryon, where $F_A \leftrightarrow F_V$ and $D_A \leftrightarrow D_V$.

3.3.3 Coupled-channel states

A list of all the coupled channels considered in this work is given in Table 3.1. T_i are the isospin-1/2 to -3/2 transition matrices and are normalized by $T_i^\dagger T_j = \delta_{ij} - \sigma_i \sigma_j / 3$, together with $T \cdot T^\dagger = 1$. As already mentioned, the Pauli matrices σ_i act on the isospin-doublet fields N and Ξ . By providing the list of coupled-channel states with specific isospin (I) and strangeness (S), the phase convention of the states is specified.

Table 3.1: The definition of coupled-channel states (I, S) with isospin (I) and strangeness (S) involving only octet baryon states. T_i are the isospin 1/2 to 3/2 transition matrices and are normalized by $T_i^\dagger T_j = \delta_{ij} - \sigma_i \sigma_j / 3$.

(0,2)	(1,2)	$(\frac{1}{2}, 1)$	$(\frac{3}{2}, 1)$
$\left(\begin{array}{c} \frac{1}{\sqrt{2}} (\bar{\Xi} N) \end{array} \right)$	$\left(\begin{array}{c} \frac{1}{\sqrt{2}} (\bar{\Xi} \bar{\sigma} N) \end{array} \right)$	$\left(\begin{array}{c} (\bar{\Lambda} N) \\ \frac{1}{\sqrt{3}} (\bar{\Sigma} \cdot \sigma N) \\ - (i \sigma_2 \bar{\Xi}^t \Lambda) \\ \frac{1}{\sqrt{3}} (\bar{\sigma} i \sigma_2 \bar{\Xi}^t \cdot \Sigma) \end{array} \right)$	$\left(\begin{array}{c} (\bar{\Sigma} \cdot T N) \\ (\Sigma \cdot T i \sigma_2 \bar{\Xi}^t) \end{array} \right)$
(0,0)	(1,0)	(2,0)	$(\frac{1}{2}, -1)$
$\left(\begin{array}{c} \frac{1}{\sqrt{2}} (\bar{N} N) \\ (\bar{\Lambda} \Lambda) \\ \frac{1}{\sqrt{3}} (\bar{\Sigma} \Sigma) \\ \frac{1}{\sqrt{2}} (\bar{\Xi} \Xi) \end{array} \right)$	$\left(\begin{array}{c} \frac{1}{\sqrt{2}} (\bar{N} \bar{\sigma} N) \\ \frac{1}{i \sqrt{2}} (\bar{\Sigma} \times \Sigma) \\ \frac{1}{\sqrt{2}} (\bar{\Xi} \bar{\sigma} \Xi) \\ (\bar{\Lambda} \bar{\Sigma}) \\ (\bar{\Sigma} \Lambda) \end{array} \right)$	$\left(\begin{array}{c} (\bar{\Sigma} \cdot S \cdot \Sigma) \end{array} \right)$	$\left(\begin{array}{c} - (i \sigma_2 \bar{N}^t \Lambda) \\ \frac{1}{\sqrt{3}} (\bar{\sigma} i \sigma_2 \bar{N}^t \cdot \Sigma) \\ (\bar{\Lambda} \Xi) \\ \frac{1}{\sqrt{3}} (\bar{\Sigma} \cdot \bar{\sigma} \Xi) \end{array} \right)$
$(\frac{3}{2}, -1)$	(0,-2)	(1,-2)	
$\left(\begin{array}{c} (\Sigma \cdot T i \sigma_2 \bar{N}^t) \\ (\bar{\Sigma} \cdot T \Xi) \end{array} \right)$	$\left(\begin{array}{c} \frac{1}{\sqrt{2}} (\bar{N} \Xi) \end{array} \right)$	$\left(\begin{array}{c} \frac{1}{\sqrt{2}} (\bar{N} \bar{\sigma} \Xi) \end{array} \right)$	

3.4 The scattering of spin-1/2 particles

Once the Lagrange density is given, the question arises, how can one calculate the scalar functions F_i that describe the scattering of spin-1/2 particles.

As presented in Sec. 2.3, the scattering of spin-1/2 particles is described by the on-shell scattering amplitude

$$T_{\frac{1}{2} \frac{1}{2} \rightarrow \frac{1}{2} \frac{1}{2}} = \sum_{i=1}^4 \sum_{\pm} F_i^{\pm} \langle T_{\pm}^{(i)} \rangle_{\frac{1}{2} \frac{1}{2} \rightarrow \frac{1}{2} \frac{1}{2}} \quad (3.33)$$

$$\begin{aligned} T^{(1)} &= \mathbb{1} \times \mathbb{1}, & T^{(2)} &= \gamma_\mu \times \gamma^\mu, \\ T^{(3)} &= \mathbb{1} \times \not{k}, & T^{(4)} &= \not{k} \times \mathbb{1}, \end{aligned}$$

in terms of eight scalar functions F_i^\pm , where the on-shell interaction is given by the $\langle \cdots \rangle$ notation used in Eq. 3.33,

$$\begin{aligned} \langle \bar{\Gamma} \times \Gamma \rangle_{\frac{1}{2}\frac{1}{2} \rightarrow \frac{1}{2}\frac{1}{2}}^\pm &= \left(\bar{u}(\bar{p}_1) \bar{\Gamma} P_\pm v(\bar{p}_2) \right) \left(\bar{v}(p_2) P_\pm \Gamma u(p_1) \right), \\ P_+ &= \mathbb{1}, \quad P_- = \gamma_5; \end{aligned} \quad (3.34)$$

where for notational clarity the reference to the helicities of initial and final states has been suppressed. The invariant amplitudes F_{1-4}^\pm are functions of the Mandelstam variables s, t and u and depend on the on-shell evaluation of the scattering amplitudes only. We introduce a set of eight auxiliary helicity amplitudes

$$\begin{aligned} \phi_{ij}^\pm &= \frac{1}{d_{+\lambda, \bar{\lambda}}^{(J_0)}(\theta)} \langle \bar{\lambda}_1, \bar{\lambda}_2 | T | +\lambda_1, +\lambda_2 \rangle \pm \frac{(-1)^{S_1-S_2}}{d_{-\lambda, \bar{\lambda}}^{(J_0)}(\theta)} \langle \bar{\lambda}_1, \bar{\lambda}_2 | T | -\lambda_1, -\lambda_2 \rangle, \\ J_0 &= \text{Min}(|\bar{\lambda}|, |\lambda|), \end{aligned} \quad (3.35)$$

where $\lambda = \lambda_1 - \lambda_2$ and $\bar{\lambda} = \bar{\lambda}_1 - \bar{\lambda}_2$ are the total helicities of the initial and final state, respectively, i and j correspond to the labels of the incoming and outgoing states. With the definition for the parity eigenstates for the $\frac{1}{2}\frac{1}{2}$ system given in Eq. 2.25, the explicit definition of the auxiliary helicity amplitudes takes the form

$$\begin{aligned} \phi_{11}^\pm &= \left\langle \frac{1}{2}, \frac{1}{2} \left| T \right| \frac{1}{2}, \frac{1}{2} \right\rangle \pm \left\langle \frac{1}{2}, \frac{1}{2} \left| T \right| -\frac{1}{2}, -\frac{1}{2} \right\rangle, \\ \phi_{12}^\pm &= -\frac{1}{\sqrt{2} \sin \frac{\theta}{2} \cos \frac{\theta}{2}} \left\langle \frac{1}{2}, \frac{1}{2} \left| T \right| \frac{1}{2}, -\frac{1}{2} \right\rangle \pm \frac{1}{\sqrt{2} \sin \frac{\theta}{2} \cos \frac{\theta}{2}} \left\langle \frac{1}{2}, \frac{1}{2} \left| T \right| -\frac{1}{2}, \frac{1}{2} \right\rangle, \\ \phi_{21}^\pm &= \frac{1}{\sqrt{2} \sin \frac{\theta}{2} \cos \frac{\theta}{2}} \left\langle \frac{1}{2}, -\frac{1}{2} \left| T \right| \frac{1}{2}, \frac{1}{2} \right\rangle \pm \frac{1}{\sqrt{2} \sin \frac{\theta}{2} \cos \frac{\theta}{2}} \left\langle \frac{1}{2}, -\frac{1}{2} \left| T \right| -\frac{1}{2}, -\frac{1}{2} \right\rangle, \\ \phi_{22}^\pm &= \frac{1}{\sin^2 \frac{\theta}{2}} \left\langle \frac{1}{2}, -\frac{1}{2} \left| T \right| \frac{1}{2}, -\frac{1}{2} \right\rangle \pm \frac{1}{\cos^2 \frac{\theta}{2}} \left\langle \frac{1}{2}, -\frac{1}{2} \left| T \right| -\frac{1}{2}, \frac{1}{2} \right\rangle. \end{aligned} \quad (3.36)$$

The auxiliary helicity amplitudes given in Eq. 3.36 can be evaluated both by using the decomposition given in Eq. 3.33, as well as making use of the interaction described by the Lagrange density. By using the decomposition of the scattering

amplitude T into invariant amplitudes, we derive the expressions of the auxiliary helicity amplitudes for a generic interaction

$$\begin{aligned}
\phi_{11}^{\pm} &= \mp 2 \bar{\alpha}_{\mp} \alpha_{\mp} F_1^{\pm} \mp 2 (\bar{\beta}_{\mp} \beta_{\mp} - \bar{\beta}_{\pm} \beta_{\pm} \cos \theta) F_2^{\pm} \\
&\quad \mp \bar{\alpha}_{\mp} ((\bar{E}_1 - \bar{E}_2) \beta_{\mp} + 2 \bar{p} \beta_{\pm} \cos \theta) F_3^{\pm} \\
&\quad \mp \alpha_{\mp} ((E_1 - E_2) \bar{\beta}_{\mp} + 2 p \bar{\beta}_{\pm} \cos \theta) F_4^{\pm}, \\
\phi_{12}^{\pm} &= 2\sqrt{2} \bar{\beta}_{\pm} \alpha_{\pm} F_2^{\pm} - 2\sqrt{2} \bar{\alpha}_{\mp} \alpha_{\pm} \bar{p} F_3^{\pm}, \\
\phi_{21}^{\pm} &= 2\sqrt{2} \beta_{\pm} \bar{\alpha}_{\pm} F_2^{\pm} - 2\sqrt{2} \alpha_{\mp} \bar{\alpha}_{\pm} p F_4^{\pm}, \\
\phi_{22}^{\pm} &= \pm 4 \bar{\alpha}_{\pm} \alpha_{\pm} F_2^{\pm},
\end{aligned} \tag{3.37}$$

together with the inverted relations

$$\begin{aligned}
F_1^{\pm} &= \mp \frac{1}{2 \bar{\alpha}_{\mp} \alpha_{\mp}} \phi_{11}^{\pm} + \frac{1}{4 \sqrt{2} \bar{\alpha}_{\mp} \alpha_{\pm} \alpha_{\mp} \bar{p}} (\beta_{\mp} (\bar{E}_1 - \bar{E}_2) + 2 \beta_{\pm} \bar{p} \cos \theta) \phi_{12}^{\pm} \\
&\quad + \frac{1}{4 \sqrt{2} \bar{\alpha}_{\mp} \bar{\alpha}_{\pm} \alpha_{\mp} p} (\bar{\beta}_{\mp} (E_1 - E_2) + 2 \bar{\beta}_{\pm} p \cos \theta) \phi_{21}^{\pm} \\
&\quad \mp \frac{1}{\bar{\alpha}_{\mp} \bar{\alpha}_{\pm} \alpha_{\mp} \alpha_{\pm} \bar{p} p} \left[\bar{\beta}_{\mp} \beta_{\pm} \bar{p} (E_1 - E_2) \right. \\
&\quad \left. + \bar{\beta}_{\pm} \beta_{\mp} p (\bar{E}_1 - \bar{E}_2) + 2 \bar{p} p (\bar{\beta}_{\mp} \beta_{\mp} + \bar{\beta}_{\pm} \beta_{\pm} \cos \theta) \right] \\
F_2^{\pm} &= \pm \frac{1}{4 \bar{\alpha}_{\pm} \alpha_{\pm}} \phi_{22}^{\pm}, \\
F_3^{\pm} &= -\frac{1}{2 \sqrt{2} \bar{\alpha}_{\mp} \alpha_{\pm} \bar{p}} \phi_{12}^{\pm} \pm \frac{\bar{\beta}_{\pm}}{4 \bar{\alpha}_{\pm} \bar{\alpha}_{\mp} \alpha_{\pm} \bar{p}} \phi_{22}^{\pm}, \\
F_4^{\pm} &= -\frac{1}{2 \sqrt{2} \bar{\alpha}_{\pm} \alpha_{\mp} p} \phi_{12}^{\pm} \pm \frac{\beta_{\pm}}{4 \bar{\alpha}_{\mp} \alpha_{\mp} \alpha_{\pm} p} \phi_{22}^{\pm},
\end{aligned} \tag{3.38}$$

where p and \bar{p} are the center-of-mass momenta in the incoming and outgoing channels, respectively, and we recall the definitions of α_{\pm} and β_{\pm} from Eq. 2.37.

Table 3.2: t -channel coupling constants $[C_{[8]}^{(I,S)}]_{ab}$ specifying the interaction strength as defined in Eq. 3.39. Octet states a and b are defined in Table 3.1.

(I,S)	$(a, b) : [C_{\pi}^{(I,S)}]_{a,b}$	$(a, b) : [C_{\eta}^{(I,S)}]_{a,b}$	$(a, b) : [C_K^{(I,S)}]_{a,b}$
(0,2)	$(1, 1) : 3(F_A^2 - D_A^2)$	$(1, 1) : \frac{1}{3}(9F_A^2 - D_A^2)$	
(1,2)	$(1, 1) : -(F_A^2 - D_A^2)$	$(1, 1) : \frac{1}{3}(9F_A^2 - D_A^2)$	
$(\frac{1}{2}, 1)$	$(1, 2) : 2D_A(F_A + D_A)$	$(1, 1) : -\frac{2}{3}D_A(3F_A - D_A)$	$(1, 3) : -\frac{1}{3}(9F_A^2 - D_A)^2$
	$(2, 2) : 4F_A(F_A + D_A)$	$(2, 2) : \frac{2}{3}D_A(3F_A - D_A)$	$(1, 4) : (F_A - D_A)(3F_A - D_A)$
	$(3, 4) : 2D_A(F_A - D_A)$	$(3, 3) : -\frac{2}{3}D_A(3F_A + D_A)$	$(2, 3) : -(3F_A + D_A)(F_A + D_A)$
	$(4, 4) : 4F_A(F_A - D_A)$	$(4, 4) : \frac{2}{3}D_A(3F_A + D_A)$	$(2, 4) : -(F_A^2 - D_A^2)$
$(\frac{3}{2}, 1)$	$(1, 1) : -2F_A(F_A + D_A)$	$(1, 1) : \frac{2}{3}D_A(3F_A - D_A)$	$(1, 2) : 2(F_A^2 - D_A^2)$
	$(2, 2) : -2F_A(F_A - D_A)$	$(2, 2) : \frac{2}{3}D_A(3F_A + D_A)$	
(0,0)	$(1, 1) : 3(F_A + D_A)^2$	$(1, 1) : \frac{1}{3}(3F_A - D_A)^2$	$(1, 2) : \frac{\sqrt{2}}{3}(3F_A + D_A)^2$
	$(2, 3) : \frac{4}{\sqrt{3}}D_A^2$	$(2, 2) : \frac{4}{3}D_A^2$	$(1, 3) : \sqrt{6}(F_A - D_A)^2$
	$(3, 3) : 8F_A^2$	$(3, 3) : \frac{4}{3}D_A^2$	$(2, 4) : \frac{\sqrt{2}}{3}(3F_A - D_A)^2$
	$(4, 4) : 3(F_A - D_A)^2$	$(4, 4) : \frac{1}{3}(3F_A + D_A)^2$	$(3, 4) : \sqrt{6}(F_A + D_A)^2$
(1,-2)	$(1, 1) : -(F_A^2 - D_A^2)$	$(1, 1) : \frac{1}{3}(9F_A^2 - D_A^2)$	

Table 3.2: Continued. t -channel coupling constants $[C_{[8]}^{(I,S)}]_{ab}$ specifying the interaction strength as defined in Eq. 3.39. Octet states a and b are defined in Table 3.1.

(I,S)	$(a, b) : [C_{\pi}^{(I,S)}]_{a,b}$	$(a, b) : [C_{\eta}^{(I,S)}]_{a,b}$	$(a, b) : [C_K^{(I,S)}]_{a,b}$
(1,0)	$(1, 1) : -(F_A + D_A)^2$ $(2, 2) : 4F_A^2$ $(2, 4) : -\frac{4\sqrt{6}}{3}F_A D_A$ $(2, 5) : -\frac{4\sqrt{6}}{3}D_A F_A$ $(3, 3) : -(F_A - D_A)^2$ $(4, 5) : \frac{4}{3}D_A^2$	$(1, 1) : \frac{1}{3}(3F_A - D_A)^2$ $(2, 2) : \frac{4}{3}D_A^2$ $(3, 3) : \frac{1}{3}(3F_A + D_A)^2$ $(4, 4) : -\frac{4}{3}D_A^2$ $(5, 5) : -\frac{4}{3}D_A^2$	$(1, 2) : 2(F_A - D_A)^2$ $(1, 4) : \frac{\sqrt{6}}{3}(3F_A + D_A)(F_A - D_A)$ $(1, 5) : \frac{\sqrt{6}}{3}(3F_A + D_A)(F_A - D_A)$ $(2, 3) : 2(F_A + D_A)^2$ $(3, 4) : -\frac{\sqrt{6}}{3}(3F_A - D_A)(F_A + D_A)$ $(3, 5) : -\frac{\sqrt{6}}{3}(3F_A - D_A)(F_A + D_A)$
(2,0)	$(1, 1) : -4F_A^2$	$(1, 1) : \frac{4}{3}D_A^2$	
$(\frac{1}{2}, -1)$	$(1, 2) : 2D_A(F_A + D_A)$ $(2, 2) : 4F_A(F_A + D_A)$ $(3, 4) : 2D_A(F_A - D_A)$ $(4, 4) : 4F_A(F_A - D_A)$	$(1, 1) : -\frac{2}{3}D_A(3F_A - D_A)$ $(2, 2) : \frac{2}{3}D_A(3F_A - D_A)$ $(3, 3) : -\frac{2}{3}D_A(3F_A + D_A)$ $(4, 4) : \frac{2}{3}D_A(3F_A + D_A)$	$(1, 3) : \frac{1}{3}(9F_A^2 - D_A^2)$ $(1, 4) : -(3F_A - D_A)(F_A - D_A)$ $(2, 3) : (F_A + D_A)(3F_A + D_A)$ $(2, 4) : (F_A^2 - D_A^2)$
$(\frac{3}{2}, -1)$	$(1, 1) : -2F_A(F_A + D_A)$ $(2, 2) : -2F_A(F_A - D_A)$	$(1, 1) : \frac{2}{3}D_A(3F_A - D_A)$ $(2, 2) : \frac{2}{3}D_A(3F_A + D_A)$	$(1, 2) : -2(F_A^2 - D_A^2)$
(0,-2)	$(1, 1) : 3(F_A^2 - D_A^2)$	$(1, 1) : \frac{1}{3}(9F_A^2 - D_A^2)$	

3.4.1 Invariant amplitudes for the t -channel exchange of a pseudoscalar meson

We first consider the case of the t -channel exchange of a pseudoscalar meson. In this case, the scattering amplitudes takes the expression

$$\begin{aligned} M_{t,[8]} &= \frac{C_{[8]}^{(I,S)}}{4f^2} (\bar{u}(\bar{p}_1)\gamma_5 \not{q} u(p_1)) S_{[8]}(p_1 - \bar{p}_1) (\bar{v}(p_2)\gamma_5 \not{q} v(\bar{p}_2)) \\ &= -\frac{C_{[8]}^{(I,S)}}{4f^2} \frac{(M_1 + \bar{M}_1)(M_2 + \bar{M}_2)}{t - m_{[8]}^2 + i\epsilon} (\bar{u}(\bar{p}_1)\gamma_5 u(p_1)) (\bar{v}(p_2)\gamma_5 v(\bar{p}_2)) \end{aligned} \quad (3.39)$$

where $C_{[8]}^{(I,S)}$ is given in Table 3.2 and $m_{[8]}$ is the mass of the exchange pseudoscalar meson. Using this definition of the scattering amplitude, one gets for the auxiliary helicity amplitudes

$$\begin{aligned} \phi_{11}^{\pm} &= -\frac{C_{[8]}^{(I,S)}}{4f^2} \frac{(M_1 + \bar{M}_1)(M_2 + \bar{M}_2)}{2(t - m_{[8]}^2 + i\epsilon)} (\pm \bar{\alpha}_{\mp} \alpha_{\mp} \mp \bar{\beta}_{\mp} \beta_{\mp} \\ &\quad \mp \bar{\alpha}_{\pm} \alpha_{\pm} \cos \theta \pm \bar{\beta}_{\pm} \beta_{\pm} \cos \theta) , \\ \phi_{22}^{\pm} &= -\frac{C_{[8]}^{(I,S)}}{4f^2} \frac{(M_1 + \bar{M}_1)(M_2 + \bar{M}_2)}{t - m_{[8]}^2 + i\epsilon} (\pm \bar{\alpha}_{\pm} \alpha_{\pm} \mp \bar{\beta}_{\pm} \beta_{\pm}) , \\ \phi_{12}^{\pm} &= -\frac{C_{[8]}^{(I,S)}}{4f^2} \frac{(M_1 + \bar{M}_1)(M_2 + \bar{M}_2)}{t - m_{[8]}^2 + i\epsilon} (\pm \alpha_{\pm} \bar{\beta}_{\pm} \mp \beta_{\pm} \bar{\alpha}_{\pm}) , \\ \phi_{21}^{\pm} &= -\frac{C_{[8]}^{(I,S)}}{4f^2} \frac{(M_1 + \bar{M}_1)(M_2 + \bar{M}_2)}{t - m_{[8]}^2 + i\epsilon} (\pm \bar{\alpha}_{\pm} \beta_{\pm} \mp \bar{\beta}_{\pm} \alpha_{\pm}) . \end{aligned}$$

By substituting these values for the auxiliary helicity amplitudes in Eq. 3.38, the invariant functions F_i^{\pm} describing the t -channel exchange of a pseudoscalar meson are

$$\begin{aligned} F_1^{\pm} &= -\frac{C_{[8]}^{(I,S)}}{4f^2} \left(\frac{1}{4} + \frac{1}{s} \bar{k} \cdot k \right) \frac{(M_1 + \bar{M}_1)(M_2 + \bar{M}_2)}{t - m_{[8]}^2 + i\epsilon} , \\ F_2^{\pm} &= \frac{C_{[8]}^{(I,S)}}{4f^2} \frac{1}{4} \frac{(M_1 + \bar{M}_1)(M_2 + \bar{M}_2)}{t - m_{[8]}^2 + i\epsilon} \left[1 - \frac{(M_1 \pm M_2)(\bar{M}_1 \pm \bar{M}_2)}{s} \right] , \end{aligned}$$

$$\begin{aligned}
F_3^\pm &= \frac{C_{[8]}^{(I,S)}}{4f^2} \frac{(M_1 + \bar{M}_1)(M_2 + \bar{M}_2)}{t - m_{[8]}^2 + i\epsilon} \frac{M_1 \pm M_2}{2s}, \\
F_4^\pm &= \frac{C_{[8]}^{(I,S)}}{4f^2} \frac{(M_1 + \bar{M}_1)(M_2 + \bar{M}_2)}{t - m_{[8]}^2 + i\epsilon} \frac{\bar{M}_1 \pm \bar{M}_2}{2s},
\end{aligned} \tag{3.40}$$

where k and \bar{k} are the relative four-momenta in the incoming and outgoing channel, respectively. As seen from the expressions above, the invariant amplitudes F_{1-4} are functions of the Mandelstam variables s and t , the rest masses of the incoming and outgoing baryons, respectively, and the rest mass of the exchange bosons. Moreover, they have no kinematical zeros or poles, keeping only the dynamical singularity given by the t -channel pole $t = m_{[8]}^2$.

3.4.2 Invariant amplitudes for the t -channel exchange of a vector meson

The t -channel exchange of a vector meson in the tensor representation is given by

$$M_{t,[9]} = M_{V,[9]} + M_{VT,[9]} + M_{TV,[9]} + M_{T,[9]}, \tag{3.41}$$

where $M_{V,[9]}$ describes the t -channel exchange of a vector meson in the tensor representation when the magnetic moments are turned to zero, $M_{T,[9]}$ describes the t -channel vector-meson exchange with the interaction reduced only to the tensor couplings, $M_{TV,[9]}$ and $M_{VT,[9]}$ represent the t -channel vector meson exchange with mixed couplings.

The scattering amplitude $M_{V,[9]}$ describing only the vector part of the t -channel exchange of a vector meson takes, in the tensor representation, the form

$$M_{V,[9]} = \frac{C_{V,[9]}^{(I,S)}}{m_V^2} (\bar{u}(\bar{p}_1) \gamma_\mu q_\nu u(p_1)) S_V^{\mu\nu,\alpha\beta}(q) (\bar{v}(p_2) \gamma_\alpha q_\beta v(\bar{p}_2)), \tag{3.42}$$

where $S_V^{\mu\nu,\alpha\beta}(q)$ is the vector-meson propagator with mass m_V and momentum $q = p_1 - \bar{p}_1$. The coupling constants specifying the interaction strength are given in Tables 3.3 and 3.4, with F_1 and F_2 taking the value F_V , D_1 and D_2 the value D_V , and G_1 and G_2 the value G_V .

Using the equivalence:

$$q_\nu S^{\mu\nu,\alpha\beta}(q)q_\beta = \frac{(q^\mu q^\alpha - q^2 g^{\mu\alpha})}{q^2 - m^2 + i\epsilon},$$

the expression of the scattering amplitude describing the vector part of the interaction becomes:

$$M_{V,[9]} = \frac{C_{V,[9]}^{(I,S)}}{m_V^2(t - m_V^2 + i\epsilon)} \left\{ (\bar{u}(\bar{p}_1)\not{q}u(p_1)) (\bar{v}(p_2)\not{q}v(\bar{p}_2)) \right. \\ \left. - t (\bar{u}(\bar{p}_1)\gamma_\mu u(p_1)) (\bar{v}(p_2)\gamma^\mu v(\bar{p}_2)) \right\}. \quad (3.43)$$

The invariant amplitudes describing the process are

$$F_1^\pm = \frac{C_{V,[9]}^{(I,S)}}{m_V^2(t - m_V^2 + i\epsilon)} \left\{ (M_1 - \bar{M}_1)(M_2 - \bar{M}_2) \left(\frac{k \cdot \bar{k}}{s} + \frac{1}{4} \right) \mp t \right\},$$

$$F_2^\pm = \frac{C_{V,[9]}^{(I,S)}}{m_V^2(t - m_V^2 + i\epsilon)} \times \left\{ \frac{(M_1 - \bar{M}_1)(M_2 - \bar{M}_2)((M_1 \pm M_2)(\bar{M}_1 \pm \bar{M}_2) + s)}{4s} \pm \frac{t}{2} \right\},$$

$$F_3^\pm = -\frac{C_{V,[9]}^{(I,S)}}{m_V^2(t - m_V^2 + i\epsilon)} \frac{(M_1 - \bar{M}_1)(M_2 - \bar{M}_2)(M_1 \pm M_2)}{2s},$$

$$F_4^\pm = -\frac{C_{V,[9]}^{(I,S)}}{m_V^2(t - m_V^2 + i\epsilon)} \frac{(M_1 - \bar{M}_1)(M_2 - \bar{M}_2)(\bar{M}_1 \pm \bar{M}_2)}{2s}. \quad (3.44)$$

The scattering amplitude $M_{T,[9]}$ describing the t -channel exchange of a vector meson in the tensor representation, when the interaction is reduced to the magnetic moments, is given by

$$M_{T,[9]} = \frac{m_V^2 C_{T,[9]}^{(I,S)}}{16f^2} (\bar{u}(\bar{p}_1)\sigma_{\mu\nu}u(p_1)) S_V^{\mu\nu,\alpha\beta}(q) (\bar{v}(p_2)\sigma_{\alpha\beta}v(\bar{p}_2)), \quad (3.45)$$

where the coupling coefficients are given in Tables 3.3 and 3.4, with F_1 and F_2 taking the value F_T , D_1 and D_2 the value D_T , and G_1 and G_2 the value G_T . The invariant

amplitudes calculated with the interaction given in Eq. 3.45 are

$$\begin{aligned}
F_1^\pm &= \frac{C_{T,[9]}^{(I,S)}}{16f^2(t - m_V^2 + i\epsilon)} \left\{ 2 \left(3 - \frac{4k \cdot \bar{k}}{s} \right) (t - m_V^2) \right. \\
&\quad + 4 \left(\frac{k \cdot \bar{k}}{s} + \frac{1}{4} \right) (2(M_1 \bar{M}_1 + M_2 \bar{M}_2) + 2s + t) \\
&\quad \left. - 2(M_1 + \bar{M}_1 \mp M_2 \mp \bar{M}_2)^2 \mp 4(M_1 + \bar{M}_1)(M_2 + \bar{M}_2) \right\} , \\
F_2^\pm &= \frac{C_{T,[9]}^{(I,S)}}{16f^2(t - m_V^2 + i\epsilon)} \left\{ - \frac{2(t - m_V^2)(M_1 \pm M_2)(\bar{M}_1 \pm \bar{M}_2)}{s} \right. \\
&\quad + \frac{((M_1 \pm M_2)(\bar{M}_1 \pm \bar{M}_2) + s)(2(M_1 \bar{M}_1 + M_2 \bar{M}_2) + 2s + t)}{s} \\
&\quad \left. - 2(M_1 + \bar{M}_1 \pm M_2 \pm \bar{M}_2)^2 \pm 2(M_1 + \bar{M}_1)(M_2 + \bar{M}_2) \right\} , \\
F_3^\pm &= \frac{C_{T,[9]}^{(I,S)}}{16f^2(t - m_V^2 + i\epsilon)} \left\{ \frac{4(t - m_V^2)(M_1 \pm M_2)}{s} \right. \\
&\quad \left. - \frac{2(M_1 \pm M_2)(2(M_1 \bar{M}_1 + M_2 \bar{M}_2) + 2s + t)}{s} \right. \\
&\quad \left. + 4(M_1 + \bar{M}_1 \pm M_2 \pm \bar{M}_2) \right\} , \\
F_4^\pm &= \frac{C_{T,[9]}^{(I,S)}}{16f^2(t - m_V^2 + i\epsilon)} \left\{ \frac{4(t - m_V^2)(\bar{M}_1 \pm \bar{M}_2)}{s} \right. \\
&\quad \left. - \frac{2(\bar{M}_1 \pm \bar{M}_2)(2(M_1 \bar{M}_1 + M_2 \bar{M}_2) + 2s + t)}{s} \right. \\
&\quad \left. + 4(M_1 + \bar{M}_1 \pm M_2 \pm \bar{M}_2) \right\} .
\end{aligned}$$

In the case of mixed vertices, the scattering amplitudes $M_{VT,[9]}$ and $M_{TV,[9]}$ are

$$M_{VT,[9]} = \frac{C_{VT,[9]}^{(I,S)}}{4f} (\bar{u}(\bar{p}_1)(-i\gamma_\mu p_\nu)u(p_1)) S_V^{\mu\nu,\alpha\beta}(q) (\bar{v}(p_2)\sigma_{\alpha\beta}v(\bar{p}_2)) , \quad (3.46)$$

$$M_{TV,[9]} = \frac{C_{TV,[9]}^{(I,S)}}{4f} (\bar{u}(\bar{p}_1)\sigma_{\mu\nu}u(p_1)) S_V^{\mu\nu,\alpha\beta}(q) (\bar{v}(p_2)(i\gamma_\alpha p_\beta)v(\bar{p}_2)) , \quad (3.47)$$

with q the exchange momentum. The coupling coefficients implied by Eq. 3.46 are given in Tables 3.3 and 3.4, with F_1 , D_1 , and G_1 taking the values F_V , D_V , and G_V , respectively, and F_2 , D_2 , and G_2 taking the values F_T , D_T , and G_T , respectively. For the coupling coefficients implied by Eq. 3.47 the values of F_1 , D_1 , G_1 and F_2 , D_2 ,

and G_2 are interchanged with respect to the previous case. The scattering amplitudes $M_{VT,[9]}$ and $M_{TV,[9]}$ given above can be simplified by using the following identities for the contraction of one of the indices of the propagator $S_V^{\mu\nu,\alpha\beta}(q)$ with the four-momentum of the propagating particle q

$$\begin{aligned} q_\nu S_V^{\mu\nu,\alpha\beta}(q) &= \frac{g^{\mu\alpha}q^\beta - g^{\mu\beta}q^\alpha}{t - m_V^2 + i\epsilon}, \\ S_V^{\mu\nu,\alpha\beta}(q) q_\beta &= -\frac{g^{\mu\alpha}q^\nu - g^{\nu\alpha}q^\mu}{t - m_V^2 + i\epsilon}. \end{aligned} \quad (3.48)$$

The corresponding expressions of the scattering amplitudes reduce to

$$\begin{aligned} M_{VT,[9]} &= \frac{C_{VT,[9]}^{(I,S)}}{4f(t - m_V^2 + i\epsilon)} (\bar{u}(\bar{p}_1)\gamma_\mu u(p_1)) \left(\bar{v}(p_2) [\not{p}, \gamma^\mu]_- v(\bar{p}_2) \right), \\ M_{TV,[9]} &= \frac{C_{TV,[9]}^{(I,S)}}{4f(t - m_V^2 + i\epsilon)} \left(\bar{u}(\bar{p}_1) [\gamma_\mu, \not{p}, u]_- (p_1) \right) (\bar{v}(p_2)\gamma^\mu v(\bar{p}_2)). \end{aligned} \quad (3.49)$$

The eight invariant amplitudes calculated for the interaction described by $M_{VT,[9]}$ are

$$\begin{aligned} F_1^\pm &= \frac{C_{VT,[9]}^{(I,S)}}{4f(t - m_V^2 + i\epsilon)} \left\{ (M_1 + \bar{M}_1) \left(\frac{1}{2} - 2\frac{k \cdot \bar{k}}{s} \right) \pm M_2 \pm \bar{M}_2 \right\}, \\ F_2^\pm &= \frac{C_{VT,[9]}^{(I,S)}(M_1 + \bar{M}_1)}{4f(t - m_V^2 + i\epsilon)} \left\{ \frac{1}{2} - \frac{(M_1 \pm M_2)(\bar{M}_1 \pm \bar{M}_2)}{2s} \right\}, \\ F_3^\pm &= \frac{C_{VT,[9]}^{(I,S)}}{4f(t - m_V^2 + i\epsilon)} \left\{ \frac{(M_1 + \bar{M}_1)(M_1 \pm M_2)}{s} - 2 \right\}, \\ F_4^\pm &= \frac{C_{VT,[9]}^{(I,S)}}{4f(t - m_V^2 + i\epsilon)} \left\{ \frac{(M_1 + \bar{M}_1)(\bar{M}_1 \pm \bar{M}_2)}{s} - 2 \right\}. \end{aligned} \quad (3.50)$$

The invariant amplitudes for the interaction described by $M_{TV,[9]}$ are

$$\begin{aligned} F_1^\pm &= \frac{C_{TV,[9]}^{(I,S)}}{4f(t - m_V^2 + i\epsilon)} \left\{ (M_2 + \bar{M}_2) \left(\frac{1}{2} - \frac{2k \cdot \bar{k}}{s} \right) \pm M_1 \pm \bar{M}_1 \right\}, \\ F_2^\pm &= \frac{C_{TV,[9]}^{(I,S)}(M_2 + \bar{M}_2)}{4f(t - m_V^2 + i\epsilon)} \left\{ \frac{1}{2} - \frac{(M_1 \pm M_2)(\bar{M}_1 \pm \bar{M}_2)}{2s} \right\}, \\ F_3^\pm &= \frac{C_{TV,[9]}^{(I,S)}}{4f(t - m_V^2 + i\epsilon)} \left\{ \frac{(M_1 \pm M_2)(M_2 + \bar{M}_2)}{s} \mp 2 \right\}, \end{aligned}$$

$$F_4^\pm = \frac{C_{TV,[9]}^{(I,S)}}{4f(t - m_V^2 + i\epsilon)} \left\{ \frac{(\bar{M}_1 \pm \bar{M}_2)(M_2 + \bar{M}_2)}{s} \mp 2 \right\} . \quad (3.51)$$

Table 3.3: Coupling constants $[C_{[9]}^{(I,S)}]_{ab}$ specifying the interaction strength for the t -channel exchange of the isospin triplet ρ_μ and isospin doublet K_μ . States a and b have been defined in Table 3.1.

(I,S)	$(a, b) : [C_{\rho_\mu}^{(I,S)}]_{a,b}$	$(a, b) : [C_{K_\mu}^{(I,S)}]_{a,b}$
(0,2)	(1, 1) : $\frac{3}{4}(F_1 + D_1)(F_2 - D_2)$	
(1,2)	(1, 1) : $-\frac{1}{4}(F_1 + D_1)(F_2 - D_2)$	
$(\frac{1}{2}, 1)$	(1, 2) : $\frac{1}{2}D_2(F_1 + D_1)$	(1, 3) : $-\frac{1}{12}(3F_1 + D_1)(3F_2 - D_2)$
	(2, 2) : $F_2(F_1 + D_1)$	(1, 4) : $\frac{1}{4}(F_1 - D_1)(3F_2 - D_2)$
	(3, 4) : $\frac{1}{2}D_1(F_2 - D_2)$	(2, 3) : $-\frac{1}{4}(3F_1 + D_1)(F_2 + D_2)$
	(4, 4) : $F_1(F_2 - D_2)$	(2, 4) : $-\frac{1}{4}(F_1 - D_1)(F_2 + D_2)$
$(\frac{3}{2}, 1)$	(1, 1) : $-\frac{1}{2}F_2(F_1 + D_1)$	(1, 2) : $\frac{1}{2}(F_1 - D_1)(F_2 + D_2)$
	(2, 2) : $-\frac{1}{2}F_1(F_2 - D_2)$	
(0,0)	(1, 1) : $\frac{3}{4}(F_1 + D_1)(F_2 + D_2)$	(1, 2) : $\frac{\sqrt{2}}{12}(3F_1 + D_1)(3F_2 + D_2)$
	(2, 3) : $\frac{1}{\sqrt{3}}D_1D_2$	(1, 3) : $\frac{\sqrt{6}}{4}(F_1 - D_1)(F_2 - D_2)$
	(3, 3) : $2F_1F_2$	(2, 4) : $\frac{\sqrt{2}}{12}(3F_1 - D_1)(3F_2 - D_2)$
	(4, 4) : $\frac{3}{4}(F_1 - D_1)(F_2 - D_2)$	(3, 4) : $\frac{\sqrt{6}}{4}(F_1 + D_1)(F_2 + D_2)$
(1,0)	(1, 1) : $-\frac{1}{4}(F_1 + D_1)(F_2 + D_2)$	(1, 2) : $\frac{1}{2}(F_1 - D_1)(F_2 - D_2)$
	(2, 2) : F_1F_2	(1, 4) : $\frac{\sqrt{6}}{12}(3F_2 + D_2)(F_1 - D_1)$
	(2, 4) : $-\frac{\sqrt{6}}{3}F_1D_2$	(1, 5) : $\frac{\sqrt{6}}{12}(3F_1 + D_1)(F_2 - D_2)$
	(2, 5) : $-\frac{\sqrt{6}}{3}D_1F_2$	(2, 3) : $\frac{1}{2}(F_1 + D_1)(F_2 + D_2)$
	(3, 3) : $-\frac{1}{4}(F_1 - D_1)(F_2 - D_2)$	(3, 4) : $-\frac{\sqrt{6}}{12}(3F_2 - D_2)(F_1 + D_1)$
	(4, 5) : $\frac{1}{3}D_1D_2$	(3, 5) : $-\frac{\sqrt{6}}{12}(3F_1 - D_1)(F_2 + D_2)$
(2,0)	(1, 1) : $-F_1F_2$	
$(\frac{1}{2}, -1)$	(1, 2) : $\frac{1}{2}D_1(F_2 + D_2)$	(1, 3) : $\frac{1}{12}(3F_1 - D_1)(3F_2 + D_2)$
	(2, 2) : $F_1(F_2 + D_2)$	(1, 4) : $-\frac{1}{4}(3F_1 - D_1)(F_2 - D_2)$
	(3, 4) : $\frac{1}{2}D_2(F_1 - D_1)$	(2, 3) : $\frac{1}{4}(F_1 + D_1)(3F_2 + D_2)$
	(4, 4) : $F_2(F_1 - D_1)$	(2, 4) : $\frac{1}{4}(F_2 - D_2)(F_1 + D_1)$
$(\frac{3}{2}, -1)$	(1, 1) : $-\frac{1}{2}F_1(F_2 + D_2)$	(1, 2) : $-\frac{1}{2}(F_2 - D_2)(F_1 + D_1)$
	(2, 2) : $-\frac{1}{2}F_2(F_1 - D_1)$	
(0,-2)	(1, 1) : $\frac{3}{4}(F_1 - D_1)(F_2 + D_2)$	
(1,-2)	(1, 1) : $-\frac{1}{4}(F_1 - D_1)(F_2 + D_2)$	

Table 3.4: Coupling constants $[C_{[9]}^{(I,S)}]_{ab}$ specifying the interaction strength for the t -channel exchange of the isospin singlets ω_μ and ϕ_μ . States a and b are defined in Table 3.1.

(I, S)	$(a, b) : [C_{\omega_\mu}^{(I,S)}]_{a,b}$	$(a, b) : [C_{\phi_\mu}^{(I,S)}]_{a,b}$
$(0, 2)$	$(1, 1) : \frac{1}{4}(F_1 + D_1 + 2G_1)(-F_2 + D_2 + 2G_2)$	$(1, 1) : \frac{1}{2}(-F_1 + D_1 + G_1)(F_2 + D_2 + G_2)$
$(1, 2)$	$(1, 1) : \frac{1}{4}(F_1 + D_1 + 2G_1)(-F_2 + D_2 + 2G_2)$	$(1, 1) : \frac{1}{2}(-F_1 + D_1 + G_1)(F_2 + D_2 + G_2)$
$(\frac{1}{2}, 1)$	$(1, 1) : \frac{1}{6}(F_1 + D_1 + 2G_1)(D_2 + 3G_2)$	$(1, 1) : \frac{1}{6}(-F_1 + D_1 + G_1)(4D_2 + 3G_2)$
	$(2, 2) : \frac{1}{2}(F_1 + D_1 + 2G_1)(D_2 + G_2)$	$(2, 2) : \frac{1}{2}(-F_1 + D_1 + G_1)G_2$
	$(3, 3) : \frac{1}{6}(D_1 + 3G_1)(-F_2 + D_2 + 2G_2)$	$(3, 3) : \frac{1}{6}(4D_1 + 3G_1)(F_2 + D_2 + G_2)$
	$(4, 4) : \frac{1}{2}(D_1 + G_1)(-F_2 + D_2 + 2G_2)$	$(4, 4) : \frac{1}{2}(F_2 + D_2 + G_2)G_1$
$(\frac{3}{2}, 1)$	$(1, 1) : \frac{1}{2}(F_1 + D_1 + 2G_1)(D_2 + G_2)$	$(1, 1) : \frac{1}{2}(-F_1 + D_1 + G_1)G_2$
	$(2, 2) : \frac{1}{2}(D_1 + G_1)(-F_2 + D_2 + 2G_2)$	$(2, 2) : \frac{1}{2}(F_2 + D_2 + G_2)G_1$
$(0, 0)$	$(1, 1) : \frac{1}{4}(F_1 + D_1 + 2G_1)(F_2 + D_2 + 2G_2)$	$(1, 1) : \frac{1}{2}(-F_1 + D_1 + G_1)(-F_2 + D_2 + G_2)$
	$(2, 2) : \frac{1}{9}(D_1 + 3G_1)(D_2 + 3G_2)$	$(2, 2) : \frac{1}{18}(4D_1 + 3G_1)(4D_2 + 3G_2)$
	$(3, 3) : (D_1 + G_1)(D_2 + G_2)$	$(3, 3) : \frac{1}{2}G_1G_2$
	$(4, 4) : \frac{1}{4}(-F_1 + D_1 + 2G_1)(-F_2 + D_2 + 2G_2)$	$(4, 4) : \frac{1}{2}(F_1 + D_1 + G_1)(F_2 + D_2 + G_2)$

Table 3.4: Continued. Coupling constants $[C_{[9]}^{(I,S)}]_{ab}$ specifying the interaction strength for the t -channel exchange of the isospin singlets ω_μ and ϕ_μ . States a and b are defined in Table 3.1.

(I,S)	$(a,b) : [C_{\omega_\mu}^{(I,S)}]_{a,b}$	$(a,b) : [C_{\phi_\mu}^{(I,S)}]_{a,b}$
(1,0)	(1,1) : $\frac{1}{4}(F_1 + D_1 + 2G_1)(F_2 + D_2 + 2G_2)$	(1,1) : $\frac{1}{2}(-F_2 + D_2 + G_2)(-F_1 + D_1 + G_1)$
	(2,2) : $(D_1 + G_1)(D_2 + G_2)$	(2,2) : $\frac{1}{2}G_1G_2$
	(3,3) : $\frac{1}{4}(-F_1 + D_1 + 2G_1)(-F_2 + D_2 + 2G_2)$	(3,3) : $\frac{1}{2}(F_1 + D_1 + G_1)(F_2 + D_2 + G_2)$
	(4,4) : $\frac{1}{3}(D_2 + 3G_2)(D_1 + G_1)$	(4,4) : $\frac{1}{6}(4D_2 + 3G_2)G_1$
	(5,5) : $\frac{1}{3}(D_1 + 3G_1)(D_2 + G_2)$	(5,5) : $\frac{1}{6}(4D_1 + 3G_1)G_2$
(2,0)	(1,1) : $(D_1 + G_1)(D_2 + G_2)$	(1,1) : $\frac{1}{2}G_1G_2$
$(\frac{1}{2}, -1)$	(1,1) : $\frac{1}{6}(F_2 + D_2 + 2G_2)(D_1 + 3G_1)$	(1,1) : $\frac{1}{6}(-F_2 + D_2 + G_2)(4D_1 + 3G_1)$
	(2,2) : $\frac{1}{2}(F_2 + D_2 + 2G_2)(D_1 + G_1)$	(2,2) : $\frac{1}{2}(-F_2 + D_2 + G_2)G_1$
	(3,3) : $\frac{1}{6}(D_2 + 3G_2)(-F_1 + D_1 + 2G_1)$	(3,3) : $\frac{1}{6}(4D_2 + 3G_2)(F_1 + D_1 + G_1)$
	(4,4) : $\frac{1}{2}(D_2 + G_2)(-F_1 + D_1 + 2G_1)$	(4,4) : $\frac{1}{2}(F_1 + D_1 + G_1)G_2$
$(\frac{3}{2}, -1)$	(1,1) : $\frac{1}{2}(F_2 + D_2 + 2G_2)(D_1 + G_1)$	(1,1) : $\frac{1}{2}(-F_2 + D_2 + G_2)G_1$
	(2,2) : $\frac{1}{2}(D_2 + G_2)(-F_1 + D_1 + 2G_1)$	(2,2) : $\frac{1}{2}(F_1 + D_1 + G_1)G_2$
(0,-2)	(1,1) : $\frac{1}{4}(F_2 + D_2 + 2G_2)(-F_1 + D_1 + 2G_1)$	(1,1) : $\frac{1}{2}(-F_2 + D_2 + G_2)(F_1 + D_1 + G_1)$
(1,-2)	(1,1) : $\frac{1}{4}(F_2 + D_2 + 2G_2)(-F_1 + D_1 + 2G_1)$	(1,1) : $\frac{1}{2}(-F_2 + D_2 + G_2)(F_1 + D_1 + G_1)$

DYNAMICALLY GENERATED RESONANCES IN THE N/D METHOD

As already discussed, the most general scattering matrix S has to be covariant, analytical, unitary and crossing symmetric. Building a scattering matrix that obeys all these requirements is a very difficult task. The main question that arises is, given a particular Lagrangian for the interaction, how to construct a coupled-channel scattering amplitude that complies with the requirements stated above. We are looking for a scattering amplitude $T_{ab}^{(JP)}(\sqrt{s})$ that obeys the once-subtracted partial-wave dispersion-integral equation

$$\begin{aligned} T_{ab}^{(JP)}(\sqrt{s}) &= U_{ab}^{(JP)}(\sqrt{s}) + \int_{thres.}^{+\infty} \frac{dw}{\pi} \frac{\sqrt{s} - \mu_M}{w - \mu_M} \frac{\Delta T_{ab}^{(JP)}(w)}{w - \sqrt{s} - i|\epsilon|}, \quad (4.1) \\ \Delta T_{ab}^{(JP)}(\sqrt{s}) &= \frac{1}{2i} \left[T_{ab}^{(JP)}(\sqrt{s} + i|\epsilon|) - T_{ab}^{(JP)}(\sqrt{s} - i|\epsilon|) \right], \end{aligned}$$

where $U_{ab}^{(JP)}(\sqrt{s})$ is a function that contains all the contributions from the left-hand cuts only, J is the total angular momentum, P denotes parity and a, b are the labels of the incoming and outgoing channels. The use of the once-subtracted dispersion integral has the advantage of facilitating the renormalization of the scattering amplitude at the energy point μ_M , called the matching scale. The value of μ_M is chosen such that, provided the driving potential $U_{ab}^{(JP)}(\sqrt{s})$ is crossing symmetric, the scattering amplitude $T_{ab}^{(JP)}(\sqrt{s} = \mu_M) = U_{ab}^{(JP)}(\sqrt{s} = \mu_M)$ is also crossing symmetric. Based on Eq. 4.1, if we incorporate unitarity

$$\Delta T_{ab}^{(JP)}(\sqrt{s}) = \sum_{c,d} \left[T_{ac}^{(JP)}(\sqrt{s}) \right]^\dagger \rho_{cd}^{(JP)}(\sqrt{s}) T_{db}^{(JP)}(\sqrt{s}), \quad (4.2)$$

we have to solve for the coupled-channel calculation the non-linear integral equation

$$T_{ab}^{(JP)}(\sqrt{s}) = U_{ab}^{(JP)}(\sqrt{s}) + \sum_{c,d} \int_{thres.}^{+\infty} \frac{dw}{\pi} \frac{\sqrt{s} - \mu_M}{w - \mu_M} \frac{T_{ac}^{(JP)}(w) \rho_{cd}^{(JP)}(w) [T_{db}^{(JP)}(w)]^\dagger}{w - \sqrt{s} - i|\epsilon|}, \quad (4.3)$$

where the phases-space matrix $\rho_{cd}^{(JP)}(\sqrt{s})$ vanishes identically below threshold.

4.1 N/D method

The N/D method allows one to obtain a general solution of Eq. 4.3 making use of the left-hand discontinuities of the amplitude $T_{ab}^{J\pm}(\sqrt{s})$. It linearizes the nonlinear integral equation derived from unitarity and the partial-wave dispersion relation with a finite number of subtractions. Originally introduced by Chew and Mandelstam [37] for a single channel, it has been extended to a coupled-channel formulation by Bjorken [38]. In the N/D method, the partial-wave amplitude $T_{ab}^{(JP)}(\sqrt{s})$ is written as

$$T_{ab}^{(JP)}(\sqrt{s}) = \sum_c \left[D_{ac}^{(JP)}(\sqrt{s}) \right]^{-1} N_{bc}^{(JP)}(\sqrt{s}), \quad (4.4)$$

in such a way that $N_{ab}^{(JP)}(\sqrt{s})$ contains only the contributions from left-hand cuts and poles and $D_{ab}^{(JP)}(\sqrt{s})$ is an analytic function everywhere except for the right-hand cut. It is also necessary that $D_{ab}^{(JP)}(\sqrt{s})$ has no zeros [37]. We are free to multiply both the numerator and the denominator with a factor, therefore we are free to normalize $D_{ab}^{(JP)}(\sqrt{s})$ at the subtraction point μ_M [66]. We first take the Ansatz (for more details see [37, 38, 67])

$$D_{ab}^{(JP)}(\sqrt{s}) = \delta_{ab} - \sum_c \int_{thres.}^{+\infty} \frac{dw}{\pi} \frac{\sqrt{s} - \mu_M}{w - \mu_M} \frac{N_{ac}^{(JP)}(w) \rho_{cb}^{(JP)}(w)}{w - \sqrt{s}}. \quad (4.5)$$

The denominator function $D_{ab}^{(JP)}(\sqrt{s})$ described by Eq. 4.5 is analytic except for the right-hand branch points. Its discontinuity across the right-hand cut is

$$\begin{aligned} \Delta D_{ab}(\sqrt{s}) &= \frac{1}{2i} \left[D_{ab}^{(+)}(\sqrt{s}) - D_{ab}^{(-)}(\sqrt{s}) \right] \\ &= - \sum_c N_{ac}(\sqrt{s}) \rho_{cb}(\sqrt{s}) \end{aligned} \quad (4.6)$$

for $D_{ab}^{(\pm)}(\sqrt{s}) = D_{ab}(\sqrt{s} \pm i\epsilon)$ with $\epsilon > 0$, where, for clarity, we have suppressed the reference to the angular momentum J and parity P and used that $N_{ab}(\sqrt{s})$ has left-hand contributions only. We have also used that the phasespace $\rho_{ab}(\sqrt{s})$ vanishes identically below threshold. Eq. 4.4 can be cast into the form

$$N_{ab}(\sqrt{s}) = \sum_c D_{ac}(\sqrt{s}) T_{cb}(\sqrt{s}). \quad (4.7)$$

The function $N_{ab}(\sqrt{s})$ that solves the nonlinear singular integral equation given in Eq. 4.1 can be calculated by solving the linear integral equation [37]

$$\begin{aligned} N_{ab}(\sqrt{s}) = & U_{ab}(\sqrt{s}) \\ & + \sum_{c,d} \int_{thres.}^{+\infty} \frac{dw}{\pi} \frac{\sqrt{s} - \mu_M}{w - \mu_M} \frac{N_{ac}(w) \rho_{cd}(w) [U_{cb}(w) - U_{cb}(\sqrt{s})]}{w - \sqrt{s}}, \end{aligned} \quad (4.8)$$

which is a once-subtracted dispersion integral for the numerator function $N_{ab}(\sqrt{s})$. From a mathematical point of view, the linear integral equation above falls in the class of Fredholm equations of the second kind [68].

The crucial point, however, lies in the analyticity of the driving potential $U_{ab}(\sqrt{s})$ along the right-hand unitarity cut. The numerator function $N_{ab}(\sqrt{s})$ is determined completely by the knowledge of the driving potential in the physical region and by its asymptotic behavior. A driving potential not complying with the desired asymptotic behavior may lead to arbitrary cutoff parameters or to arbitrary assumptions about the properties of distant singularities (the high-energy behavior of the input potential is closely related to distant singularities in crossed channels) [69]. However, an analytical continuation of the potential can be performed from small to high energies, such that it comports with the desired asymptotic behavior [70]. Once Eq. 4.8 has been solved, Eq. 4.5 determines the denominator $D_{ab}(\sqrt{s})$, leading therefore to a complete determination of $T_{ab}(\sqrt{s})$. However, the preceding discussion has some weak points, since zeros of the denominator function correspond to poles of the scattering amplitude $T_{ab}(\sqrt{s})$. This fact has two related consequences. First, we can not say *a priori* that the solution given by Eq. 4.8 leads to an acceptable solution of Eq. 4.3, since $D_{ab}(\sqrt{s})$ may have some zeros that would correspond to spurious poles in the scattering amplitude $T_{ab}(\sqrt{s})$ not present in the original form of Eq. 4.3. Secondly, any

solution of a Fredholm integral equation is a meromorphic function. A meromorphic function is a holomorphic function on the complex plane (or an open subdomain) except a set of isolated points, which are poles for the function. The poles of the numerator $N_{ab}(\sqrt{s})$ would correspond to poles of the scattering amplitude $T_{ab}(\sqrt{s})$ in an unphysical sheet. Moreover, one may add an arbitrary meromorphic function, corresponding to a solution of the homogeneous Fredholm equation, to the numerator, which would correspond to additional poles of the scattering amplitude. The arbitrariness coming from the possible addition of meromorphic functions has been first shown by Castillejo, Dalitz and Dyson [71] and is a common feature of the solution of dispersion equations. The poles of the meromorphic function are known as CDD poles after their discoverers. CDD poles are unwanted since the scattering amplitude should be determined unambiguously for a given generalized potential $U_{ab}(\sqrt{s})$. The physical solution to the N/D equation is *unique* provided that no CDD poles occur. The reasoning is essentially that, first of all, one may show that for large values of angular momentum J , the relevant solution of the N/D equations will not contain CDD poles. Secondly, the solution will be analytical in J and an analytic continuation of the solution from high values of J to lower values of J is possible and leads to solutions of the N/D equations without CDD poles [72].

The presence of a pole in the solution of the scattering amplitude would correspond to a dynamically generated resonance or to a ‘ghost’ state, depending if the pole is situated in a physical or unphysical sheet [72]. Ghosts may arise from a strongly repulsive potential and are associated with unphysical, wrong-sign residues of the scattering amplitude at the pole. In the following sections, certain specific examples are given in which we further study the implications of the N/D method described above and attempt to generate a resonance state. The technique applied in these examples assumes a system of two coupled-channels, that will be solved with the N/D method. We will show that by adjusting the strength of the interaction one is able to generate resonances dynamically.

Before we can assert anything about the solutions of the linear integral equation 4.8, we must investigate whether it is nonsingular. The condition for the integral equa-

tion [72]

$$\begin{aligned}\phi(\sqrt{s}) &= f(\sqrt{s}) + \int dw \phi(w) K(w, \sqrt{s}), \\ K(w, \sqrt{s}) &= h_1(w) G(w, \sqrt{s}) h_2(\sqrt{s}), \\ G(\sqrt{s}, w) &= G^\dagger(w, \sqrt{s}), \quad h_1(\sqrt{s}) > 0, \quad h_2(\sqrt{s}) > 0\end{aligned}\quad (4.9)$$

to be nonsingular is that the integral

$$\int \int dw dw' h_1(w) h_2(w) |G(w, w')|^2 h_1(w') h_2(w') \quad (4.10)$$

should converge on the given domain of integration. We identify

$$\begin{aligned}\phi(\sqrt{s}) &= \frac{N_{ab}(\sqrt{s})}{\sqrt{s} - \mu_M}, & f(\sqrt{s}) &= \frac{U_{ab}(\sqrt{s})}{\sqrt{s} - \mu_M}, \\ G(\sqrt{s}, t) &= \frac{U(\sqrt{s}) - U(w)}{\pi(\sqrt{s} - w)}, & h_1(\sqrt{s}) &= \rho_{cd}(\sqrt{s}), \quad h_2(w) = 1.\end{aligned}$$

We must therefore examine the convergence of the integral

$$\int \int dw dw' \rho(w) \left| \frac{U(w) - U(w')}{\pi(w - w')} \right|^2 \rho(w'). \quad (4.11)$$

Finding a solution for the integral equation 4.9, implies evaluating the inverse of the operator $1 - K$. The inverse exists provided none of the eigenvalues of K is equal to 1. By adjusting the strength of the interaction with an arbitrary factor α , we in fact determine the solution of

$$\phi(\sqrt{s}) = \alpha f(\sqrt{s}) + \alpha \int dw \phi(w) K(\sqrt{s}, w). \quad (4.12)$$

In this case, according to Fredholm theory, the inverse of the operator $1 - \alpha K$ should exist but for a finite number of values for α .

To summarize, once provided the solution of the integral equation for $N_{ab}(\sqrt{s})$, we can evaluate the denominator $D_{ab}(\sqrt{s})$, whose values can be used to evaluate the

scattering amplitudes $T_{ab}(\sqrt{s})$ as implied by

$$N_{ab}(\sqrt{s}) = U_{ab}(\sqrt{s}) \quad (4.13)$$

$$\begin{aligned}
 & + \sum_{c,d} \int_{thres.}^{+\infty} \frac{dw}{\pi} \frac{\sqrt{s} - \mu_M}{w - \mu_M} \frac{N_{ac}(w) \rho_{cd}(w) [U_{cb}(w) - U_{cb}(\sqrt{s})]}{w - \sqrt{s}} \\
 D_{ab}(\sqrt{s}) &= \delta_{ab} - \sum_c \int_{thres.}^{+\infty} \frac{dw}{\pi} \frac{\sqrt{s} - \mu_M}{w - \mu_M} \frac{N_{ac}(w) \rho_{cb}(w)}{w - \sqrt{s}} \\
 T_{ab}(\sqrt{s}) &= \sum_c D_{ac}^{-1}(\sqrt{s}) N_{cb}(\sqrt{s}). \quad (4.14)
 \end{aligned}$$

4.2 Single-channel calculation

We start our analysis with the study of a single-channel problem. We assume a single nucleon anti-nucleon state where the interaction is given as a t -channel exchange of a vector meson. We recall here the expression of the Lagrange interaction

$$\begin{aligned}
 \mathcal{L}_{VB} &= \frac{F_V}{2m_V} \text{tr} (\bar{B} \gamma_\mu [\partial_\nu V^{\mu\nu}, B]_-) + \frac{D_V}{2m_V} \text{tr} (\bar{B} \gamma_\mu [\partial_\nu V^{\mu\nu}, B]_+) \\
 &+ \frac{G_V}{2m_V} \text{tr} (\bar{B} \gamma_\mu B) \text{tr} (\partial_\nu V^{\mu\nu}) + \frac{F_T m_V}{8f} \text{tr} (\bar{B} \sigma_{\mu\nu} [V^{\mu\nu}, B]_-) \quad (4.15) \\
 &+ \frac{D_T m_V}{8f} \text{tr} (\bar{B} \sigma_{\mu\nu} [V^{\mu\nu}, B]_+) + \frac{G_T m_V}{8f} \text{tr} (\bar{B} \sigma_{\mu\nu} B) \text{tr} (V^{\mu\nu}).
 \end{aligned}$$

We perform the calculations in a partial-wave basis, where the partial-wave decomposition for a $\frac{1}{2} \bar{\frac{1}{2}} \rightarrow \frac{1}{2} \bar{\frac{1}{2}}$ has been provided in Eq. 2.42 and it can be summarized in the following form

$$\begin{aligned}
 T_{ij}^{JP}(\sqrt{s}) &= \sum_{k,\pm} \lambda_{ij,k}^{JP}(\sqrt{s}, J) A_k^{JP}(s) \quad (4.16) \\
 A_k^{JP}(s) &= \left(\frac{s}{\bar{p}p} \right)^J \int_{-1}^1 d \cos \theta F_k^P(s, t) P_J(\cos \theta)
 \end{aligned}$$

where $T_{ij}^{JP}(\sqrt{s})$ is the scattering amplitude with a given angular momentum J and parity P , i and j are the indices of the covariant basis state for the given incoming and outgoing channel, respectively, k labels the number of the invariant amplitude, and $\lambda(\sqrt{s}, J)$ is a function arising from the decomposition of the covariant partial-wave amplitudes into invariants. The invariant amplitudes $F_k^P(s, t)$ for the t -channel

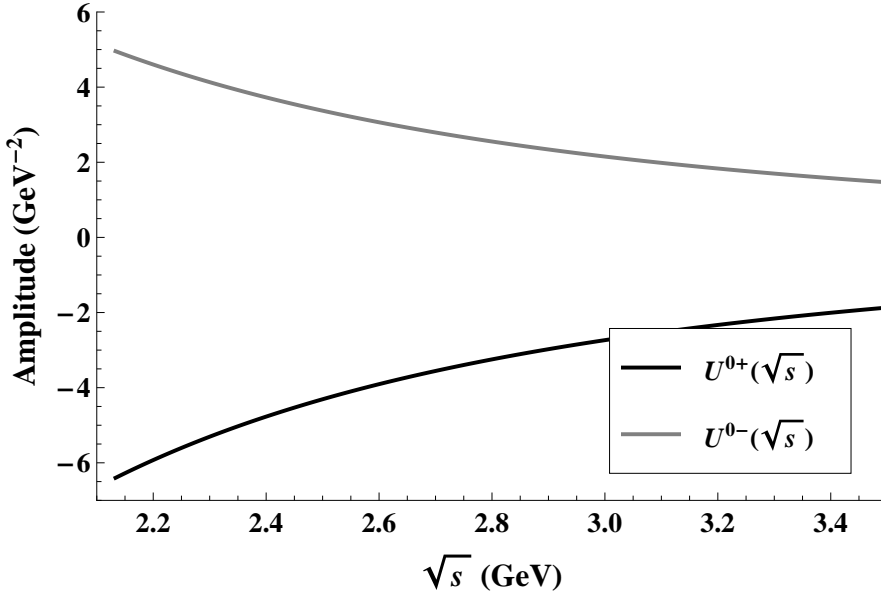


Figure 4.1: Driving potential for $J = 0$, positive (black line) and negative (gray line) parity.

exchange of a vector meson have been calculated in section 3.4. In general, their exact structure depends on the type of particles in the incoming and outgoing channel as well as on the type of the exchange particle. However, it is clear from the structures calculated in chapter 3 that evaluating the covariant partial-wave amplitudes is reduced to evaluating the integrals

$$\left(\frac{s}{\bar{p}p}\right)^J \int_{-1}^1 d\cos\theta \frac{P_J(\cos\theta)}{t - m^2}, \quad (4.17)$$

$$\left(\frac{s}{\bar{p}p}\right)^J \int_{-1}^1 d\cos\theta t^a P_J(\cos\theta). \quad (4.18)$$

The evaluation of the integral in Eq. 4.18 gives the result

$$\begin{aligned} \left(\frac{s}{\bar{p}p}\right)^J \int_{-1}^1 d\cos\theta t^a P_J(\cos\theta) &= \\ &= \left(\frac{s}{\bar{p}p}\right)^J \int_{-1}^1 d\cos\theta (\Delta + 2\bar{p}p \cos\theta)^a P_J(\cos\theta) \end{aligned}$$

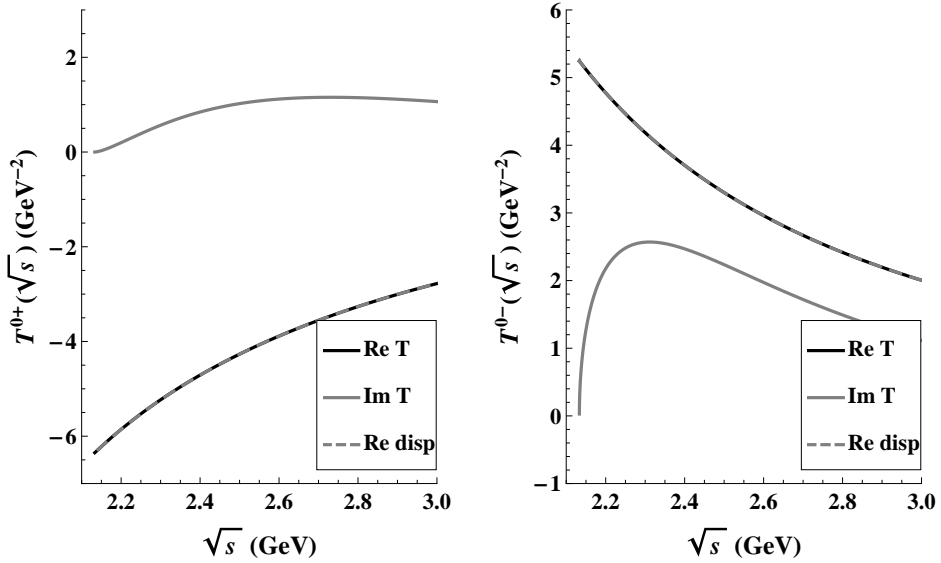


Figure 4.2: Real and imaginary parts of the partial wave scattering amplitude calculated with Eq. 4.14, for $J = 0$, positive (left) and negative (right) parity. The black line is the real part of the scattering amplitude, the solid gray line is the imaginary part of the scattering amplitude increased by a factor 10. The dashed gray line is the result of the original, nonlinear integral equation 4.1.

$$= \binom{a}{J} \frac{2J!}{(2J+1)!!} \Delta^a \left(\frac{2s}{\Delta} \right)^J \quad (4.19)$$

whereas the evaluation of the integral in 4.17 may give rise to the t -channel cut.

We calculate the driving potential for the coupled-channel system characterized by $(I, S) = (3/2, 1)$, where we first limit ourselves to the lightest channel. The masses of the fermion and antifermion are $M_1 = M_N = 0.939$ GeV and $M_2 = M_{\Sigma} = 1.195$ GeV, respectively. For a $\frac{1}{2} \frac{1}{2}$ system with one channel where the exchange particle is taken to be a vector meson, the t -channel cut lies below threshold. However, in our coupled-channel approach, we require information about the driving potential from the lowest threshold and the t -channel cut may enter in our energy range. In order to avoid this problem, we have used vector meson masses larger by

1.5 GeV than the normal masses. We refer to [69, 70] for a detailed discussion on a systematic method for performing the analytical continuation of the driving potential to the both subthreshold energy range and to large values of \sqrt{s} .

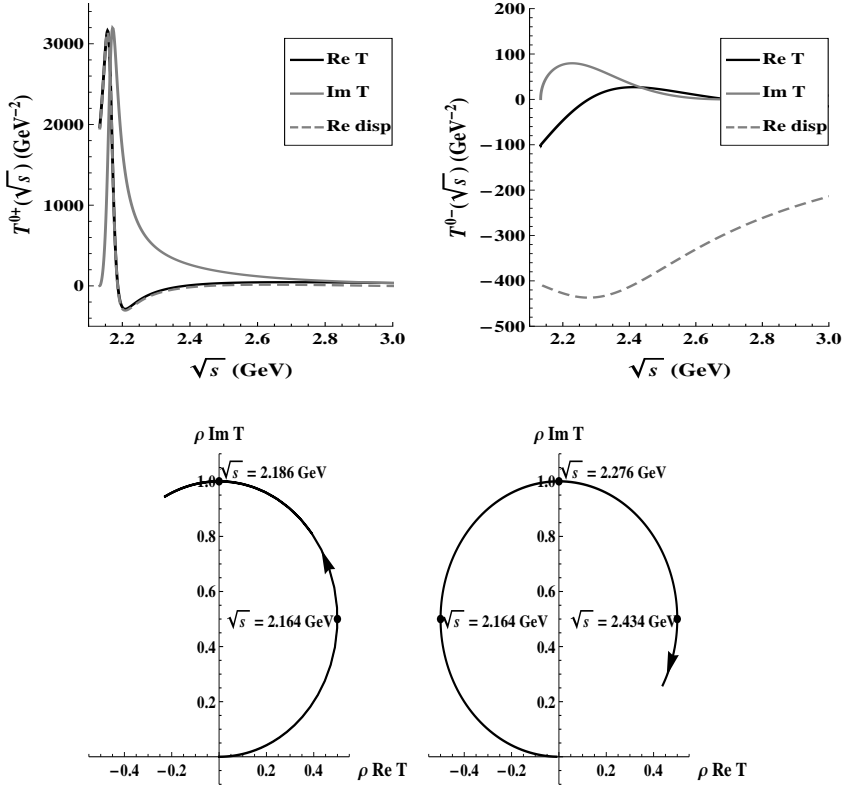


Figure 4.3: Real and imaginary parts of the partial-wave scattering amplitude calculated with Eq. 4.14, for $J = 0$, positive (left) and negative (right) parity. The black line is the real part of the scattering amplitude, the solid gray line is the imaginary part of the scattering amplitude. The dashed gray line is the result of the original, nonlinear integral equation 4.3. We have increased the strength of the driving potential by a factor $\alpha = -100$.

The driving potential is presented in Fig. 4.1. The potential obeys the imposed condition of approaching a constant amplitude for large values of the center-of-mass energy \sqrt{s} for both parities. Similarly to the discussion in [19], the crossing condition

is imposed such that for the channel with the smallest threshold, it holds $s = t$ for $s = \mu_M^2$ and $u = 0$. This leads to a value of $\mu_M^2 = M_1^2 + M_2^2$.

In Figure 4.2 the partial-wave scattering amplitudes $T^{0\pm}(\sqrt{s})$ are shown starting from the threshold $\sqrt{s} = 2.134$ GeV up to $\sqrt{s} = 3$ GeV for both positive (left) and negative (right) parity. The amplitudes have been calculated using Eq. 4.14. The black line is the real part of the scattering amplitude, the solid gray line is the imaginary part of the scattering amplitude, increased by a factor 10 to be visible on the same scale. The dashed gray line is the result of the original, nonlinear integral equation 4.1. As imposed by unitarity, the imaginary part of the scattering amplitude becomes zero at the opening threshold. It can be seen that the solution of the N/D method verifies the original nonlinear integral equation 4.1 that combines unitarity and analyticity.

In order to test whether it is possible to generate resonances in an N/D coupled-channel approach, we arbitrarily increase the strength of the potential by a scalar factor. For a driving potential increased by a factor $\alpha = -100$, the scattering amplitude $T^{0+}(\sqrt{s})$ shows a resonance at $\sqrt{s} = 2.186$ GeV with a width $\Gamma = 0.044$ GeV in the $J^P = 0^+$ sector. The resonance position was taken at the maximum of the peak in the imaginary part of the scattering amplitude, whereas the width was taken as the full width at half-maximum of the peak. Using the imaginary part of the scattering amplitude, calculated with the N/D method, as input to the dispersion relation Eq. 4.1, we can check if the solution is analytical. As can be seen from Fig. 4.3 there is a good agreement between the real part evaluated with the N/D approach (solid black line) and the real part evaluated from the once-subtracted integral equation 4.1 (dashed gray line) for $T^{0+}(\sqrt{s})$. However, in the case of the scattering amplitude $T^{0-}(\sqrt{s})$, a ghost state has been generated at $\sqrt{s} = 2.276$ GeV with a width $\Gamma = 0.135$ GeV, as can be seen from the Argand diagram. The point (0,0) on the Argand diagram corresponds to the threshold energy. However, causality is not obeyed in this case, since the representative point ($\rho \text{ Re}T$, $\rho \text{ Im}T$) moves around the unitarity circle in a clockwise direction. In this case, the linear integral equation 4.8 should be solved again, as suggested in [67], with a CDD pole added to the solution for $N_{ab}(\sqrt{s})$.

4.3 Coupled-channel effects

In this section, the dynamic role of coupling between channels is analyzed. We investigate the effect of the second channel, for which the mass of the fermion is $M_1 = M_\Sigma = 1.195$ GeV and the mass of the antifermion is $M_2 = M_\Xi = 1.315$ GeV. The channel coupling displaces the poles originally present in the isolated channels and builds up effects on its own. We focus mainly on the question of how strong should the coupled-channel interaction be in order to create a pole of its own.

For the system of two coupled channels, the driving potential for a given angular momentum J and parity P takes the form

$$U^{(JP)}(\sqrt{s}) = \begin{pmatrix} U_{11}^{(JP)}(\sqrt{s}) & U_{12}^{(JP)}(\sqrt{s}) \\ U_{21}^{(JP)}(\sqrt{s}) & U_{22}^{(JP)}(\sqrt{s}) \end{pmatrix} \quad (4.20)$$

where $U_{11}^{(JP)}(\sqrt{s})$ and $U_{22}^{(JP)}(\sqrt{s})$ are the diagonal interactions, and $U_{12}^{(JP)}(\sqrt{s})$ is the coupled-channel interaction. Figure 4.4 shows the driving potentials $U_{11}^{(0\pm)}(\sqrt{s})$, $U_{12}^{(0\pm)}(\sqrt{s}) = U_{21}^{(0\pm)}(\sqrt{s})$ and $U_{22}^{(0\pm)}(\sqrt{s})$. The driving potential evaluated in the kinematical basis is real and smooth at the crossing of the second threshold for both parities, implying that the kinematical dependence present in the partial-wave helicity amplitudes has been removed.

We recall the definition of the phases-space density

$$\rho_{\pm, \frac{1}{2} \frac{1}{2}}^J(s) = \frac{1}{(2J+1)\pi} \left(\frac{p}{\sqrt{s}} \right)^{2J-1} \times \begin{pmatrix} \frac{p^2 (s-M_\pm^2)}{4s^2} & \frac{J p^2 M_\pm}{2s\sqrt{s}} \\ \frac{J p^2 M_\pm}{2s\sqrt{s}} & \frac{J (s-M_\mp^2) ((J+1)s + J M_\pm^2)}{4s^2} \end{pmatrix}, \quad (4.21)$$

where $M_\pm = M_1 \pm M_2$.

4.3.1 Zero coupling

We first test our procedure in the case of no coupling between the states and we set the coupled-channel interaction $U_{12}^{(JP)}(\sqrt{s}) = 0$, while independently the strength of the diagonal interaction is increased. In this case, the N/D method should give the

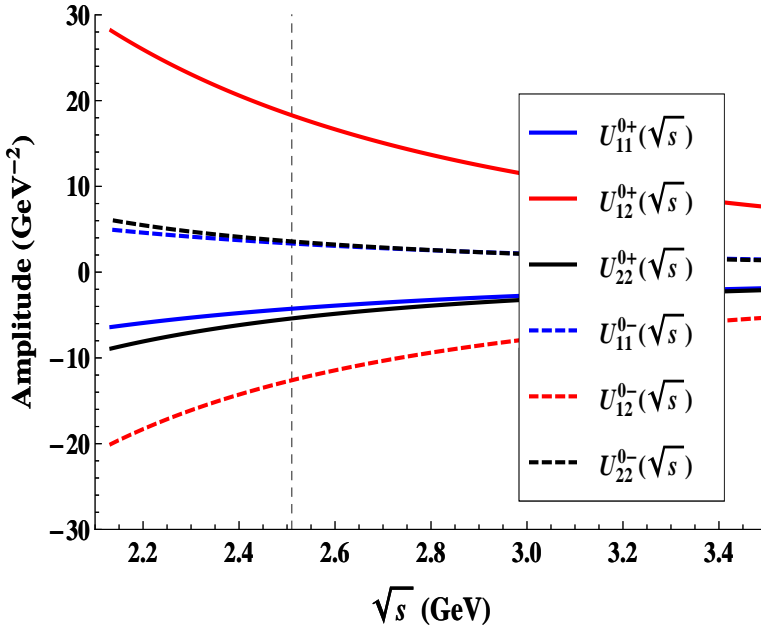


Figure 4.4: Behavior of the driving potential $U_{ab}^{0\pm}$ with energy. The dashed vertical line corresponds to the second threshold.

same result for the coupled-channel procedure as for the case when the two channels are evaluated separately. Figure 4.5 shows the calculated partial-wave amplitudes $T_{11}^{0+}(\sqrt{s})$ (left panel) and $T_{11}^{0-}(\sqrt{s})$ (right panel) for a diagonal interaction increased with a factor $\alpha_{11} = \alpha_{22} = -100$. It can be seen that the partial-wave amplitude $T_{11}^{0+}(\sqrt{s})$ is the same as in Fig. 4.3. This finding implies that the solution of the N/D method with one channel is the same as for the case when more channels are added which are extremely weakly coupled to the first. Since the amplitude $T_{22}^{0+}(\sqrt{s})$ is an analytic function, it can be continued to values of the energies below the threshold, even if they do not correspond to a physical regime. In this case, the imaginary part of the amplitude is zero below the threshold of the second channel, confirming that indeed there is no loss of probability to other channels. Moreover, the real part of the amplitude corresponding to these energies is given mainly by the analytic continuation of $U_{22}^{(JP)}(\sqrt{s})$.

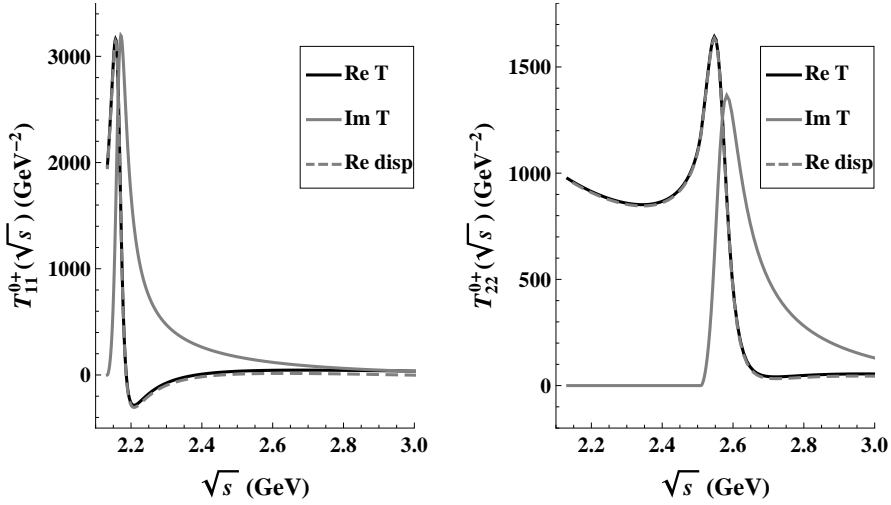


Figure 4.5: Real and imaginary parts of the partial-wave scattering amplitude for $J^P = 0^+$. The black line is the real part of the scattering amplitude, the solid gray line is the imaginary part of the scattering amplitude. The dashed gray line is the result of the original, nonlinear integral equation 4.1. We have increased the strength of the driving potential $\alpha_{11} = \alpha_{22} = -100$.

4.3.2 Intermediate coupling

We study the effect of the coupled-channel interaction in the case when the diagonal driving potential in channel-1 is small, the coupled-channel interaction has intermediate values and the interaction in channel-2 is large. Figure 4.6 shows the result of the coupled-channel calculation of the scattering amplitudes for $J^P = 0^+$ (top) and $J^P = 0^-$ (bottom). For positive parity, the potential $U_{11}^{0+}(\sqrt{s})$ is increased by the factor $\alpha_{11} = 1$, the off-diagonal interaction is increased by a factor $\alpha_{12} = 10$ and the potential $U_{22}^{0+}(\sqrt{s})$ is increased by the factor $\alpha_{22} = -100$. The resonance produced originally by the strong interaction in channel-2 is now seen in all partial waves amplitudes T_{ij}^{0+} due to the coupled-channel effects.

For opposite parity, the potential $U_{11}^{0-}(\sqrt{s})$ is increased by the factor $\alpha_{11} = -1$,

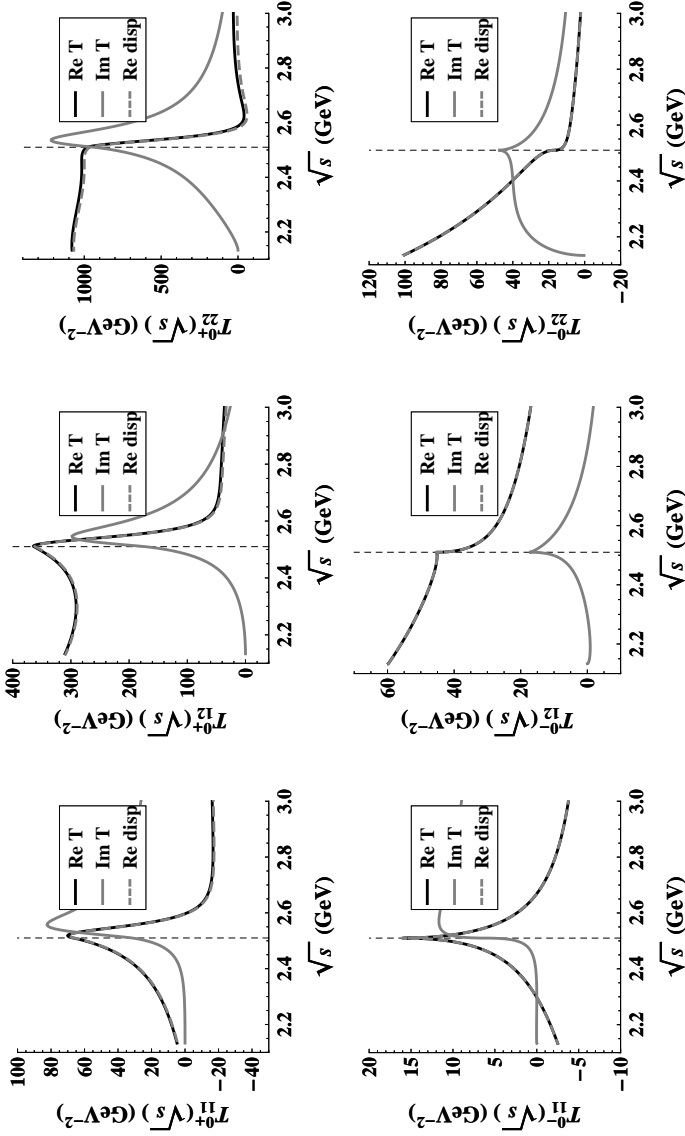


Figure 4.6: Real and imaginary parts of the partial-wave scattering amplitude for $J^P = 0^+$ (top) and $J^P = 0^-$ (bottom). The dashed vertical line corresponds to the second threshold. The dashed gray line is the result of the once-subtracted dispersion integral in Eq. 4.1.

the off-diagonal interaction is increased by a factor $\alpha_{12} = -3$ and the potential $U_{22}^{0-}(\sqrt{s})$ is increased by the factor $\alpha_{22} = 10$. A clear signature of the analytic structure is the occurrence of a cusp structure at threshold. The slope of $\text{Im}T_{11}^{0+}$ for $\sqrt{s} = 2.51$ GeV (at the opening of the second threshold) is smaller than for opposite parity. As a consequence, we obtain a much more pronounced cusp-like behavior of $\text{Im}T_{11}^{0-}$ at the threshold. The difference is mainly due to the change in the definition of the phases-space for the two parities. The real part of the amplitudes as calculated from the once-subtracted dispersion integral given in Eq. 4.1 reproduce exactly the ones obtained from the coupled-channel approach.

4.3.3 Strong coupled-channel interaction

A further distinct case in the study of the coupled-channel effects is the situation when the diagonal interactions $U_{aa}(\sqrt{s})$ are small compared to the coupled-channel interaction $U_{ab}(\sqrt{s})$, with $a \neq b$. We will analyze the extreme situation when the diagonal interactions $U_{11}(\sqrt{s}) = U_{22}(\sqrt{s}) = 0$. Figure 4.7 shows the result for the scattering amplitudes for a strong offdiagonal driving potential for $J^P = 0^+$, as well as the Argand diagram for the diagonal amplitudes. The real part of the scattering amplitude evaluated with the once-subtracted dispersion integral reproduces accurately the kinks at the thresholds; this implies that in this case analyticity is obeyed, but more subtraction points may be needed.

Below the opening of the second channel, the diagonal scattering amplitude $T_{11}(\sqrt{s})$ is realized by the interaction with the virtual second state. When the second channel opens, there is an increase in the $\text{Im}T$ due to an increase in the phases-space of the second channel. The Argand diagram implies the presence of a resonance for the first channel (gray line), in the close vicinity of the threshold. This resonance is due solely to the coupled-channel effects.

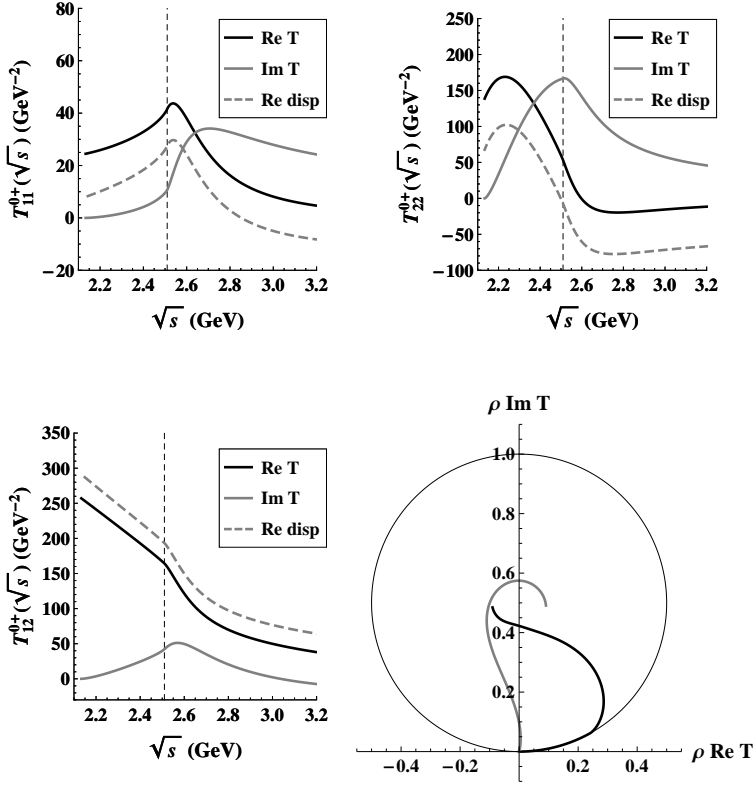


Figure 4.7: Real and imaginary parts of the partial-wave scattering amplitude for $J^P = 0^+$. The black line is the real part of the scattering amplitude, the solid gray line is the imaginary part of the scattering amplitude. The dashed gray line is the result of the original, nonlinear integral equation 4.1. In the bottom right, the Argand diagram of the $T_{11}(\sqrt{s})$ (black line) and $T_{22}(\sqrt{s})$ (gray line).

SUMMARY AND CONCLUSIONS

In this thesis, we have constructed a scattering matrix obeying the constraints from unitarity, analyticity, covariance and crossing symmetry at a given energy. Unitarity, derived from the principle of conservation of probability imposes an interdependence of the real and imaginary parts. Causality of the scattering matrix relates the real and imaginary parts of the amplitudes by (causal) dispersion relations. In addition, the same analytical expression for the scattering amplitude should describe the processes obtained by the permutation of initial- and final-state particles.

The covariant partial-wave amplitudes are an excellent starting point for analyzing baryon-antibaryon scattering in a covariant coupled-channel approach that takes into account the constraints set by micro-causality and coupled-channel unitarity. Making use of the $SU(3)$ Lagrangian presented in chapter 3, for the scattering of two spin-1/2 particles, the invariants describing the t -channel exchange of pseudoscalar and vector mesons have been presented. However, the procedure remains the same for any given interaction involving spin-1/2 or spin-3/2 particles. We evaluate a set of auxiliary helicity amplitudes ϕ_{ij}^{\pm} as defined in Eq. 3.35 by using the interaction given by the effective field Lagrangian as well as the decompositions of the generic interaction into invariants, as defined in chapter 2. The invariant functions F_i^{JP} can be immediately calculated by analytically solving the system of linear equations.

We have first studied the structure of the partial-wave amplitudes expressed in the helicity formalism of Jacob and Wick for the scattering of two spin-1/2, two spin-3/2 particles, and a spin-1/2 off a spin-3/2 particle. Although one can easily write down and calculate helicity partial-wave amplitudes, these scalar amplitudes are

correlated at certain energies or have poles, even if the S-matrix elements themselves are regular at the corresponding points. These singularities are in a sense spurious, reflecting only the nature of the decomposition. As an intermediate step, for each of the scattering processes involving spin-1/2 and spin-3/2 particles, we have identified complete sets of invariants that parameterize the scattering amplitudes of the various processes. These amplitudes are frame independent and kinematically unconstrained. They are expected to satisfy the Mandelstam dispersion-integral representation.

Based on the analytical expressions that describe the decomposition of helicity partial-wave amplitudes into invariants, we have built transformation matrices from the helicity basis to a new kinematic-free basis. We have tested that any parity conserving interaction can be decomposed into this set of invariants. The matrix elements of any tensors evaluated in the new kinematic-free basis are free from kinematical singularities, retaining only the singularities described by the dynamics of the process. The covariant partial-wave amplitudes evaluated in the kinematical-free basis have convenient analytic properties that justify the use of uncorrelated dispersion-integral relations.

As a further step, we have constructed a projector algebra that solves the two-body Bethe-Salpeter scattering equation in the limit of short range forces. The existence and smoothness of such a projector basis is closely related to the existence of covariant partial-wave amplitudes. The derivation of such projectors was presented for the scattering of two spin-1/2 particles. Explicit expressions for such projectors were presented for the two simplest reactions.

The $SU(3)$ Lagrange density has been used to calculate the driving interaction for the N/D method to construct a scattering amplitude that obeys constraints from unitarity, analyticity and crossing symmetry at a specific energy. We have performed a series of calculations for a 2×2 coupled-channel interaction. The results of the scattering amplitudes calculated for different interaction strengths have been presented in chapter 4. We have investigated the effects of a weak, intermediate and strong coupling on the covariant partial-wave amplitudes calculated with the N/D method. In the N/D approach the structure of the T -matrix may be influenced by the high-energy structure of the driving potential. This is partially compensated by the subtraction in the dispersion integral and by imposing the proper asymptotic be-

havior of the driving potential. One important feature of the N/D method is that it can produce resonances across the whole energy regime, even for the cases when a single channel is involved. However, the solution of the N/D equation is a meromorphic function. This implies that the amplitudes calculated with the N/D method may present additional poles corresponding to the generation of ghosts. The treatment of ghosts requires a more elaborate procedure, which has not been pursued in this thesis.

In conclusion, for the processes involving the scattering of spin-1/2 and spin-3/2 particles, we have developed a set of bases transformations from the helicity basis as introduced by Jacob and Wick to a new kinematic-free basis. These transformations have been used to evaluate covariant partial-wave amplitudes that are kinematically unconstrained, a required ingredient for the calculation of the scattering amplitude using uncorrelated dispersion integrals. We have also shown that the N/D method leads to an analytical and unitary amplitude in such a way that it may lead to the dynamical generation of resonances, both for the single channel problem, as well as a result of the coupled-channel effects.

A numerical coupled-channel calculation has been performed for the scattering off spin-1/2 particles with the t -channel exchange of vector mesons. As a next step, a systematic treatment of the t - and u -channel cuts must be implemented for the scattering amplitudes. The driving interaction must be extended to include pseudoscalar mesons as exchange particles. Moreover, the channel space must be extended to include spin-3/2 particles, for which the covariant partial-wave amplitudes have been calculated in this thesis. Also, covariant partial-wave amplitudes must be used to extend the coupled-channel space with meson-nucleon states and meson-meson states.

The theoretical predictions must be confirmed by comparing with experimental data. The PANDA experiment will be in a unique position to provide high quality experimental data, even for channels with exotic isospin and strangeness, by making use of hadron probes, which have large expected cross sections. The theoretical-predicted resonances, that have been generated dynamically by using the N/D method, must be identified by comparison with experimental data. The calculations can be then used to make predictions for new states of the hadron spectrum. A good understanding of the predicted theoretical states and of the hadron spectra will allow for an identification of the nature of the hadronic states, such as gluonic hadrons or glueballs.

Also, theoretical predictions can be used as input for a partial-wave analysis in the sense that it provides additional relations between the real and imaginary parts of the scattering amplitudes.

EXPANSION IN LEGENDRE POLYNOMIALS

The helicity partial-wave amplitudes are expressed in terms of Legendre polynomials and the invariant amplitudes. We first eliminate the trivial angular dependence of the helicity partial-wave amplitudes and introduce a set of auxiliary helicity amplitudes

$$\phi_{ij}^{\pm} = \frac{1}{d_{+\lambda, \bar{\lambda}}^{(J_0)}(\theta)} \langle \bar{\lambda}_1, \bar{\lambda}_2 | T | +\lambda_1, +\lambda_2 \rangle \pm \frac{(-1)^{S_1-S_2}}{d_{-\lambda, \bar{\lambda}}^{(J_0)}(\theta)} \langle \bar{\lambda}_1, \bar{\lambda}_2 | T | -\lambda_1, -\lambda_2 \rangle ,$$

$$J_0 = \text{Min} (|\bar{\lambda}|, |\lambda|) , \quad (\text{A.1})$$

where $\lambda = \lambda_1 - \lambda_2$ and $\bar{\lambda} = \bar{\lambda}_1 - \bar{\lambda}_2$ is the total helicity of the initial and final state, respectively. Partial-wave matrix elements can now be expressed in terms of the auxiliary amplitudes ϕ_{ij}^{\pm} and the Legendre polynomials $P_n(\cos \theta)$. It holds

$$\begin{aligned} t_{\pm, ij}^J &= \langle \bar{\lambda}_1, \bar{\lambda}_2 | T_J | \lambda_1, \lambda_2 \rangle \pm (-1)^{S_1-S_2} \langle \bar{\lambda}_1, \bar{\lambda}_2 | T_J | -\lambda_1, -\lambda_2 \rangle \\ &= \int_{-1}^1 \frac{d \cos \theta}{2} \left[\left(\phi_{ij}^+ + \phi_{ij}^- \right) d_{\lambda_j, \lambda_i}^{(J_0)}(\theta) d_{\lambda_j, \lambda_i}^{(J)}(\theta) \right. \\ &\quad \left. \pm \left(\phi_{ij}^+ - \phi_{ij}^- \right) d_{-\lambda_j, \lambda_i}^{(J_0)}(\theta) d_{-\lambda_j, \lambda_i}^{(J)}(\theta) \right] , \end{aligned} \quad (\text{A.2})$$

where the product of two Wigner rotation functions $d_{\lambda_j, \lambda_i}^{(J_0)}(\theta) d_{\lambda_j, \lambda_i}^{(J)}(\theta)$ can be expressed in terms of the Legendre polynomials by making use of

$$d_{\lambda_j, \lambda_i}^{(J_0)}(\theta) d_{\lambda_j, \lambda_i}^{(J)}(\theta) = \sum_{n=|J-J_0|}^{n=J+J_0} (-1)^{\lambda_j-\lambda_i} (2n+1)$$

$$\times \begin{pmatrix} J_0 & J & n \\ -\lambda_j & \lambda_j & 0 \end{pmatrix} \begin{pmatrix} J_0 & J & n \\ -\lambda_i & \lambda_i & 0 \end{pmatrix} P_n(\cos \theta) . \quad (\text{A.3})$$

PROJECTORS FOR THE $\frac{1}{2}\frac{1}{2} \rightarrow \frac{1}{2}\frac{1}{2}$ REACTION

The expressions of the projectors provided in (2.41) can be further simplified by using appropriate building blocks, that are derived by suitable derivatives of the function $Y_J^{(n)}(\bar{r}, r, s)$. We write

$$\begin{aligned}
\partial^\mu Y_J^{(n)} &\equiv \frac{\partial}{\partial r^\mu} Y_J^{(n)}(\bar{r}, r, s) = (J - n) \frac{r^\mu}{r^2} Y_J^{(n)} \\
&\quad + \left(\frac{\bar{r}^2 r^2}{s^2} \right)^{(J-n)/2} P_J^{(n+1)}(x) \left[-\frac{\bar{r}^\mu}{\sqrt{\bar{r}^2 r^2}} + \frac{\bar{r} \cdot r}{\sqrt{\bar{r}^2 r^2}} \frac{r^\mu}{r^2} \right] \\
&= -\frac{\bar{r}^\mu}{s} Y_J^{(n+1)} - \frac{r^\mu}{s} \frac{\bar{r}^2}{s} Y_{J-1}^{(n+1)}, \\
\bar{\partial}^\mu Y_J^{(n)} &\equiv \frac{\partial}{\partial \bar{r}^\mu} Y_J^{(n)}(\bar{r}, r, s) = \\
&= -\frac{r^\mu}{s} Y_J^{(n+1)} - \frac{\bar{r}^\mu}{s} \frac{r^2}{s} Y_{J-1}^{(n+1)}, \\
\bar{\partial}^\mu \partial^\nu Y_J^{(n)} &= -\frac{\bar{r}^\nu}{s} \bar{\partial}^\mu Y_J^{(n+1)} - \frac{r^\nu}{s^2} \bar{\partial}^\mu Y_{J-1}^{(n+1)} \\
&\quad - \frac{g^{\mu\nu}}{s} Y_J^{(n+1)} - 2 \frac{\bar{r}^\mu r^\nu}{s^2} Y_{J-1}^{(n+1)}, \tag{B.1}
\end{aligned}$$

where we used

$$x P_J^{(n+1)}(x) = (J - n) P_J^{(n)}(x) + P_{J-1}^{(n+1)}(x). \tag{B.2}$$

The projectors for the $\frac{1}{2}\bar{\frac{1}{2}} \rightarrow \frac{1}{2}\bar{\frac{1}{2}}$ reaction read:

$$\begin{aligned}
 \mathcal{Y}_{\pm,11}^J &= \mp \frac{1}{s} \left(P_{\pm} \otimes P_{\pm} \right) Y_J, \\
 \mathcal{Y}_{\pm,12}^J &= \pm \frac{1}{\sqrt{s}} \left(P_{\pm} \otimes P_{\pm} \tilde{\gamma}_{\nu} \right) \partial^{\nu} Y_J, \\
 \mathcal{Y}_{\pm,21}^J &= \pm \frac{1}{\sqrt{s}} \left(\tilde{\gamma}_{\mu} P_{\pm} \otimes P_{\pm} \right) \bar{\partial}^{\mu} Y_J, \\
 \mathcal{Y}_{\pm,22}^J &= \mp \left(\tilde{\gamma}_{\mu} P_{\pm} \otimes P_{\pm} \tilde{\gamma}_{\nu} \right) \bar{\partial}^{\mu} \partial^{\nu} Y_J,
 \end{aligned} \tag{B.3}$$

where we recall the notation

$$\tilde{\gamma}^{\mu} = \gamma^{\mu} - \psi \frac{w^{\mu}}{s}. \tag{B.4}$$

PROJECTORS FOR THE $\frac{1}{2}\frac{1}{2} \rightarrow \frac{3}{2}\frac{1}{2}$ REACTION

We first provide some useful intermediate results applied in the derivation of the projectors for the $\frac{1}{2}\frac{1}{2} \rightarrow \frac{3}{2}\frac{1}{2}$ reaction. It holds

$$\begin{aligned}
 \bar{r}^\alpha \langle \tilde{\gamma}_\alpha P_\mp \otimes P_\pm \rangle_\mu &= \frac{\bar{M}_\mp}{2s} (s - \bar{M}_\pm^2) \langle P_\mp \otimes P_\pm \rangle_\mu, \\
 r^\alpha \langle P_\mp \otimes P_\pm \tilde{\gamma}_\alpha \rangle_\mu &= \frac{M_\pm}{2s} (s - M_\mp^2) \langle P_\mp \otimes P_\pm \rangle_\mu, \\
 \langle \tilde{\gamma}^\mu P_\mp \otimes P_\pm \rangle_\mu &= -\frac{\bar{M}_\pm}{s} w^\mu \langle P_\mp \otimes P_\pm \rangle_\mu, \\
 \bar{r}^\mu \langle \bar{\Gamma} \otimes \Gamma \rangle_\mu &= -\frac{s + \bar{M}_+ \bar{M}_-}{2s} w^\mu \langle \bar{\Gamma} \otimes \Gamma \rangle_\mu,
 \end{aligned} \tag{C.1}$$

where we use the notation of (B.4) and

$$\langle \bar{\Gamma} \otimes \Gamma \rangle_\mu = \bar{u}_\mu(\bar{p}_1) \bar{\Gamma} v(\bar{p}_2) \bar{v}(p_2) \Gamma u(p_1). \tag{C.2}$$

The first two on-shell identities in (C.1) resemble our previous results (2.45) used in the derivation of the $\frac{1}{2}\frac{1}{2} \rightarrow \frac{1}{2}\frac{1}{2}$ projectors. The last two identities follow from

$$\begin{aligned}
 \bar{u}_\mu(\bar{p}_1) \gamma^\mu &= 0 = \bar{u}_\mu(\bar{p}_1) p_1^\mu, \\
 \bar{p}_1^\mu &= w^\mu + 2 \bar{k}^\mu = w^\mu + 2 \bar{r}^\mu + 2 \frac{w \cdot \bar{k}}{s} w^\mu,
 \end{aligned} \tag{C.3}$$

where we recall (2.11, 2.33). Using the notations of Appendix B we obtain:

$$\begin{aligned}
\mathcal{Y}_{\pm,11}^{J,\mu} &= \pm \frac{\sqrt{2J+1}}{2s^2} \left(\tilde{p}_1 P_{\mp} \otimes P_{\pm} \right) w^{\mu} Y_J, \\
\mathcal{Y}_{\pm,12}^{J,\mu} &= \mp \frac{\sqrt{2J+1}}{2s\sqrt{s}} \left(\tilde{p}_1 P_{\mp} \otimes P_{\pm} \tilde{\gamma}_{\beta} \right) w^{\mu} \partial^{\beta} Y_J, \\
\mathcal{Y}_{\pm,21}^{J,\mu} &= \mp \frac{\sqrt{2J+1}}{2Js\sqrt{s}} \left(\tilde{p}_1 \tilde{\gamma}_{\alpha} P_{\mp} \otimes P_{\pm} \right) w^{\mu} \bar{\partial}^{\alpha} Y_J, \\
\mathcal{Y}_{\pm,22}^{J,\mu} &= \mp \frac{\sqrt{2J+1}}{2Js} \left(\tilde{p}_1 \tilde{\gamma}_{\alpha} P_{\mp} \otimes P_{\pm} \tilde{\gamma}_{\beta} \right) w^{\mu} \bar{\partial}^{\alpha} \partial^{\beta} Y_J, \\
\mathcal{Y}_{\pm,31}^{J,\mu} &= \pm \frac{\sqrt{2J+1}}{Js^2} \sqrt{s} \left[\left(P_{\mp} \otimes P_{\pm} \right) \left(s \bar{\partial}^{\mu} - 2J w^{\mu} \right) \right. \\
&\quad \left. + \left(\tilde{p}_1 \tilde{\gamma}_{\alpha} P_{\mp} \otimes P_{\pm} \right) w^{\mu} \bar{\partial}^{\alpha} \right] Y_J, \\
\mathcal{Y}_{\pm,32}^{J,\mu} &= \mp \frac{\sqrt{2J+1}}{Js} \left[\left(P_{\mp} \otimes P_{\pm} \tilde{\gamma}_{\beta} \right) s \bar{\partial}^{\mu} \partial^{\beta} \right. \\
&\quad \left. - \left(P_{\mp} \otimes P_{\pm} \tilde{\gamma}_{\beta} \right) 2J w^{\mu} \partial^{\beta} \right. \\
&\quad \left. + \left(\tilde{p}_1 \tilde{\gamma}_{\alpha} P_{\mp} \otimes P_{\pm} \tilde{\gamma}_{\beta} \right) w^{\mu} \bar{\partial}^{\alpha} \partial^{\beta} \right] Y_J, \\
\mathcal{Y}_{\pm,41}^{J,\mu} &= \pm \frac{\sqrt{2J+1}}{J(J-1)s^2} \left[\left(\tilde{\gamma}_{\alpha} P_{\mp} \otimes P_{\pm} \right) s^2 \bar{\partial}^{\mu} \bar{\partial}^{\alpha} \right. \\
&\quad \left. - \left(\tilde{\gamma}_{\alpha} P_{\mp} \otimes P_{\pm} \right) 2(J-1)s w^{\mu} \bar{\partial}^{\alpha} \right. \\
&\quad \left. + \left(\tilde{p}_1 P_{\mp} \otimes P_{\pm} \right) 4J(J-1)w^{\mu} \right] Y_J, \\
\mathcal{Y}_{\pm,42}^{J,\mu} &= \pm \frac{\sqrt{2J+1}}{J(J-1)s\sqrt{s}} \left[\left(\tilde{\gamma}_{\alpha} P_{\mp} \otimes P_{\pm} \tilde{\gamma}_{\beta} \right) s^2 \bar{\partial}^{\mu} \bar{\partial}^{\alpha} \partial^{\beta} \right. \\
&\quad \left. - \left(\tilde{\gamma}_{\alpha} P_{\mp} \otimes P_{\pm} \tilde{\gamma}_{\beta} \right) 2(J-1)w^{\mu} s \bar{\partial}^{\alpha} \partial^{\beta} \right. \\
&\quad \left. + \left(\tilde{p}_1 P_{\mp} \otimes P_{\pm} \tilde{\gamma}_{\beta} \right) 4J(J-1)w^{\mu} \partial^{\beta} \right] Y_J. \tag{C.4}
\end{aligned}$$

Note that the last four projectors in (C.4) involve structures already present in the first four projectors.

Nederlandse samenvatting

De toekomstige internationale Faciliteit voor Antiprotonen- en Ionenonderzoek [1] in Darmstadt zal één van de meeste geavanceerde faciliteiten worden voor het onderzoek naar antiproton-proton botsingen. Het Antiprotonannihilatie-experiment in Darmstadt (PANDA) heeft een breed wetenschappelijk programma waarvan de studie van exotische hadronen, 'strange'- en 'charmed'-baryonen, het spectrum van charmonium, in-medium hadroneigenschappen, gammastralingspectroscopie en de structuur van het nucleon de belangrijkste deelgebieden zijn.

Het is algemeen geaccepteerd dat de kwantumchromodynamica (QCD) de fundamentele theorie is van de sterke kernkracht. In tegenstelling tot de ladingsneutrale fotonen, die de ijkvelden zijn van de kwantumelektrodynamica (QED), kunnen de gluonen, de ijkvelden van QCD, met elkaar interacteren omdat ze kleurlading dragen. De zelfkoppeling van gluonen in QCD staat de voorspelling toe van hadronische systemen die verschillen van de klassieke quarkmodeltoestanden $\bar{q}q$ en qqq .

Er zijn mogelijkheden tot het construeren van exotische kleursinglet toestanden, zoals glueballs (gebonden gluontoestanden, gg of ggg), hybrides (toestanden die bestaan uit quarks met een sterke gluoncomponent, $q\bar{q}g$) of toestanden met een exotische 'flavor'-inhoud zoals tetraquarks ($qq\bar{q}\bar{q}$) in het geval van mesonen, en pentaquarks ($qqq\bar{q}q$) voor baryonen. Door de extra vrijheidsgraden van de gluonen kunnen de exotische toestanden spin-exotische quantumgetallen, J^{PC} , hebben die niet toegestaan zijn voor $q\bar{q}$ mesonen en andere fermion-antifermionsystemen. Zeer nauwkeurige experimentele resultaten voor de spin/pariteit bepalingen en vervalswaarschijnlijkheden zijn een doorslaggevend element voor het identificeren van de structuur van deze exotische toestanden.

Vanwege de moeilijkheden die QCD met zich meebrengt, zijn veel methoden

die de hadronische wisselwerkingen bestuderen gebaseerd op effectieve theorieën. Deze maken gebruik van de symmetrieën van de QCD Lagrangiaan om effectieve Lagrangianen op te bouwen voor de wisselwerking tussen hadronen in plaats van die tussen quarks. Als de aantrekkende kracht tussen twee hadronen sterk genoeg is, dan zou het deze twee deeltjes samen kunnen binden tot een nieuwe toestand, een dynamisch gegenereerde resonantie. Deze verschijnt dus als gevolg van de dynamiek van het systeem van de deeltjes die fungeren als de bouwstenen van het gebruikte model.

Onze aanpak begint met het benoemen van de algemene eigenschappen van een verstrooiingsamplitude: unitariteit, covariantie, analyticiteit en deeltjesverwisselings-symmetrie. De covariante partiële-golfamplitudes zijn een uitstekend beginpunt voor het analyseren van baryon-antibaryonverstrooiing in een covariante gekoppelde-kanalenaanpak die rekening houdt met causaliteit en gekoppelde-kanalenunitariteit. In hoofdstuk 2 wordt de analytische structuur van de partiële-golfamplitudes die spin-1/2 en spin-3/2 fermion-antifermionverstrooiing beschrijven, onderzocht. Partiële-golfamplitudes die zijn uitgedrukt in het helicititsformalisme van Jacob en Wick [24] kunnen oneindigheden hebben of gecorreleerd zijn op bepaalde energieën, zelfs als de matrix elementen van de verstrooiingsamplitude zelf regulier zijn in de overeenkomstige punten. Dit zijn geen echte singulariteiten, ze geven alleen het wezen van de decompositie weer; ze worden ook wel kinematische singulariteiten genoemd. Deze kinematische beperkingen in de helicititspartiële-golfamplitudes worden geëlimineerd door niet-unitaire transformatiematrices die de begin- en eindhelicititeitstoestanden op nieuwe covariante toestanden afbeelden.

Gebruikmakend van de $SU(3)$ Lagrangiaan voor de verstrooiing van twee spin-1/2 deeltjes, welke wordt gepresenteerd in hoofdstuk 3, worden de invarianten die de t -kanaal-uitwisseling van pseudoscalaire en vectormesonen beschrijven, gepresenteerd. In hoofdstuk 4 wordt de resulterende potentiaal gebruikt als de aandrijfwisselwerking voor een gekoppelde-kanaal berekening van verstrooiingsamplitudes gebaseerd op de N/D methode. We hebben een serie berekeningen uitgevoerd voor een 2×2 gekoppelde-kanalen wisselwerking. Hiermee onderzoeken wij de effecten van een zwakke, gemiddelde en sterke koppeling op de covariante partiële-golfamplitudes zoals uitgerekend met de N/D methode. Hiervoor wordt gecompenseerd door

de aandrijfpotentiaal van de dispersie-integraal af te trekken en er het juiste asymptotische gedrag aan op te leggen. Een belangrijke eigenschap van de N/D methode is dat het resonanties kan produceren over het hele energiebereik, zelfs in de gevallen waar het een enkel kanaal betreft. Helaas zijn een aantal van de gegenereerde structuren a-causaal.

Als een volgende stap moet een systematische behandeling van de oneindigheden als gevolg van structuren in t - en u -kanaalsuitwisselingsinteracties worden geïmplementeerd voor de beschrijving van de verstrooiingsamplitudes. De aandrijfpotentiaal moet zodanig worden uitgebreid dat het pseudoscalaire mesonen als uitwisselingsdeeltjes omvat. Bovendien moet de kanalenruimte uitgebreid worden om spin-3/2 deeltjes, waarvoor in dit proefschrift de covariante partiële-golfamplitudes zijn uitgerekend, te kunnen beschrijven. Daarbovenop moeten covariante partiële-golfamplitudes gebruikt worden om de gekoppelde-kanalenruimte uit te breiden met meson-nucleon en meson-meson toestanden.

Acknowledgments

*Expecting the world to treat you fairly because you are good is
like expecting an angry bull not to charge because you are a vegetarian.*

Dennis Whitman

It is difficult to overstate my gratitude to my Ph.D. supervisor, Prof. Dr. Olaf Scholten. With his enthusiasm, his inspiration, and his great efforts to explain things clearly and simply, he helped keep this project on track. It is not an understatement in saying that this thesis would have never been finished without him. Throughout my writing period, he provided encouragement, advice, and lots of good ideas. I appreciate your help and support through the last four years, and especially in the last few months. I don't want to finish this paragraph without thanking Ann and Laura for all the pleasant times.

I would like to thank Professors Diego Bettoni, Kanzo Nakayama and Klaus Peters for reading my thesis and for their nice words. I would also like to thank Prof. Herbert Löhner for providing very useful comments that have greatly improved the quality of this thesis.

I want to thank Catherine Evelyne and Liselotte Willemina for being my par-nymphs. I appreciate a lot your support and friendship.

Just to make sure I don't forget someone, I will simply thank all my colleagues, friends and family for their support in the last four years. I would like to thank my husband for his constant love, encouragement and understanding. Thank you for always being there for me.

References

- [1] FAIR - An International Accelerator Facility for Beams of Ions and Antiprotons, Conceptual Design Report, <http://www.fair-center.de>, 2001.
- [2] PANDA: <http://www-panda.gsi.de>,
- [3] W. Erni et al., Physics Performance Report for PANDA: Strong Interaction Studies with Antiprotons, PANDA Collaboration, *arXiv:hep-ex/0903.3905*, 2009.
- [4] J. G. Messchendorp, Strong interaction studies with PANDA, PANDA Collaboration, *arXiv:hep-ex/1001.0272*, 2010.
- [5] U. Wiedner, Future Prospects for Hadron Physics at PANDA, *Prog. Part. Nucl. Phys.* 66:477, 2011.
- [6] J. G. Messchendorp, Hadron Physics with Anti-Protons: The PANDA Experiment at FAIR, *eConf C070910:123*, 2007.
- [7] D. Bettoni, The PANDAexperiment at FAIR, *eConf, C070805:39*, 2007.
- [8] C. J. Morningstar and M. J. Peardon, The Glueball spectrum from an anisotropic lattice study, *Phys. Rev. D* 60:034509, 1999.
- [9] D. Acosta et al., Observation of the narrow state $X(3872) \rightarrow J/\psi \pi^+ \pi^-$ in $\bar{p}p$ collisions at $\sqrt{s} = 1.96$ TeV, *Phys. Rev. Lett.* 93:072001, 2004.
- [10] The BESIII Collaboration, Observation of a $p\bar{p}$ mass threshold enhancement in $\psi' \rightarrow \pi^+ \pi^- J/\psi (J/\psi \rightarrow \gamma p\bar{p})$ decay, *arXiv:hep-ex/1001.5328*, 2010.
- [11] Jie-Sheng Yu, Zhi-Feng Sun, Xiang Liu, and Qiang Zhao, Categorizing resonances $X(1835)$, $X(2120)$ and $X(2370)$ in the pseudoscalar meson family, *Phys. Rev. D* 83:114007, 2011.

- [12] Zhi-Gang Wang, Analysis of the X(1835) and related baryonium states with Bethe-Salpeter equation, *Eur. Phys. J.* A47:71, 2011.
- [13] J.-P. Dedonder, B. Loiseau, B. El-Bennich, and S. Wycech, On the structure of the X(1835) baryonium, *Phys. Rev.* C80:045207, 2009.
- [14] Shi-Lin Zhu, New hadron states, *Int. J. Mod. Phys.* E17:283, 2008.
- [15] Tao Huang and Shi-Lin Zhu, X(1835): A Natural candidate of eta-prime's second radial excitation, *Phys. Rev.* D73:014023, 2006.
- [16] S. Scherer and M. R. Schindler, A Chiral perturbation theory primer, *arXiv:hep-ph/0505265*, 2005.
- [17] N. Kaiser, T. Waas, and W. Weise, SU(3) chiral dynamics with coupled channels: Eta and kaon photoproduction, *Nucl. Phys.* A612:297, 1997.
- [18] J. A. Oller, E. Oset, and J. R. Pelaez, Meson-meson interaction in a nonperturbative chiral approach, *Phys. Rev.* D59:074001, 1999.
- [19] M. F. M. Lutz and E. E. Kolomeitsev, Relativistic chiral SU(3) symmetry, large N(c) sum rules and meson baryon scattering, *Nucl. Phys.* A700:193, 2002.
- [20] M. Gell-Mann, M. L. Goldberger, and W. E. Thirring, Use of causality conditions in quantum theory, *Phys. Rev.* 95:1612, 1954.
- [21] S. Mandelstam, Analytic properties of transition amplitudes in perturbation theory, *Phys. Rev.* 115:1741, 1959.
- [22] S. Mandelstam, Dispersion relations in strong-coupling physics, *Rep. Prog. Phys.* 25:99, 1962.
- [23] S. Mandelstam, Determination of the pion - nucleon scattering amplitude from dispersion relations and unitarity. General theory, *Phys. Rev.* 112:1344, 1958.
- [24] M. Jacob and G. C. Wick, On the general theory of collisions for particles with spin, *Ann. Phys.* 7:404, 1959.
- [25] G. F. Chew, M. L. Goldberger, F. E. Low, and Y. Nambu, Relativistic Dispersion Relation Approach to Photomeson Production, *Phys. Rev.* 106:1345, 1957.
- [26] Noboru Nakanishi, Proof of Partial-Wave Dispersion Relations in Perturbation Theory, *Phys. Rev.* 126:1225, 1962.

- [27] F. A. Berends, A. Donnachie, and D. L. Weaver, Photoproduction and electroproduction of pions. 1. Dispersion relation theory, *Nucl. Phys.* B4:1, 1967.
- [28] A. Gasparyan and M. F. M. Lutz, Photon- and pion-nucleon interactions in a unitary and causal effective field theory based on the chiral Lagrangian, *arXiv:hep-ph/1003.3426*, 2010.
- [29] K. Nakayama and W. G. Love, Spin structure of spin-1/2 baryon and spinless meson production amplitudes in photonic and hadronic reactions, *Phys. Rev.*, C72:034603, 2005.
- [30] K. Nakayama and F. Huang, Model-independent analysis of $p + p \rightarrow pp(^1S_0) + \gamma$, *Phys.Rev.* C82:065201, 2010.
- [31] R. H. Dalitz, On the strong interactions of the strange particles, *Rev. Mod. Phys.* 33:471, 1961.
- [32] W. Zimmermann, *Nuovo Cim.* 21 (1961) 249,
- [33] G. L. Payne and L. Schlessinger, Properties of the K Matrix in Nuclear-Reaction Theory, *Phys. Rev.* C2:1648, 1970.
- [34] E. E. Salpeter and H. A. Bethe, A Relativistic equation for bound state problems, *Phys. Rev.* 84:1232, 1951.
- [35] R. G. Newton, Scattering theory of waves and particles, ISBN: 0387109501, *Springer Verlag, New York*, 1982.
- [36] O. Scholten, S. Kondratyuk, L. van Daele, et al., Compton scattering on the proton and light nuclei in the Delta-resonance region, *Acta Phys. Polon.* B33:847, 2002.
- [37] G. F. Chew and S. Mandelstam, Theory of the Low-Energy Pion-Pion Interaction, *Phys. Rev.* 119:467, 1960.
- [38] J. D. Bjorken, Construction of coupled scattering and production amplitudes satisfying analyticity and unitarity, *Phys. Rev. Lett.* 4:473, 1960.
- [39] G. Cohen-Tannoudji, A. Morel, and H. Navelet, Kinematical singularities, crossing matrix and kinematical constraints for two-body helicity amplitudes, *Ann. Phys.* 46:239, 1968.
- [40] J. S. Ball, Application of the Mandelstam Representation to Photoproduction of Pions from Nucleons, *Phys. Rev.* 124:2014, 1961.

- [41] A. O. Barut, I. Muzinich, and D. N. Williams, Construction of Invariant Scattering Amplitudes for Arbitrary Spins and Analytic Continuation in Total Angular Momentum, *Phys. Rev.* 130:442, 1963.
- [42] Y. Hara, Analyticity Properties of Helicity Amplitudes and Construction of Kinematical Singularity-Free Amplitudes for Any Spin, *Phys. Rev.* 136:B507, 1964.
- [43] J. D. Jackson and G. E. Hite, Kinematic Singularities and Threshold Relations for Helicity Amplitudes, *Phys. Rev.* 169:1248, 1968.
- [44] Ling-Lie Chau Wang, General Method of Constructing Helicity Amplitudes Free from Kinematic Singularities and Zeros, *Phys. Rev.* 142:1187, 1966.
- [45] J. Franklin, Threshold Kinematic Constraints and Correlations of Helicity Amplitudes, *Phys. Rev.* 170:1606, 1968.
- [46] M. D. Scadron and H. F. Jones, Covariant M functions for higher spin, *Phys. Rev.* 173:1734, 1968.
- [47] W. A. Bardeen and W. K. Tung, Invariant amplitudes for photon processes, *Phys. Rev.* 173:1423, 1968.
- [48] M. F. M. Lutz and E. E. Kolomeitsev, On charm baryon resonances and chiral symmetry, *Nucl. Phys.* A730:110, 2004.
- [49] W. Rarita and J. Schwinger, On a theory of particles with half integral spin, *Phys. Rev.* 60:61, 1941.
- [50] J. Nieves and E. Ruiz Arriola, Bethe-Salpeter approach for meson-meson scattering in chiral perturbation theory, *Phys. Lett.* B455:30, 1999.
- [51] M. F. M. Lutz, Effective chiral theory of nucleon-nucleon scattering, *Nucl. Phys.* A677:241, 2000.
- [52] J. Nieves and E. Ruiz Arriola, Bethe-Salpeter approach for unitarized chiral perturbation theory, *Nucl. Phys.* A679:57, 2000.
- [53] M. F. M. Lutz, G. Wolf, and B. Friman, Scattering of vector mesons off nucleons, *Nucl. Phys.* A706:431, 2002.
- [54] M. Lutz and E. Kolomeitsev, Covariant Meson-Baryon Scattering with Chiral and Large N_c Constraints, *Found. Phys.* 31:1671, 2001.

- [55] H. Fritzsch and M. Gell-Mann, Current algebra: Quarks and what else? *eConf*, C720906V2:135, 1972.
- [56] W. J. Marciano and H. Pagels, Quantum Chromodynamics: A Review, *Phys. Rept.* 36:137, 1978.
- [57] Chen-Ning Yang and R. L. Mills, Conservation of Isotopic Spin and Isotopic Gauge Invariance, *Phys. Rev.* 96:191, 1954.
- [58] J. Goldstone, Field Theories with Superconductor Solutions, *Nuovo Cim.* 19:154, 1961.
- [59] S. Weinberg, Dynamical approach to current algebra, *Phys. Rev. Lett.* 18:188, 1967.
- [60] Steven Weinberg, Phenomenological Lagrangians, *Physica A*96:327, 1979, Festschrift honoring Julian Schwinger on his 60th birthday.
- [61] E. E. Jenkins, QCD baryons in the $1/N(c)$ expansion, *UCSD-PTH-01-21*:36, 2001.
- [62] E. E. Jenkins, Chiral Lagrangian for baryons in the $1/N(c)$ expansion, *Phys. Rev.* D53:2625, 1996.
- [63] E. E. Jenkins, Large $N(c)$ baryons, *Ann. Rev. Nucl. Part. Sci.* 48:81, 1998.
- [64] A. Semke and M. F. M. Lutz, Baryon self energies in the chiral loop expansion, *Nucl. Phys.* A778:153, 2006.
- [65] J. J. de Swart, The Octet Model and its Clebsch-Gordan Coefficients, *Rev. Mod. Phys.* 35:916, 1963.
- [66] S. Ciulli, C. Pomponiu, I. Sabba-Stefanescu, and G. Steinbrecher, Tautologies and optimization of N/D equations, *Phys. Rev.* D8:455, 1973.
- [67] A. Gasparyan and M. F. M. Lutz, Photon- and pion-nucleon interactions in a unitary and causal effective field theory based on the chiral Lagrangian, *Nucl. Phys.* A848:126, 2010.
- [68] E. I. Fredholm, Sur une classe d'equations fonctionnelles, *Acta Math.* 27:365, 1903.
- [69] M. F. M. Lutz and E. E. Kolomeitsev, private communication, 2008.
- [70] J. Hofmann, *Coupled-channel study of axial-vector mesons with realistic t - and u -channel exchanges*, PhD thesis.

- [71] L. Castillejo, R. H. Dalitz, and F. J. Dyson, Low's scattering equation for the charged and neutral scalar theories, *Phys. Rev.* 101:453, 1956.
- [72] S. Mandelstam, Regge poles as consequences of analyticity and unitarity, *Ann. Phys.* 21:302, 1963.